**The Dissertation Committee for Mary Elizabeth Ramsey Certifies that this is the approved version of the following dissertation:**

# MOLECULAR MECHANISMS UNDERLYING STEROID HORMONE ACTION DURING SEX DETERMINATION IN THE RED-EARED SLIDER TURTLE, *Trachemys scripta elegans*

**Committee:**

David Crews, Supervisor

Jim Bull

Creagh Bruener

Thane Wibbels

John Wallingford

# MOLECULAR MECHANISMS UNDERLYING STEROID HORMONE ACTION DURING SEX DETERMINATION IN THE RED-EARED SLIDER TURTLE, *Trachemys scripta elegans*

**by**

**Mary Elizabeth Ramsey, B.A.**

**Dissertation**

Presented to the Faculty of the Graduate School of

The University of Texas at Austin

in Partial Fulfillment

of the Requirements

for the Degree of

**Doctor of Philosophy**

**The University of Texas at Austin**

**May, 2007**

# Dedication

To James and Diego, Frida, Tim, Bunchy and Pearl

## Acknowledgements

Thanks first and foremost to David Crews. Thanks to my committee, in particular Creagh Bruener who has been incredibly supportive throughout this whole process. Thanks to Crews Lab members past – Emily Willingham, Alice Fleming, Raymond Porter, Sarah Woolley, and Jon Sakata. Thanks to Crews Lab members present – Christina Shoemaker, Nicholas Sanderson, and Brian Dias. Thanks also to Molly Cummings and the Cummings Lab. And of course thanks to James for putting up with all this….

# MOLECULAR MECHANISMS UNDERLYING STEROID HORMONE ACTION DURING SEX DETERMINATION IN THE RED-EARED SLIDER TURTLE, *Trachemys scripta elegans*

Publication No._____

Mary Elizabeth Ramsey, Ph.D.

The University of Texas at Austin, 2007

Supervisor: David Crews

Many reptiles, including the red-eared slider turtle (Trachemys scripta elegans), exhibit temperature-dependent sex determination (TSD). Temperature determines sex during a temperature sensitive period (TSP), when gonadal sex is labile to both temperature and hormones – particularly estrogen. Estrogen production is a key step in ovarian differentiation for many vertebrates, including TSD reptiles, and temperature-based differences in aromatase expression during the TSP may be a critical step in ovarian determination. Steroidogenic factor-1 (Sf1) is a key gene in vertebrate sex determination and regulates steroidogenic enzymes, including aromatase. The biological actions of steroid hormones are mediated by their receptors, defined here as the classic transcriptional regulation of target genes. To elucidate the mechanism of estrogen action estrogen during sex determination, I examined aromatase, Sf1, ERα, ERβ, and AR

expression in slider turtle gonads before, during and after the TSP, as well as following sex reversal via temperature or steroid hormone manipulation by administering exogenous estradiol (E2) or aromatase inhibitor (AI) to the eggshell.

Sf1 is expressed at higher levels during testis development and following male-producing temperature shift and AI treatment, while aromatase increases during ovary determination and feminizing temperature shift and E2 treatment. My results do not lend support to a role for Sf1 in the regulation of aromatase expression during slider turtle sex determination, but do support a critical role for estrogen in ovarian development.

Estrogen receptor α and AR levels spike at the female-producing temperature just as aromatase levels are increasing during ovarian sex determination, while ERβ remains constant and only increases late in ovarian differentiation – well after estrogen levels have increased, indicating that ERα and ERβ may have distinct roles in slider turtle ovarian development. Estrogen receptor α and ERβ are expressed along developing sex cords in the absence of estrogen (AI treatment). When shifted to female-producing temperatures, embryos maintain medullary ERα and AR expression while ERβ is reduced. By contrast, ERα and ERβ redirect to the cortex in E2-created ovaries. Warmer temperature and E2 result in the same endpoint (ovarian development), but may entail different steroid signaling patterns between temperature- and estrogen-induced feminization.

# Table of Contents

# List of Tables

## List of Figures

# Chapter 1: Introduction

## BACKGROUND

Sex determination can be thought of as the decision point(s) wherein the gonad will initiate differentiation towards becoming a testis or an ovary. A variety of sex-determining systems exist among vertebrates, and these range from primarily genotypic to primarily environmental (Sarre et al., 2004; Manolakou et al., 2006). Among amniotes, mammals and birds exhibit genotypic sex determination (GSD) and sex-specific gene expression on heteromorphic sex chromosomes determines the sex of the developing embryo. The mechanisms of sex determination among reptiles range from GSD-type systems with or without heteromorphic sex chromosomes to systems where sex is determined via an environmental cue or even a combination of genotypic and environmental cues (Sarre et al., 2004). Here, I am concerned with temperature-dependent sex determination (TSD), a sex-determining mechanism found in many egg-laying turtles, some lizards, and all crocodilians (Bull, 1980; Janzen and Paukstis, 1991).

The triggers for initiating sex-determining networks are diverse. Gonadal sex in many eutherian mammals appears to be determined by the presence or absence of SRY, a gene expressed on the short arm of the Y chromosome (Gubbay et al., 1990; Sinclair et al., 1990), so that XX individuals are female and XY individuals are male, although some microtine and akodont rodents and mole voles do not strictly adhere to this mode of sex determination (Graves, 2002; Marchal et al., 2003). In birds, a ZZ/ZW sex determining

system exists and females are the heterogametic sex, although the exact trigger is unknown. Both XX/XY and ZZ/ZW systems are found in reptiles, fish, and amphibians with GSD. In addition, many of these groups, regardless of triggering mechanism, are also sensitive to epigenetic factors such as temperature and steroid hormones in their sex determination (Baroiller et al., 1999; Wallace et al., 1999; Sarre et al., 2004; Manolakou et al., 2006).

While the triggers underlying sex determination are diverse, the genes involved in sex determination and differentiation that respond to those triggers - though not necessarily their expression pattern or developmental timing - are conserved across vertebrate groups. Homologues for genes first discovered in mammals such as Dmrt1, Sox9, Mis, Dax1, WT1, Wnt4, and FoxL2, have been found in fish (Guan et al., 2000), amphibians (Shibata et al., 2002), birds (Clinton, 1998; Smith and Sinclair, 2001), and reptiles (Spotila et al., 1998; Kettlewell et al., 2000; Western et al., 2000; Maldonado et al., 2002; Shoemaker et al., 2007)

An important conserved feature of vertebrate sex determination is the ability of steroid hormones to influence either genotypic (except for eutherian mammals) or temperature-induced sex determination and differentiation. In most vertebrate groups, estrogen plays a prominent role in female sex differentiation. Exogenous estrogen application can induce transient feminization in birds (Scheib, 1983) and permanent sex reversal in fish (Baroiller et al., 1999), amphibians (Wallace et al., 1999) and reptiles, including those with TSD (Bull et al., 1988). Nonaromatizable androgens cannot override all-female producing temperatures (Wibbels and Crews, 1992), but they can

produce all males from an intermediate (1:1 sex ratio) temperature (Wibbels and Crews, 1995), indicating a possible role for androgens in sex determination as well.

The biological actions of steroid hormones are mediated through ligand-specific binding to their respective receptors (Tsai and O'Malley, 1994). Correspondingly, steroid receptors such as androgen receptor (AR), estrogen receptor α (ERα), and estrogen receptor β (ERβ), as well as aromatase, the enzyme that converts testosterone to estradiol, are highly conserved in adult and embryonic reproductive tissues. Also conserved is Sf1, a gene with multiple roles during sexual development across vertebrate groups, including regulation of aromatase (Morohashi and Omura, 1996; Parker et al., 2002). AR, ERα and ERβ expression patterns are critical markers for steroid hormone action. Aromatase expression indicates possible embryonic production of estrogen, and *Sf1* is a master steroidogenic regulator. Examining the developmental expression profiles of AR, ERα, ERβ, aromatase, and *Sf1* will illuminate the interplay between temperature and sex steroid hormone action in slider turtle sex determination.

**RED-EARED SLIDER TURTLE MODEL SYSTEM**

The red-eared slider turtle, *Trachemys Scripta elegans,* is well characterized histologically over development. The onset and duration of temperature and hormonal sensitivity during sex determination have been delineated in the slider turtle (Wibbels et al., 1991; Wibbels et al., 1994). Slider turtle developmental staging is outlined in Table1. Sex is determined during a temperature-sensitive period (TSP) encompassing about the middle third of development. At female-producing temperatures, the TSP extends from about Stages 14-19, while at male-producing temperatures it extends from about Stages 14-20/21. The urogenital ridge first forms around stage 13, and hatching occurs at stage

26. The TSP and the ensuing phase of gonadal differentiation can be further divided into three phases: bipotential gonad (Stages 14-16, when the gonad is morphologically bipotential although temperature may already be exerting its action), sex determination (Stages 17-19/20, when the sexual trajectory of the gonadal primordium is still flexible), and gonadal commitment/differentiation (Stages 20/21-hatch, when the final gonadal morphology develops and sex is irreversible). The TSP encompasses the bipotential and sex determination phases of gonadal development (Table1).

Incubation at high temperature (31°C) produces 100% females, while incubation at low temperature (26°C) produces 100% males. Temperatures intermediate to these extremes produce varying ratios of males to females, and 29.2° is considered the threshold temperature where 1:1 sex ratio is produced (Wibbels et al., 1991). In the slider turtle, shifting eggs from 31°C → 26° or the parallel shift from 26° → 31° during the TSP results in almost 100% sex reversal. During the TSP, application of exogenous estradiol ($E_2$) on eggs incubating at 26°C produces 100% sex reversal, while blocking embryonic estrogen production with aromatase inhibitor (AI) at a female-biased temperature (29.4°C) results in male hatchlings (Wibbels et al., 1993; Crews and Bergeron, 1994).

## ROLE OF STEROID HORMONES AND STEROIDOGENIC ENZYMES IN *T. SCRIPTA* SEX DETERMINATION

Steroid hormones, in particular estrogen, may be a proximate mechanism responding to a temperature trigger (Crews et al., 1994; Pieau and Dorizzi, 2004). Because of the ability to sex reverse embryos by altering estrogen availability, steroid

signaling pathways may be important components of the slider turtle sex -determining pathway; but their mechanism of action in TSD is not well understood.

Early studies on TSD established steroidogenic capability and activity before, during, and after the TSP in slider turtle adrenal-kidney-gonad (AKG) tissue (White and Thomas, 1992a) as well as the presence of steroid hormones in serum and whole embryos (White and Thomas, 1992c). Embryos incubating at male-producing temperatures are more steroidogenically active (White and Thomas, 1992b), and contain more T and $E_2$ during early- to mid-TSP and more progesterone (P) in the middle of the TSP than 31°C embryos (White and Thomas, 1992c). Expression of SF-1, an important regulator of steroidogenic enzymes including aromatase, exhibits a sexually dimorphic pattern of expression in the slider turtle and is upregulated following masculinizing temperature shifts and AI treatments (Fleming et al., 1999; Fleming and Crews, 2001). Until the present work (Chapter 2), researchers had not found sex-specific differences in slider turtle gonadal aromatase expression or activity during the TSP (Willingham et al., 2000; Murdock and Wibbels, 2003).

The developing AKG tissue is rich in steroid hormones and their precursors. Beyond endogenous steroidogenic activity, yolk is an important extraembryonic source of steroid hormones available to the developing embryo. Measurements of yolk steroid levels in slider turtle eggs show differential uptake of estrogen, testosterone and progesterone (Bowden et al., 2002), although this uptake did not differ by incubation temperature. Estrogen (2.4ng/g yolk at oviposition) declines to nondetectable yolk levels by the beginning of the TSP, so it is possible that early gonadal steroid hormone receptor

expression could precede embryonic aromatase activity and may transduce hormone signals from extraembryonic sources.

## ESTROGEN RECEPTORS (ER)

The estrogen receptor exists in two primary isoforms, ERα and ERβ (Nilsson et al., 2001). Both are members of the nuclear receptor superfamily of transcription factors and are activated on binding an estrogenic ligand. ERs mediate the genomic biological effects of estrogens in all vertebrate groups. In mammals, estrogens play an important role in the development of female secondary sex characteristics. ERα and ERβ expression occurs in male and female adult (Pelletier et al., 2000) and developing (Jefferson et al., 2000) reproductive tracts. During development, female mice express ERα in fetal ovarian interstitial cells and throughout developing Müllerian duct structures, while ERβ is found primarily in granulosa cells (mouse postnatal day or PND 1). In males, both ERα and ERβ are found in the fetal testis, with ERα in interstitial cells, and ERβ in developing spermatagonia. Although exogenous estrogen treatments have been shown to sex-reverse male marsupials (Coveney et al., 2001), estrogens have been thought unnecessary for normal female differentiation in eutherian mammals. Female ER knockout (ERKO) mice for ERα (Lubahn et al., 1993) and ERβ (Krege et al., 1998) both develop normal reproductive tracts, although ERα are infertile and ERβ are subfertile. It was not until αβERKO mice were created that estrogen-related sex reversal was observed in a eutherian mammal (Couse et al., 1999; Dupont et al., 2000). Double knockout (αβERKO) female mice show grossly normal prenatal female differentiation, including development of Müllerian duct-derived structures, but soon show age-related disruptions in normal ovarian function. Immature αβERKO females display precocious ovarian maturation (including accelerated folliculogenesis), probably due to disruptions

in estrogen-mediated LH regulation in the hypothalamus-pituitary-gonad axis. Adult αβERKO females undergo partial sex reversal, including germ cell loss and development of seminiferous tubule-like structures containing Sertoli-like cells with elevated Mis (a protein secreted by Sertoli cells that directs Müllerian duct regression) and Sox9 levels (Couse et al., 1999; Dupont et al., 2003). Although this sex-reversal seems to be a transdifferentiation of mature granulosa cells into Sertoli-like cells rather than a developmental phenomenon, it is illustrative of the plasticity of gonadal cellular organization.

In birds, ER mRNA is detected very early (day 3.5; just after formation of the primordial gonad) in the female genital ridge, and is expressed in male and female gonads as well as in the developing Müllerian duct and external genitalia of both sexes (Andrews et al., 1997; Smith et al., 1997). As gonads are differentiating (days 7.5-12.5), both males and females show higher ER mRNA levels in the left gonad than the right, but while the female right gonad regresses, males develop full-size right and left testes (Andrews et al., 1997). Other researchers (Nakabayashi et al., 1998) found ER mRNA restricted to the cortical region of the left ovary, and only transient expression in the left testis. The above works did not differentiate between ERα and ERβ isoforms, but presumably reflect ERα expression pattern. Avian ERβ is present in adult testis and ovary tissue (Foidart et al., 1999), however to my knowledge a compete ontogeny of avian ERβ gonadal expression has not been published.

Even less is known about ERα and ERβ in TSD reptiles. Early work localized $E_2$ uptake sites in crocodile gonads during gonadal differentiation (Smith and Joss, 1994), although in slider turtle AKG tissue $^3H$-$E_2$ accumulation was reported in the adrenal and

mesonephros tissue rather than the gonad itself (Gahr et al., 1992). Preliminary ERα *in situ* hybridization results in our lab (Bergeron et al., 1998) indicated ERα mRNA expression is gonad-specific within the AKG during development. Contrary to cortical localization in the bird ovary, ERα mRNA expression in the developing slider turtle ovary is diffuse and scattered throughout the medullary compartment while expression in the developing testis became localized in the developing testicular cords (Bergeron et al., 1998; Chapter 3). The present work reports the first developmental expression analysis of ERβ transcript in a TSD reptile.

**ANDROGEN RECEPTOR**

The androgen receptor is also a member of the nuclear receptor superfamily of transcription factors. AR mediates physiological effects of androgens and regulates target genes upon ligand binding. Among other roles, androgen-bound AR is an important regulator of spermatogenesis as well as masculinization of the reproductive tract and external genitalia (Haqq and Donahoe, 1998). AR is known to be important in the development of a masculine phenotype from XY individuals with androgen insensitivity syndrome. Due to nonfunctional AR, the gonad is a testis, but outer genitalia are feminized due to the failure to masculinize the internal reproductive tract (Brinkmann et al., 1996). In the adult rat, immunohistochemistry experiments show that AR protein is expressed in the Sertoli, peritubular myoid, and Leydig cells of the testis, while the ovary shows AR staining in granulosa and theca cells (Pelletier et al., 2000). During mammalian development, AR does not appear to play a direct role in early testis differentiation, and instead expression is mainly confined to Wolffian-derived accessory sex structures and external genitalia. In the rat, expression of AR protein in the fetal

reproductive system begins after testis differentiation has begun and seems to be confined to mesenchymal mesonephric cells underlying the developing Wolffian duct (beginning rat day 16.5). Expression later extends into the epithelial cells of the Wolffian duct (rat day 17-18) and testis-specific expression first appears in peritubular and interstitial cells (possibly of mesonephric origin), though it is never detected in fetal Sertoli or Leydig cells (Majdic et al., 1995). Immunostaining studies with fetal ovine testis tissue (Sweeney et al., 1997) indicate that AR protein is not expressed in the developing testis until after the onset of testicular differentiation and the appearance of testicular cords. AR appears in interstitial cell nuclei on day 40 of gestation, well after pre-Sertoli and pre-Leydig cells already express AMH and 3β-HSD respectively, and after seminiferous cords are organized. Here too, it would appear that Sertoli and Leydig cell AR expression is delayed until pubertal onset of spermatogenesis. Recently, AR knockout mice (ARKO) have been reported (Yeh et al., 2002). Male ARKO mice have female-like appearance and body weight, reduced testis size (80% reduction), ambiguous external genitalia, agenesis of some Wolffian duct-derived structures (vas deferens, epididymis, seminal vesicle, prostate), disrupted spermatogenesis (arrested at pachytene spermatocytes), testis cell disruptions such as hypertrophied Leydig cells and reduced numbers of mature peritubular myoid cells, lower serum T concentrations, and decreased bone volume. Male ARKO mice do not retain Müllerian duct-derived structures (no oviducts, uterus, vaginal opening) so as with androgen insensitivity syndrome individuals, normal Mis regulation and function occurs in the absence of AR. Female ARKO mice are subfertile. They form normal-appearing ovaries but experience problems with folliculogenesis and normal cycling at puberty (Hu et al., 2004).

In the chicken, AR is present in both testes and ovaries during development, but is expressed at higher levels in the left ovary than the testis (Katoh et al., 2006). Interestingly, *in ovo* treatment of female chick embryos with the AR antagonist flutamide resulted in disorganization of ovarian cortical development. This disorganization was rescued by co-application of either testosterone or estradiol with flutamide, indicating a possible role for androgen signaling in sex-specific aromatase action in ovarian development (Katoh et al., 2006).

In contrast to mammalian systems, AR may play a more prominent role in reptile gonad development. In the slider turtle, treatment with DHT (a nonaromatizable androgen) during the TSP results in male hatchlings from pivotal temperatures, and inhibition of reductase, the enzyme that converts testosterone into DHT, sex-reverses from a male-biased temperature. Combined treatment with DHT and $E_2$ at pivotal temperatures as well as treatment with high concentrations of testosterone at female-biased temperatures produces some individuals with ovotestes (Wibbels et al., 1992; Crews and Bergeron, 1994; Wibbels and Crews, 1995). These results point to possible AR involvement within the developing gonad during the TSP. AR expression coupled with testosterone production in fetal Leydig cells may be important in creating an early endocrine microenvironment necessary for normal testis development.

**AROMATASE**

Cytochrome P450 aromatase is encoded by the CYP19 gene. It is a heme-binding protein that catalyzes the conversion of androgens to estrogens (Simpson et al., 1994). Aromatase has been found in all vertebrate groups, and it exists as multiple isoforms in most species, either through alternative splicing (Simpson et al., 1994) or through

separate genes (Trant et al., 2001). In adult mammals, aromatase is expressed in brain, bone, adipose, ovary, and placental tissues (Simpson et al., 1994). During development, aromatase expression is typically localized in the developing brain and gonad. Mouse aromatase mRNA levels are very low in developing ovarian tissue, although somewhat higher in the embryonic testis (Greco and Payne, 1994). The ovaries of aromatase knockout (ArKO) female mice contain granulosa cells, but individuals are infertile due to arrested folliculogenesis and ovulatory failure (Fisher et al., 1998). Female ArKO mice also show underdeveloped genitalia and mammary glands. Postnatal ovaries of female ArKO mice fed a soy-free diet exhibit the same sex-reversed phenotype seen in αβERKO ovaries (Britt et al., 2001; Britt et al., 2002). Male ArKO mice are initially fertile with normal testis development (although they do show elevated testosterone, LH, and FSH). As male ArKO mice mature, however, they demonstrate progressive infertility (Robertson et al., 1999), pointing to an important role for aromatase, and therefore estrogen, in male germ cell development.

Estrogens and embryonic aromatase activity play a critical role in bird sex determination and differentiation. A single treatment with aromatase inhibitor (AI) during the bipotential phase of gonadal development permanently sex reverses genetically female chickens (Elbrecht and Smith, 1992). Although chicken ER mRNA is found in both males and females (where it localizes to the cortical region of the developing left ovary), aromatase expression is female-specific and found throughout the medullary region of both left and right ovaries (Yoshida et al., 1996; Andrews et al., 1997; Smith et al., 2003). Aromatase expression does not begin until the onset of ovarian differentiation (day 6.5) and well after the onset of ER mRNA expression (day 3.5) (Andrews et al., 1997). During sex-reversal after AI treatment (administered at day 3

when the gonad is still undifferentiated), aromatase levels drop during the normal time of ovarian differentiation, while Mis increases toward control male levels (Nishikimi et al., 2000).

Sexually dimorphic gonadal aromatase expression in species with temperature-sensitive sex determining mechanisms may be directly or indirectly affected by the temperature cue itself. Gonadal aromatase is responsive to temperature in an amphibian with GSD (Kuntz et al., 2003). In the newt *P. waltl,* a species with a ZZ/ZW sex determining system, incubation at high temperature during a thermo-sensitive period of sexual development results in phenotypic male ZW offspring. Gonadal aromatase mRNA levels are downregulated during heat treatment (32 °C) to typical ZZ levels, but do not respond to heat treatment after sex determination is completed.

Of particular interest here is the action of aromatase in estrogen-sensitive TSD reptiles. Because of the sex-reversing power of $E_2$ and AI treatments during the TSP of gonadal development, much research on TSD reptiles has concerned possible temperature-dependent regulation of steroidogenesis. Early research on the pond turtle (*E. orbicularis*) showed that gonadal aromatase levels are higher at female-producing temperatures (although the rise comes late in the TSP), and that temperature shifts to feminizing temperature increase aromatase activity (Desvages and Pieau, 1992). In the diamondback terrapin (*Malaclemys terrapin*), aromatase is sexually dimorphic in both the brain and the gonad (Jeyasuria and Place, 1998). Gonadal aromatase levels are higher at female-producing temperatures late- and post-TSP (Jeyasuria and Place, 1997). Brain aromatase levels are higher at feminizing temperatures early in the TSP, but are downregulated as the TSP progresses, while correspondingly upregulated at male-

producing temperature and downregulated in the gonad. Therefore, one hypothesis on the interaction of temperature and aromatase in TSD reptiles postulates an interaction between brain and gonadal aromatase activity throughout the TSP. According to this hypothesis, at the onset of the TSP, high brain aromatase levels in the female negatively feed back on brain aromatase (so lower aromatase in the brain is feminizing) and positively feed back on gonadal aromatase (so higher aromatase in the gonad is feminizing) (Jeyasuria and Place, 1998). One reason the search for an extragonadal source for differential aromatase expression was so appealing is that earlier work in the slider turtle (Willingham et al., 2000; Murdock and Wibbels, 2003) did not detect a rise in aromatase until late in ovarian differentiation (post-TSP). However, both these experiments used AKG tissue as the source of measurement rather than isolated gonad. In a more sensitive assay using gonad tissue, we were able to resolve a female-temperature specific increase in aromatase during the TSP itself (Chapter 2), giving support to the hypothesis that differential aromatase in the gonad itself is an early marker of ovarian commitment. Indeed, Merchant-Larios and colleagues (Moreno-Mendoza et al., 2001) found that temperature shifts with gonadal organ cultures could change *Sox9* (an early Sertoli cell marker that exhibits higher male expression in all vertebrate groups) levels. In the sea turtle (*Lepidochelys olivacea)*, shifts to feminizing temperatures downregulated *Sox9*, while shifts to masculinizing temperatures upregulated *Sox9*. These results point to a temperature sensing mechanism at the gonad that does not depend on brain-gonad feedback.

## EXPERIMENTAL QUESTIONS

The experiments presented here concern the interaction between steroid hormones and temperature during sex determination and differentiation in the slider turtle. In the

current work, I examined gonadal expression changes in steroid hormone production (aromatase), regulation (*Sf1*), and signal transduction (steroid hormone receptors ERα, ERβ, and AR) during development at male- and female-producing temperatures. I utilized the lability of sex determination in the slider turtle to study how changes in temperature (sex reversal via temperature shift in both male → female, and female → male directions) or steroid hormone environment (sex reversal via estradiol ($E_2$) application at the male-producing temperature or aromatase inhibitor (AI) application at a female-biased temperature) alter steroid hormone signaling.

Chapter 2 concerns temperature-specific estrogen production and its regulation during gonadal development. It utilizes whole mount *in situ* hybridization and quantitative real-time PCR (qPCR) to determine 1) Is gonadal aromatase differentially expressed at female-producing temperature during the TSP? 2) Do *Sf1* expression patterns correlate with aromatase? 3) Do aromatase and *Sf1* localization patterns change in response to sex-reversing treatments? 4) Do these changes support a role for *Sf1* regulation of aromatase during sex determination at the female-producing temperature?

Chapter 3 concerns temperature-specific steroid hormone signal transduction during slider turtle development. It utilizes whole mount *in situ* hybridization and qPCR to determine 1) Are ERα, ERβ, and AR differentially expressed between male- and female-producing temperatures during the TSP? 2) Do ERα, ERβ, and AR localization patterns change in response to sex-revering treatments? 3) Do temperature- and estrogen-based sex reversal affect parallel changes in steroid signaling?

Chapter 4 concerns gene expression measures in adrenal-kidney-gonad (AKG) complexes versus isolated gonad tissue. It utilizes qPCR to determine if measurements based on total AKG tissue accurately reflect their expression in the gonad. A related question is whether gene expression in the components of the AKG are additive.

# Chapter 2: Gonadal Expression of *Sf1* and aromatase during sex determination in the red-eared slider turtle (*Trachemys scripta*), a reptile with temperature-dependent sex determination

## INTRODUCTION

Two primary forms of sex determination exist among vertebrates. In genotypic sex determination (GSD) a genetic factor such as the *Sry* gene found on the mammalian Y chromosome determines sex. In environmental sex determination, environmental cues dictate sex determination. One form of environmental sex determination found in many egg-laying reptiles is temperature-dependent sex determination (TSD). In the red-eared slider turtle (*Trachemys scripta elegans*), gonadal sex is determined by incubation temperature during a temperature-sensitive period (TSP) spanning about the middle third of development (Wibbels et al., 1991a). The TSP and the ensuing phase of gonadal differentiation can be further divided into three phases: bipotential gonad (Stages 14-15, when the gonad is morphologically bipotential although temperature may already be exerting its action), sex determination (Stages 16-19, when the sexual trajectory of the gonadal primordium is still flexible), and gonadal commitment/differentiation (Stages 20-hatch, when the final gonadal morphology develops and sex is irreversible). During the TSP, warmer temperatures (31° C) produce 100% female hatchlings and cooler temperatures (26° C) produce 100% males, while intermediate temperatures produce mixed sex ratios. For example, an incubation temperature of 29.4° C results in an 80:20 female-biased sex ratio. Sex determination is labile throughout the TSP, and shifting embryos from 31→26° C or 26→31° C reverses sex outcome (Wibbels et al., 1991a).

While the actual triggering mechanisms that initiate a sex-determining gene cascade are diverse, many aspects of sex determination, and more particularly, gonadal differentiation, are remarkably conserved across vertebrate groups. Genes implicated in mammalian sex determination and gonadal differentiation such as *Sox9*, *Dmrt1*, *Mis*, *Sf1*, *Wnt4*, *Dax1*, and *FoxL2* have also been found in avian and reptile species, including reptiles with TSD (Fleming et al., 1999; Govoroun et al., 2004; Kettlewell et al., 2000; Loffler et al., 2003; Maldonado et al., 2002; Murdock and Wibbels, 2003b; Smith et al., 1999b; Spotila et al., 1998; Western et al., 1999; Western et al., 2000).

Another conserved feature of vertebrate sex determination is the ability of steroid hormones to influence either GSD (except in eutherian mammals) or TSD. In many vertebrates, estrogen plays a prominent role in the differentiation of ovaries. Application of estrogen during the period of sexual differentiation will induce partial to complete sex reversal in marsupials (Coveney et al., 2001), transient feminization in birds (Scheib, 1983) and permanent sex reversal in fish (Baroiller et al., 1999), amphibians (Wallace et al., 1999), and reptiles (Bull et al., 1988). In the slider turtle, application of estrogen to the egg during the TSP overrides a male-determining temperature cue and produces all female hatchlings that are morphologically indistinguishable from females produced via warmer female-determining temperatures (Wibbels et al., 1993). Similarly, inhibition of Cyp19a1 (hereafter referred to as aromatase), the enzyme that converts testosterone to estradiol ($E_2$), during the TSP produces male hatchlings from female-biased temperatures (Crews and Bergeron, 1994; Crews et al., 1994). This effect is also conserved. For example, inhibiting aromatase early in development permanently sex reverses genetically female chickens (Elbrecht and Smith, 1992) and creates males from an all-female parthenogenic lizard species (Wennstrom and Crews, 1995; Wibbels and Crews, 1994).

Because estrogens and aromatase inhibitors can override a temperature cue for sex determination in TSD reptiles, it has been hypothesized that temperature-based changes in estrogen levels are a critical step for ovarian development (Crews et al., 1994; Pieau and Dorizzi, 2004). If temperature and estrogen action are intimately linked in TSD, then examining aromatase expression in the gonad becomes critical to understanding the complex interplay between temperature, steroid hormones, and other sex-determining genes that underlie sex determination in a TSD reptile. Of particular interest in this context is *Sf1*, a gene known to regulate the expression of gonadal steroidogenic enzymes including aromatase (Morohashi and Omura, 1996; Parker et al., 2002). *Sf1* is critical in vertebrate sex determination and differentiation regardless of sex-determining mechanism. Beyond its steroidogenic functions, Sf1 is required for maintenance of the early bipotential gonad and plays a critical role in testis differentiation. *Sf1* mRNA is expressed at higher levels in developing mammalian testes (Ikeda et al., 1994), a pattern conserved in the slider turtle (Fleming et al., 1999). *Sf1* is also responsive to sex-reversing treatments: *Sf1* levels increase with a male-producing temperature shift and aromatase inhibitor (AI) treatment and will decrease with the corresponding female-producing shift and exogenous estrogen application (Fleming and Crews, 2001).

The current study localizes *Sf1* and aromatase mRNA expression using whole mount *in situ* hybridization at male- and female-producing temperatures from the early bipotential gonad through the TSP and sexual differentiation. We also document changes in *Sf1* and aromatase localization in response to sex-reversing treatment by temperature shifts and application of exogenous estrogen or aromatase inhibitor to incubating eggs

during the TSP. Finally, quantitative real-time PCR (qPCR) is used to quantify *Sf1* and aromatase mRNA levels in isolated gonad tissue from embryos incubating at male- and female-producing temperatures.

## METHODS

### Tissue collection

Red-eared slider turtle *(T. scripta)* eggs were purchased from Robert Clark (Clark Turtle Farms, Hammond LA). The eggs were picked up within 24 hours of laying so all embryos in each group/shipment were at roughly equivalent developmental stages. To control for possible clutch effects, collected eggs were randomized on site. Eggs were kept at room temperature (22° C) in Texas until candled to establish viability, at which time they were further randomized and placed into trays (35/tray) containing 1:1 vermiculite and water mix and placed in incubators (Precision, Chicago, IL) at 26° C (male-producing temperature), 29.4° C (female-biased temperature), or 31° C (female-producing temperature). Temperatures within the incubators were monitored continuously with HOBO recording devices (Onset Computer Corporation, Bourne, MA) as well as checked daily using calibrated shelf thermometers. To avoid small temperature gradient effects, the egg trays were rotated daily within the incubator. A few eggs (2-3) were dissected at regular intervals to assess developmental stage (Yntema, 1968). Embryos were harvested at Stages 15, 17, 19, 21, and 23. Adrenal-kidney-gonad (AKG) or isolated gonad tissue was rapidly dissected and processed for experimental use (see below).

In addition to eggs incubated at constant temperatures, eggs were manipulated either by shifting them to a different temperature (Table 1) or by chemical manipulation (Table 2) with all sex-reversing treatments occurring at Stage 17 (midway through the TSP). For the temperature shifts, one group was shifted from 26 → 31° C, with another receiving the complementary shift from 31 → 26° C. For the hormone treatment, groups incubating at 26° and 31° C were treated with 5 μg estradiol-17β (Sigma, St. Louis, MO) in 5 μl 95% EtOH, each with control groups receiving EtOH vehicle. Other eggs were incubated at the intermediate temperature of 29.4° C, a temperature that produces a female-biased sex ratio (typically 80:20 female:male, see Table 2). One group was treated with 100 μg of the aromatase inhibitor (AI) fadrozole (CGS16949A, Ciba-Geigy, Summit, NJ) in 5 μl 95% EtOH with a control group treated with EtOH alone. Treated groups were harvested at Stages 19 and 23 except for estradiol-treated eggs at 31° C which were harvested at Stage 23 alone. For each treatment, a subset of eggs was allowed to develop through hatching and was sexed by gross morphology of the gonad.

**Whole mount in situ hybridization**

A 337 bp subclone of slider turtle aromatase (Accession **AF178949**) was cloned into pCR 4-TOPO vector (Invitrogen, Carlsbad, CA) according to the manufacturer's protocol. Turtle *Sf1* (Accession **AF033833**) cloning and probe length have been reported previously (Fleming et al., 1999). DIG-labeled turtle aromatase and *Sf1* antisense and sense control probes were transcribed using Megascript High Yield Transcription kit (Ambion, Austin, TX) with 33% labeled digoxigenin-11-UTP (Roche, Indianapolis, IN) and 67% unlabeled UTP, following the manufacturer's protocol. Probe integrity and abundance was assessed through gel electrophoresis.

For each gene, whole mount *in situ* hybridization (ISH) experiments were conducted on AKG tissue from 4 embryos/stage/treatment (N= 88 embryos/gene). The ISH experiments were conducted as described (Smith et al., 1999a) but modified for use with turtle tissue. Briefly, AKG tissue was fixed overnight in 4% PFA and then sequentially dehydrated with MeOH:PBTX solutions, ending in 100% MeOH for storage at -20° C. ISH was performed using hybridization solution containing 4-8 µl of DIG-labeled antisense probe. Samples were incubated overnight (4° C) with anti-digoxigenin-AP antibody (Roche) preabsorbed with embryo powder derived from whole body and AKG embryonic turtle tissue. BM purple AP substrate (Roche) was used for colorimetric detection. For each gene, color detection for all groups in a given stage was halted simultaneously. Color detection times were optimized for each gene/developmental stage and ranged from 5 – 8 hours. Detection times were as follows: St 15 SF1 5.5 hrs, Aromatase 8 hrs; St 17 SF1 7 hrs, Aromatase 7.5 hrs, St 19 SF1 7 hrs, Aromatase 7 hrs, St 23 SF1 8 hrs, Aromatase 8.5 hrs. To view internal gonadal structure/signal, whole mount tissue was sectioned on a Microm HM 500 OM cryostat (Microm International, Germany) at 25 or 40 µm thickness. No specific signal was detected in embryos hybridized with labeled sense control probe(Figure 1). . All section photographs were taken on a Nikon Eclipse 80i microscope using NIS-Elements BR 220 visualization software. LUT settings were 125-black, 255-white, and gamma .75 for all photomicrographs except for *Sf1* at Stage 15 which were visualized at 85-black due to intensity of signal. 100x photomicrographs (Figure 2) were taken on an Olympus BX61 microscope (Olympus American Inc.) using MicroFire S99808 video camera (Optronics, Goleta, CA).

**Total RNA preparation and cDNA synthesis**

Aromatase and *Sf1* are expressed in the surrounding kidney and adrenal compartments of the AKG complex as well as the gonad at both incubation temperatures (Fleming et al., 1999; White and Thomas, 1992). To isolate temperature-specific differences in expression levels within the gonad itself, gonads were excised from surrounding tissue for analysis. Because the gonad is a very small component of the AKG, gonads from multiple individuals (30-50/sample) were pooled for measurement.

Gonads were rapidly dissected away from the adjacent adrenal/kidney tissue and placed in RNAlater (Ambion) for overnight incubation at 4° C followed by storage at -80° C, or placed directly into Promega RNAgents Total RNA Isolation kit denaturing solution and stored at -80° C. Total RNA was then extracted from the gonad tissue using RNAgents Total RNA Isolation kit (Promega, Madison, WI) following the manufacturer's protocol. Total RNA abundance and purity was assessed through spectophotometry readings at 260 nm and 280 nm.

Prior to cDNA synthesis, total RNA was treated with DNase to ensure elimination of genomic DNA contamination using the Turbo DNA-Free kit (Ambion) following the manufacturer's protocol. Single-stranded cDNA was then reverse-transcribed at a concentration of 1 μg total RNA/20 μl synthesis reaction using Superscript First Strand Synthesis for RT-PCR kit (Invitrogen). cDNA synthesis was primed with both oligo-dT and random hexamers using a modified manufacturer's protocol (Invitrogen).

**Real-time qPCR**

Real-time PCR quantification results are typically normalized to a housekeeping gene, but many housekeeping genes previously considered to be constitutively expressed were found to be regulated by particular treatments, tissue types, or developmental stage (Bustin, 2002; Pfaffl, 2001). Therefore, to select an appropriate normalizing gene, five candidate slider turtle housekeeping genes (Table 3) plus slider turtle 16S rRNA sequence were tested on cDNA template derived from AKG total RNA for all stages and treatments used in these experiments. GeNORM (http://medgen.ugent.be/~jvdesomp/genorm/;Vandesompele et al., 2002) program was used to assess the most stably expressed genes. PP1 (protein phosphatase 1 gamma) was chosen based on stability of expression under experimental conditions and relative level of abundance compared to aromatase and *Sf1* transcript levels.

Real-time PCR primer sequences and amplicon size are described below (Table 4). Aromatase primers were designed using LUX primer design program (www.invitrogen.com/LUX) and *Sf1* and PP1 primers were designed using MacVector (Accelrys, Inc., San Diego, CA) software program. All primers were engineered to cross exon boundaries (estimated from human gene structure) to eliminate possible signal contamination from genomic DNA. Specificity of target was verified by gel electrophoresis.

Real-time qPCR experiments were conducted on ABI Prism 7900 real-time PCR machine (Applied Biosystems). cDNA representing 10 ng starting total RNA was used in a 10 μl reaction containing 2 μl cDNA template, 5 μl 2x Platinum SYBR Green qPCR SuperMix UDG (Invitrogen), and 5 pmol aromatase or *Sf1* primers or 3 pmol PP1

primers. Real-time qPCR parameters were 2 min at 50° C, 2 min at 95°C for denaturing, followed by 40 cycles at 15 sec 95° C, 15 sec 60° C, and 15 sec 72° C. Each gene primer pair showed no signal in no-template and no-RT controls. Relative gene expression levels were assessed using SYBR green detection chemistry. Dissociation curve analysis was performed after each assay to determine target specificity. Each sample was run in triplicate.

### Real-time qPCR data analysis

Real-time qPCR run results were first analyzed using the Applied Biosystems Sequence Detection System software (SDS 2.2.1). Relative quantification was performed by a modified comparative critical threshold (CT) method that corrects for different PCR amplification efficiencies among primer pairs (Simon, 2003). Gene expression normalized to PP1 housekeeping is given as MNE (mean normalized expression) = ($E_{pp1}$^meanCT $_{pp1}$)/( $E_{arom\ or\ Sf1}$^meanCT $_{arom\ or\ Sf1}$), where E= PCR efficiency (E=10^-(1/slope)) (Pfaffl, 2001) and meanCT is the average CT across the three replicates.

## RESULTS

### Developmental analysis of *Sf1* expression

*Sf1* is present in the gonad throughout all three phases of gonadal development. High levels of *Sf1* are expressed at both male- and female-producing temperatures at the onset of the TSP (Stage 15; Figure 2 A,G). As the gonad enters the sex-determining stages of development (Stage 17), *Sf1* expression begins to dissipate at the female-producing temperature, but at the male-producing temperature is localized to the

presumptive supporting cell lineage surrounding germ cells located predominately in the cortex at this stage of development (Figure 2 B,H; Figure 3 A,B). At Stage 19, *Sf1* expression remains diffuse throughout the medullary region in the developing ovary, while expression is more prominent at the male-producing temperature, and localizes to the developing sex cords (Figure 2 C,I). At Stage 23, when gonadal differentiation is well underway and sex outcome is irreversible, expression at the female-producing temperature continues to show scattered medullary expression as well as localization along the medullary/cortical boundary, while strong medullary striping is evident in the developing testis (Figure 2 D,J).

**Developmental analysis of aromatase expression**

Aromatase is present throughout the TSP at both male- and female-producing incubation temperatures, but localization patterns differ both according to incubation temperature and embryonic state (Figure 4). At the female-producing temperature, aromatase is localized to presumptive supporting cells surrounding germ cells in the bipotential genital ridge at the onset of the TSP (Stage 15). This female-specific localization pattern precedes organization at the male-producing temperature (Figure 4, A,G).

By the middle of the TSP (Stage 17), the gonad is still bipotential but temperature-based gene expression patterns are already beginning to direct the gonad along a developmental trajectory towards an ovary or a testis (Crews et al., 2006). At this stage, aromatase expression appears equivalent between the two temperatures, but the tendency towards higher levels of organization in the supporting cell lineage around germ cells at the female-producing temperature remains (Figure 4, B,H; Figure 3 C,D).

Importantly, this difference in organization is occurring at a developmental stage not only during the TSP, but also while aromatase abundance in the gonad itself is not markedly different between sexes (Figure 5 B).

At Stage 19, as the TSP closes at the female-producing temperature, the peri-germ cell localization pattern of aromatase persists at the female-producing temperature, and also includes some specific expression along the presumptive medullary-cortical boundary as well as increasing medullary expression. At the male-producing temperature, sex determination is still somewhat labile, but aromatase expression is beginning to organize into a striping pattern in the medullary compartment, reflecting the onset of testis differentiation and a transition away from bipotentiality (Figure 4 C,I).

During ovarian differentiation (Stage 23), aromatase expression is faint but some expression can be seen localized around the regressing medullary cords and at the cortical/medullary boundary. In the differentiating testis, localization of aromatase around nascent seminiferous tubules diminishes until it is barely perceptible at Stage 23 (Figure 4 D,J).

**Real-time quantitative PCR during development in isolated gonad tissue**

*Sf1* and aromatase transcript abundance was measured using qPCR. *Sf1* gonadal qPCR expression is higher at the male-producing temperature than the female-producing temperature across development (Figure 5 A). Aromatase abundance measured from isolated gonad tissue shows higher levels of expression at the female-producing temperature from late in the TSP (Stage 19) through ovarian differentiation (Stages

21/23) (Figure 5 B), although differences between the two temperatures do not become pronounced until later in development.

When maximum levels of expression between the two temperatures are compared (Figure 5 C), aromatase levels at the onset of the sex-determining period (Stage 17) are at their highest for an embryo incubating at a male-producing temperature (and will consequently drop and then plateau) and at their lowest for putative females. The lack of correlation between *Sf1* and aromatase abundance patterns is highlighted by examining the relationship between each gene's percent maximum expression across temperatures (Figure 5 D). The ratio of *Sf1*/aromatase shows that *Sf1* is expressed at high levels at male-producing temperature when aromatase expression is low, while aromatase is highly expressed at female-producing temperatures when *Sf1* expression is low.

**Changes in *Sf1* and aromatase expression patterns following sex reversal treatments**

***Temperature shifts***

Patterns of gene expression are altered when eggs are shifted at Stage 17 from male- to female-producing temperatures (M→F) or female- to male-producing temperatures (F→M). *Sf1* and aromatase expression patterns were analyzed following both shifts at Stages 19 (during sex determination) and 23 (during gonadal commitment/differentiation). In the M→ F shift, *Sf1* expression begins to lose the male-typical, intense medullary organization by Stage 19 (Figure 2 C,E), and by Stage 23, the differentiating ovary exhibits the female-typical, diffuse medullary signal (Figure 2 D,F). In the F→M shift, the gonad shows incipient male-typical *Sf1* expression along developing seminiferous tubules by Stage 19 (Figure 2 I,K), indicating the gonad has

already begun to reset the developmental trajectory towards testis formation. By Stage 23, male-specific *Sf1* expression along the seminiferous tubules is evident, although some cortical development remains (Figure 2 J,L).

At Stage 19, two stages after the M→ F shift, aromatase expression increased in organization compared to the unshifted control (Figure 4 C,E), with female-typical expression patterns evident by Stage 23 (Figure 4 D,F). Following the opposing F→M shift, aromatase expression is redirected away from female-specific organization by Stage 19 (Figure 4 I,K), although the gonad still shows morphological signs of ovarian-specific cortical development. By Stage 23, low-level male-specific aromatase expression patterns predominate in the developing testis, although remnants of the cortical compartment remain (Figure 4 J,L).

***Estradiol treatment at the male-producing temperature***

Treatment of eggs at the male-producing incubation temperature with exogenous estradiol-17β ($E_2$) during the TSP (Stage 17) results in all female hatchlings (Crews et al., 1994). Here we show that *Sf1* expression levels are less intense following exogenous $E_2$ treatment (Figure 6 A,B) and fall to near negligible levels during ovarian differentiation at Stage 23 (Figure 6 C,D).

In contrast, aromatase expression remains high two stages after estradiol application (Stage 19), and there is a tendency for signal to concentrate around the nascent cortical/medullary boundary and into the developing cortical compartment itself (Figure 6 G,H). This trend in cortical aromatase localization persists (Figure 6 I,J) as

hormone-induced ovarian differentiation continues (Stage 23), and is more evident in $E_2$-treated ovaries incubated at the male-producing temperature than untreated ovaries developing at female temperatures (Figure 6 J, Fig 4 J).

***Estradiol treatment at the female-producing temperature***

*Sf1* and aromatase expression patterns were also examined after application of estradiol to eggs incubating at the female-producing temperature. The feminizing effect of temperature and exogenous estrogen creates a unique phenotype featuring ovaries with enlarged cortical compartments (Figure 6 F,L). With this treatment, *Sf1* tends to exhibit more intense signal than the typically diffuse pattern exhibited in ovaries created via temperature (Figure 6 E; Figure 2 J,F) or via estradiol application at a male-producing temperature (Figure 6 D). Similarly, while light aromatase transcript can be detected in the medullary compartment of all differentiated ovaries, only ovaries receiving both feminizing temperature and estradiol treatment exhibited the intense and organized medullary signal shown here (Figure 6 K,L; Figure 4 J,F; Figure 7 G).

***Treatment with aromatase inhibitor at the female-biased incubation temperature***

Application of aromatase inhibitor (AI) during the TSP (stage 17) causes sex reversal in embryos incubating at an intermediate, female-biased (29.4° C) temperature, thus increasing the percentage of males (Crews and Bergeron, 1994). *Sf1* localization patterns are not altered at Stage 19 following application of AI (Figure 7 A,B). By Stage 23, however, *Sf1* shows more male-typical expression along the developing seminiferous tubules, while the vehicle-treated ovary exhibits negligible signal with some light expression along the cortical/medullary boundary. (Figure 7 C,D).

AI treatment also does not alter aromatase expression at Stage 19, two embryonic stages after the original application (Fig 7 E,F). However, as with the masculinizing temperature shift, aromatase localization does shift to a low-level, male-typical pattern as testis morphology becomes evident by Stage 23 (Figure 7 G,H). EtOH-treated females at the female-biased temperature exhibited similar patterns of expression as untreated 29.4° C controls (data not shown), as well as females incubating at the female-producing temperature (31°) (Figure 2 J ; Figure 4 J).

## DISCUSSION

If estrogen is a critical endogenous component in the determination and differentiation of the ovary in the slider turtle, then possible temperature-specific differences in embryonic aromatase expression or activity may be mediating the gonadal steroid hormone milieu. We report an increase in female temperature-specific aromatase expression late in the TSP itself, before sex is committed. Our data suggest a role for differential estrogen production in ovarian determination/differentiation, and supports earlier work on the pond turtle (*Emys orbicularis*), where aromatase activity increased late in the TSP at a female-producing temperature (reviewed in Pieau et al., 1999). This increase in aromatase expression is earlier in gonadal development than observed in previous studies in slider turtle (Murdock and Wibbels, 2003a; Willingham et al., 2000) or alligator (Gabriel et al., 2001; Smith et al., 1995) and is likely due to the inclusion of the kidney and adrenal components of the AKG, the tissue used in these earlier studies. The gonad is a very small fraction of the AKG complex, and kidney and adrenal transcript pools appear to reduce the sensitivity of gonad-specific measurements, as has been suggested by Pieau (Pieau and Dorizzi, 2004). Indeed, when we include the entire

AKG complex and measure aromatase expression in our qPCR assay, we also do not pick up a female-specific increase until late in ovarian development (M. Ramsey and D. Crews, unpublished data).

Aromatase expression indicates possible sites of estrogen synthesis in the developing gonad, and *Sf1* expression is examined as a possible indicator of steroidogenic regulation as well as a marker of reversal/commitment to sexual fate. In the differentiating ovary, the requirement for steroidogenesis during development – and the production of aromatase – varies across amniotes, and *Sf1* expression patterns vary accordingly. In mice, *Sf1* expression is downregulated (Ikeda et al., 1994), and aromatase is not expressed during early ovarian differentiation (Greco and Payne, 1994). However, *Sf1* expression is maintained at high levels in species that do require estrogen production during ovarian differentiation such as sheep (Quirke et al., 2001), chickens (Smith et al., 1999a) and alligators (Western et al., 2000). In the current study (Figure 5), qPCR results show higher *Sf1* expression at male- than female-producing temperatures throughout gonadal development, results consistent with previous slider turtle reports using semi-quantitative *in situ* hybridization analysis of gonadal expression (Fleming et al., 1999).

*Sf1* is present in the undifferentiated gonad at both male- and female-producing temperatures, and a regulatory relationship between *Sf1* and aromatase cannot be excluded. *Sf1* could regulate the onset of aromatase expression at the female-producing temperature, while other factors, including a positive feedback relationship with estrogen itself, could be responsible for increasing and then maintaining high aromatase levels. In this model, temperature-specific factors would also inhibit *Sf1* upregulation of aromatase at the male-producing temperature. However, our qPCR results indicate differential

patterns in abundance between *Sf1* and aromatase. *Sf1* and aromatase also exhibit sexually dimorphic patterns of specificity/organization of expression, even at phases of gonadal development when abundance is not different between the two temperatures.

Aromatase is expressed in the bipotential gonad at both temperatures, but shows an early difference in localization (Figure 4). Aromatase is more tightly localized around putative germ cells both prior to and during the sex-determining phase of gonadal development at female-producing temperatures than at male-producing temperatures. The pattern is established earlier and is more widespread across the gonad at the female-producing temperature, suggesting that differential aromatase localization preceding the TSP – particularly in the supporting cell lineage surrounding germ cells in the early bipotential gonad - may set the pattern for female-specific hormone profiles affecting ovarian differentiation later in development.

In contrast, *Sf1* expression is bipotential early in development but then becomes more sex-specific and localizes around putative germ cells at the male-producing temperature during sex determination (Figure 2). In mammals, *Sf1* is expressed in Sertoli as well as Leydig cells during testis differentiation (Ikeda et al., 1994), and its localization in the supporting cell lineage surrounding germ cells supports a conserved (non-steroidogenic?) function in slider turtle testis differentiation. The slider turtle, therefore, exhibits similarity to the mouse in terms of *Sf1* expression and testis development, but to chicken and other TSD reptile models in terms of aromatase expression and ovarian determination. This leads to the intriguing possibility that aromatase is not regulated by Sf1 in early slider turtle ovarian development. Two attractive candidates are *FoxL2* and *Lrh1*. *FoxL2* is a conserved granulosa cell marker

(Schmidt et al., 2004) also expressed in developing turtle ovaries (Crews et al., 2006; Loffler et al., 2003) that regulates aromatase in goats (Pannetier et al., 2006) and chickens (Govoroun et al., 2004; Hudson et al., 2005). Another possibility is *Lrh1*, a close relative of *Sf1* that is expressed in granulosa cells and has also been shown to regulate aromatase in the mouse ovary (Hinshelwood et al., 2003).

During gonadal differentiation after the TSP has closed, *Sf1* continues to be high in the developing testis. This expression seems to localize between the sex cords later in development, and while our experiment does not allow cell type identification, it is possible this pattern reflects steroidogenic regulation within the interstitial cell lineage. It is noteworthy, however, that light *Sf1* expression was detected in differentiating ovaries. This expression was observed not only throughout the medullary compartment as seen in chickens (Smith et al., 1999a) and sheep (Quirke et al., 2001), but also along the medullary/cortical boundary where steroidogenic enzymes including aromatase are expressed in fetal sheep ovaries (Quirke et al., 2001). These are the same two regions expressing aromatase in the slider turtle ovary, and may indicate Sf1 regulation of aromatase expression late in ovarian development.

During ovarian differentiation, aromatase expression as assayed by sectioned whole mount *in situ* hybridization is localized primarily in the medullary compartment but the intensity of signal is faint. This low level of expression is at odds with our qPCR results. Aromatase signal is reliably detected throughout putative ovaries at earlier stages of development (Figure 4G,H,I; Figure 6H; Figure 7E,F). The reduced sensitivity of the whole mount *in situ* method in the fully differentiated ovary (Figure 4J) probably results from differential aromatase probe penetration into ovarian versus testis tissue at this late

phase of differentiation. At the male-producing temperature, most aromatase expression is gone by the differentiation phase of testis development. However, pockets of expression localize to the interior of the seminiferous tubules, pointing to possible germ cell localization for aromatase in the differentiated testis. This expression pattern would agree with recent reports of aromatase expression in male germ cells in rats and humans (Carreau et al., 2001; Lambard and Carreau, 2005; Lambard et al., 2004).

Slider turtle sex determination is labile during the TSP, and normal gonadal development can be can be reversed by temperature shifts and by hormonal override of a temperature cue during the TSP (Wibbels et al., 1994). Opposing patterns of expression for *Sf1* and aromatase lead to opposite predictions during sex reversal – *Sf1* should decrease following feminizing treatment (M→F temperature shifts and estradiol treatment) and increase following masculinizing treatment (F→M temperature shifts and AI application), while aromatase should follow the opposite pattern.

Our results support these predictions. *Sf1* expression is redirected towards a diffuse female-like expression pattern following a shift from male- to female-producing temperature and exhibits the more intense, male-typical pattern following the opposing shift (Figure 2). Given the same treatment, aromatase expression is altered towards a more organized female-typical pattern following the M→F temperature shift while expression is scattered and diffuse after the shift from F→M temperature (Figure 4). These results affirm that 1) *Sf1* and aromatase exhibit specific sexually dimorphic patterns of expression that respond to temperature-based sex reversal, and 2) *Sf1* and aromatase localization patterns are not correlated during temperature-based sex reversal.

Our predictions are also supported when sex is reversed via the modulation of estrogen availability (Figures 6 and 7). Following exogenous estradiol application during the sex-determining phase at a male-producing temperature, *Sf1* localization patterns change to a low-level female-specific pattern. In contrast, aromatase expression intensified as expected following estradiol treatment, but the localization pattern was not the same as temperature-induced ovarian differentiation. In the slider turtle, as in the chicken (Smith et al., 1999a), aromatase expression is almost exclusively medullary in the differentiating ovary (Figure 4 F,J). The extension of aromatase expression into the cortical compartment late in ovarian differentiation (Figure 6 J) was unique to estrogen-created ovaries. Female-producing temperatures and estrogen production are linked in the slider turtle, but their mechanism of interaction is unknown. Along with regression of the medullary sex cords, proliferation of cells in the cortical region is a major component of ovarian differentiation in the slider turtle (Wibbels et al., 1993). Continued high levels of estrogen may be required to maintain ovarian development – particularly that of the cortical compartment – in turtles maintained at male-producing temperature. In addition, our data suggest that *Sf1* expression may not be required for aromatase maintenance during estrogen-induced ovarian development at a male-producing temperature.

Temperature and estrogen have a synergistic relationship in slider turtle sex determination (Bull et al., 1990; Crews et al., 1991; Wibbels et al., 1991b), and treating embryos already incubating at a female-producing temperature with exogenous estradiol creates hyper-feminized ovaries with enlarged cortical compartments. These "super-ovaries" give more support to the hypothesis that estrogen plays a critical role in the proliferation of cortical cells during ovarian development, and exhibit both altered expression of *Sf1* and particularly intense aromatase expression in the medullary

compartment (Figure 6 F,L). The intense aromatase expression was surprising given that aromatase expression in the medullary region was difficult to detect in fully differentiated ovaries using whole mount *in situ* hybridization. Interestingly, estrogen treatment has been shown to modulate basement membrane (BM) and extra-cellular matrix (ECM) composition in the prostate gland of estrogen-treated rats (Chang et al., 1999) and upregulate hepanarase, the enzyme that degrades hepanarase sulfate (a major polysaccharide of the BM and ECM) in MCF-7 breast cancer cells (Elkin et al., 2003). It is tempting to suggest that these estrogen-treated ovaries have modifications in the BM separating the medullary and cortical compartments of the gonad that allowed enhanced aromatase probe penetration into the interior of the ovary.

Reducing estrogen by blocking aromatase activity did not appreciably change localization patterns for either gene until late in gonadal differentiation (Figure 7). Previous work also showed a delay in *Sf1* response to AI treatment compared to temperature shifts or estrogen application (Fleming and Crews, 2001). Presumably, this delay is due to a carry-over effect from pre-existing estrogen in the gonad, as blocking aromatase activity only prevents new estrogen production.

Our results indicate that both *Sf1* and aromatase have important roles in slider turtle sex determination and differentiation. *Sf1* exhibits higher expression at male- than female-producing temperatures , indicating a conserved role in testis patterning as has been documented in mouse models. Aromatase is expressed in a female-specific manner. Both genes respond to sex-reversing treatments, but temperature and steroid treatment had different effects on sex-specific expression patterns during the sex determination phase of gonadal development. Despite its role as a regulator of steroidogenic enzymes

(including aromatase), our data do not add support to the hypothesis that *Sf1* regulates female-specific aromatase expression in the developing slider turtle ovary, but do support a critical role for estrogen in ovarian development.

Table 2-1. Effect of temperature

Table 1. Effect of temperature

| Group | Hatch sex ratio* |
|---|---|
| 26° C | 0 (65) |
| 31° C | 100 (114) |
| 26° → 31° C | 94 (38) |
| 31° → 26° C | 19 (43) |

*given as % female, (# individuals)

Table 2-2. Effect of chemical manipulation

Table 2. Effect of chemical manipulation

| Group | Hatch sex ratio* |
|---|---|
| 26° C ETOH | 0 (48) |
| 26° C E2 | 100 (53) |
| 31° C ETOH | 100 (25) |
| 31° C E2 | 100 (30) |
| 29.4° C ETOH | 82 (83) |
| 29.4° C AI | 12 (68) |

*given as % female, (# individuals)

Table 2-3. Housekeeping gene candidates and homology to *M. musculus*

Table 3. Housekeeping gene candidates and homology to *M. musculus*

| Gene | Clone length | Homology | Accession number |
|---|---|---|---|
| Beta actin | 396 | 86 | DQ848990 |
| 16S rRNA | 323 | N/A | AB090050 |
| UBED2 | 321 | 93 | DQ848992 |
| PP1 | 479 | 79 | DQ848991 |
| HPRT1 | 312 | 81 | DQ848993 |
| ALAS1 | 550 | 78 | DQ848994 |

Table 2-4. Real-time qPCR primer sequences

Table 4. Real-time qPCR primer sequences

| Gene | Amplicon (bp) | Primer sequence |
|---|---|---|
| SF1 | 103 | For 5’ - GGTGGATCGACAAGAGTTTGTGTG - 3’<br>Rev 5’ - TTTCTCCTGAGCATCCTTCGCC - 3’ |
| Aromatase | 95 | For 5’ - GCACATGGACTTTGCATCACA - 3’<br>Rev 5’ - GAACCATCATCTCCAACACACACTGGTTC - 3’ |
| PP1 | 95 | For 5’ - CAGCAGACCCTGAGAACTTCTTCCTG - 3’<br>Rev 5’ - GCGCCTCTTGCACTCATCAT - 3’ |

Figure 2-1. SF1 and aromatase whole mount *in situ* hybridization expression and probe specificity.

SF1 and aromatase are expressed along the gonad in a whole mount AKG (A, E) but not in DIG-labeled sense controls (C, G). Adjacent to each whole mount, a photomicrograph of a representative section from the pictured AKG show specific signal in gonads hybridized with DIG-labeled antisense probe (B,F) but not sense controls (D, H). Dashed lines outline sense-hybridized gonads (C,D; G,H). Pictured gonads were incubated at the female-producing temperature (FPT; 31°) and were dissected at Stage 17 (midway through the TSP). Whole mount gonads were sectioned at 40 μm thickness. Bar = 10 μm in B,D,F,H and 250 μm in A,C,E,G.

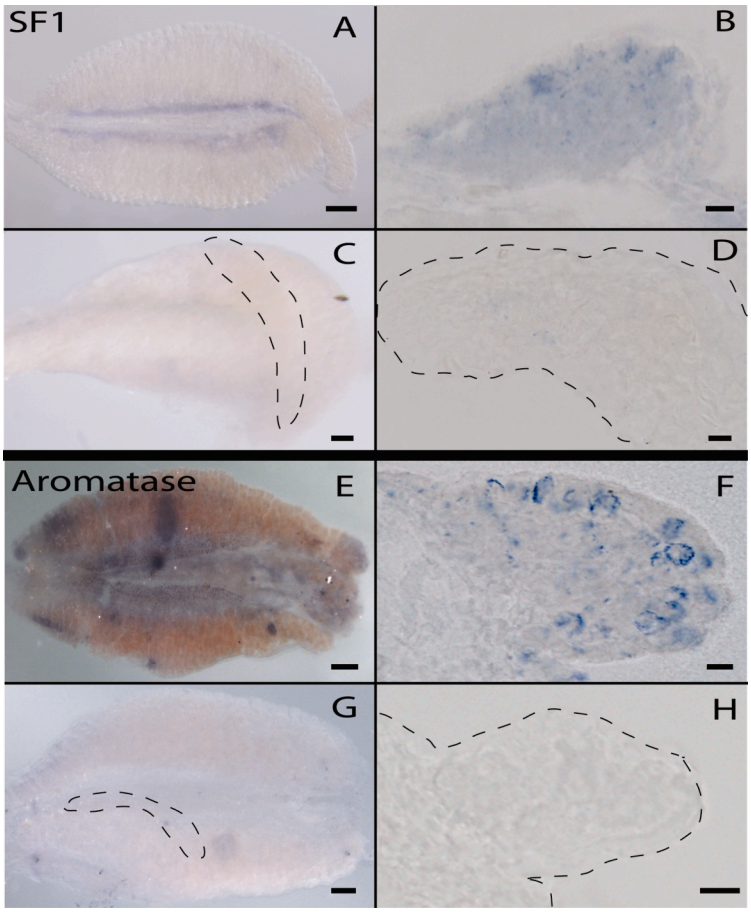

Figure 2-2. *Sf1* expression in the gonad changes over time and is altered following a sex-reversing temperature shift.

*Sf1* localization patterns differ by sex when analyzed at male-producing temperature (A-D) and female producing temperature (G-J) throughout the TSP. Embryos were shifted between incubation temperatures midway through the TSP (Stage 17). *Sf1* expression patterns are temperature-sensitive and show changes two and four stages after temperature shift from male- to female-producing temperatures (E,F) and vice versa (K,L). MPT = male-producing temperature (26° C), FPT = female-producing temperature (31° C). MPT → FPT shift = 26 → 31° C. FPT → MPT shift = 31 → 26° C. Arrow indicates cortical remnants in the temperature-shifted testis (L). Whole mount gonads were sectioned at 40 μm thickness. Bar = 10 μm.

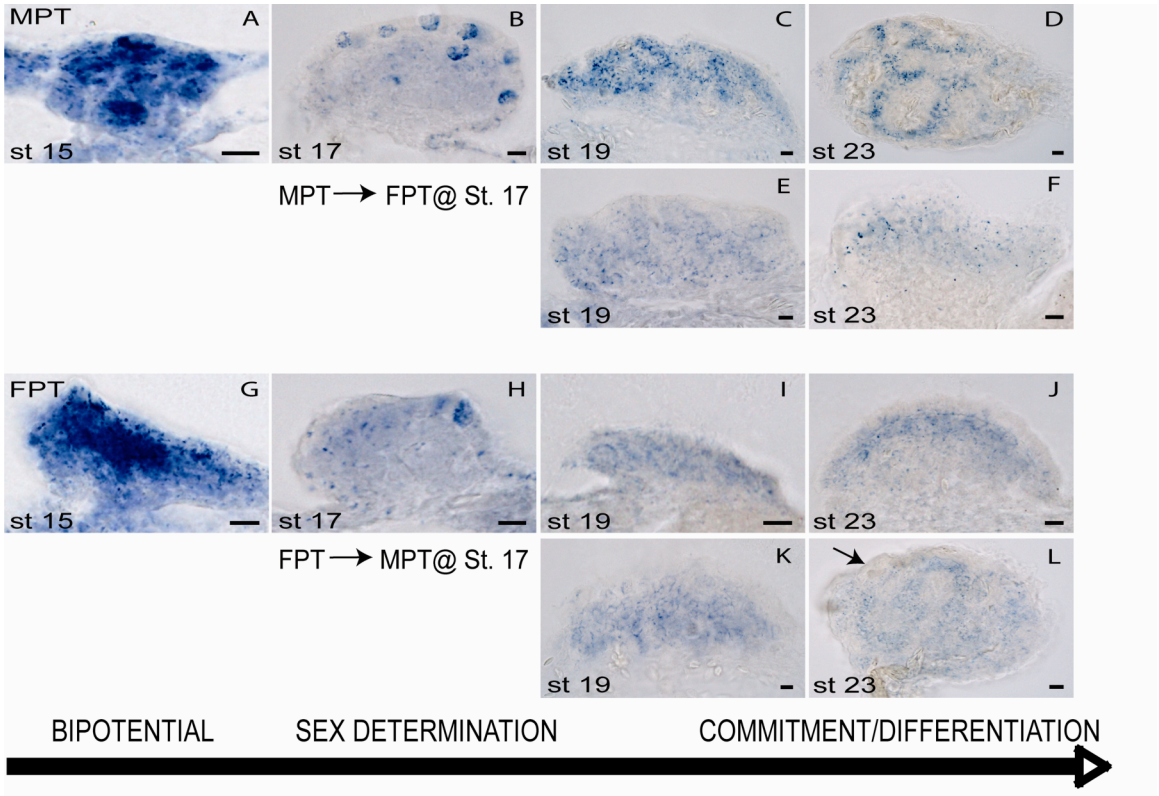

Figure 2-3. Higher magnification views of SF1 and aromatase expression during the TSP.

Photomicrographs show SF1 and aromatase localization at 40x and 100x magnification. Although the gonad is bipotential at this stage of development (Stage 17, midway through the TSP), gene expression patterns are already becoming sexually dimorphic. SF1 (A,B) at MPT and Aromatase (C,D) at FPT form ring-like structures around putative germ cells in the bipotential gonad. Arrows in A,C point to structure magnified in B,D. TSP = temperature-sensitive period. MPT = male-producing temperature (26° C). FPT = female-producing temperature (31°). Whole mount gonads were sectioned at 40 μm thickness. Bar = 10 μm.

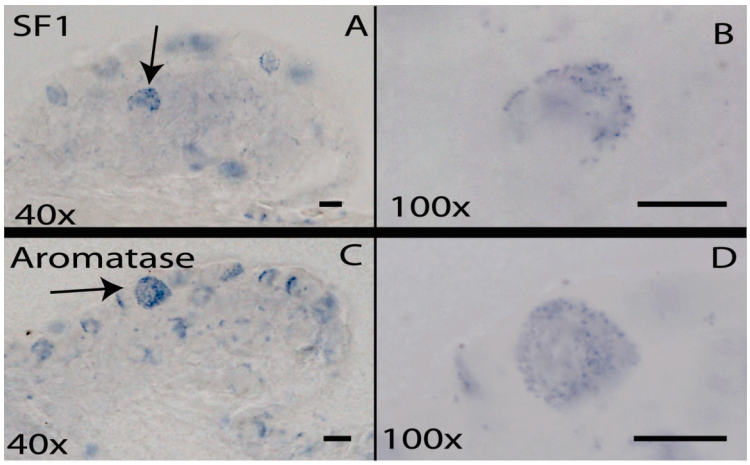

Figure 2-4. Aromatase gonadal localization is sexually dimorphic in the bipotential gonad and is altered following a sex-reversing temperature shift.

Aromatase localization is differential by sex throughout the three phases of gonadal development. Aromatase expression is more diffuse at male-producing temperatures (A-D) and more intensely localized at female-producing temperatures (G-J). Aromatase expression patterns are temperature-sensitive and are altered two and four stages after temperature shifts from male- to female-producing temperatures (E,F) and vice versa (K,L). MPT = male-producing temperature (26° C), FPT = female-producing temperature (31° C). Arrow indicates cortical remnants in the temperature-shifted testis (C,L). Whole mount gonads were sectioned at 40 μm thickness (A-C, E, G-I, K) except for Stage 23 gonads (D,F,J,L) which were sectioned at 25 μm thickness. Bar = 10 μm.

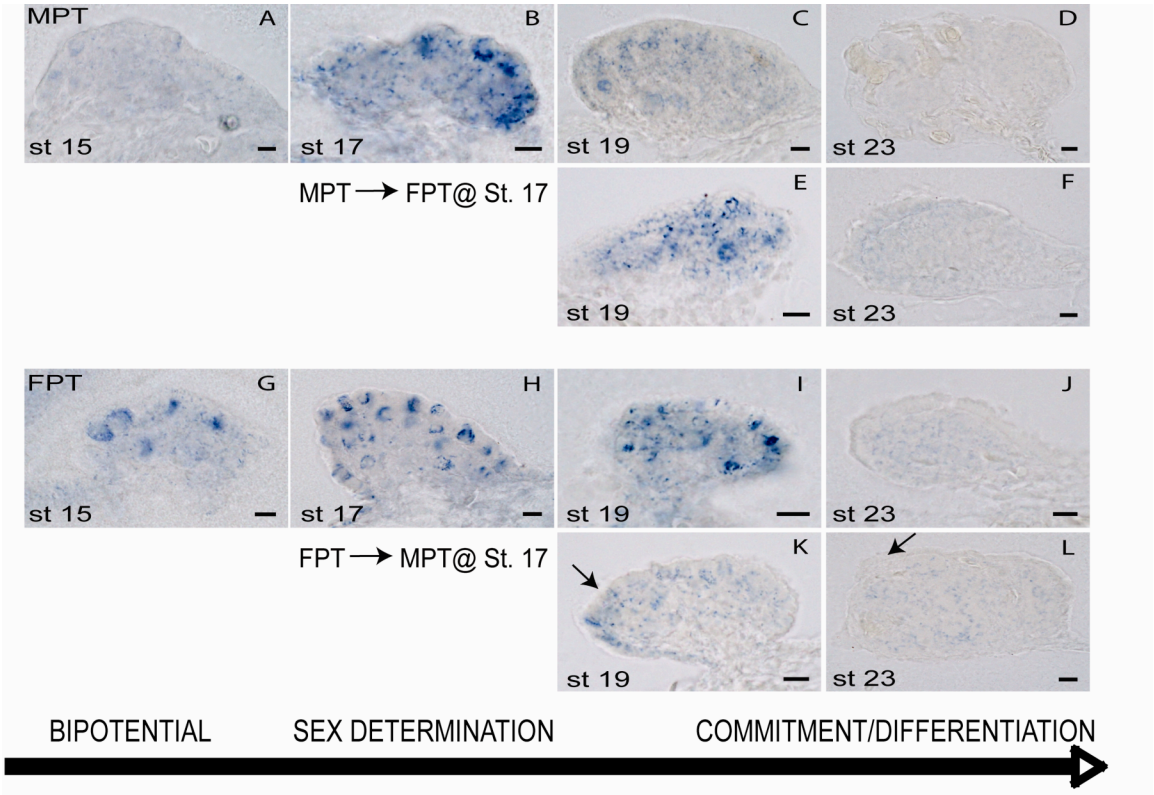

Figure 2-5. Sf1 gonadal transcript abundance in the gonad is higher at male-producing temperatures while aromatase is higher in putative ovaries.

*Sf1* and aromatase transcript was measured by real-time quantitative PCR (qPCR). Expression of *Sf1* was higher at male-producing temperature throughout the sex-determining (Stages 17-19) and gonadal differentiation (Stages 21-23) periods of development (A). Expression of aromatase was equivalent between temperatures at Stage 17, but then increased in a temperature- and sex-specific manner at female-producing temperatures (B). Individual data points are graphed onto panels A and B but may not be distinct due to similarity of measurements across replicates. Late in the MPT (Stages 21,23), aromatase was at the limit of detection for the assay, and was undetectable in two of three wells for each stage (B). Transcript abundance was measured on isolated gonad tissue from 30 – 50 pooled individuals/stage/temperature. Levels were normalized to PP1, a constitutively expressed housekeeping gene (see Experimental Procedures). Aromatase qPCR results were also analyzed by expressing each normalized value as % maximum of the highest level of expression for each temperature (C). Expression at MPT was highest (100%) at the onset of the sex-determining phase of development when the gonad is still bipotential (Stage 17), while expression at FPT was highest (100%) late in ovarian differentiation (Stage 23). The relationship between *Sf1* and aromatase qPCR results was analyzed by expressing % maximum expression across each temperature (D). % maximum expression was calculated across both temperatures for each gene such that all *Sf1* values were expressed relative to MPT Stage 17 (highest level of *Sf1* expression = 100%) and all aromatase values were expressed relative to FPT Stage 23 (highest level of aromatase expression = 100%). These relative values were then expressed as the ratio (*Sf1*/aromatase). MPT = male-producing temperature (26° C), FPT = female-producing temperature (31° C).

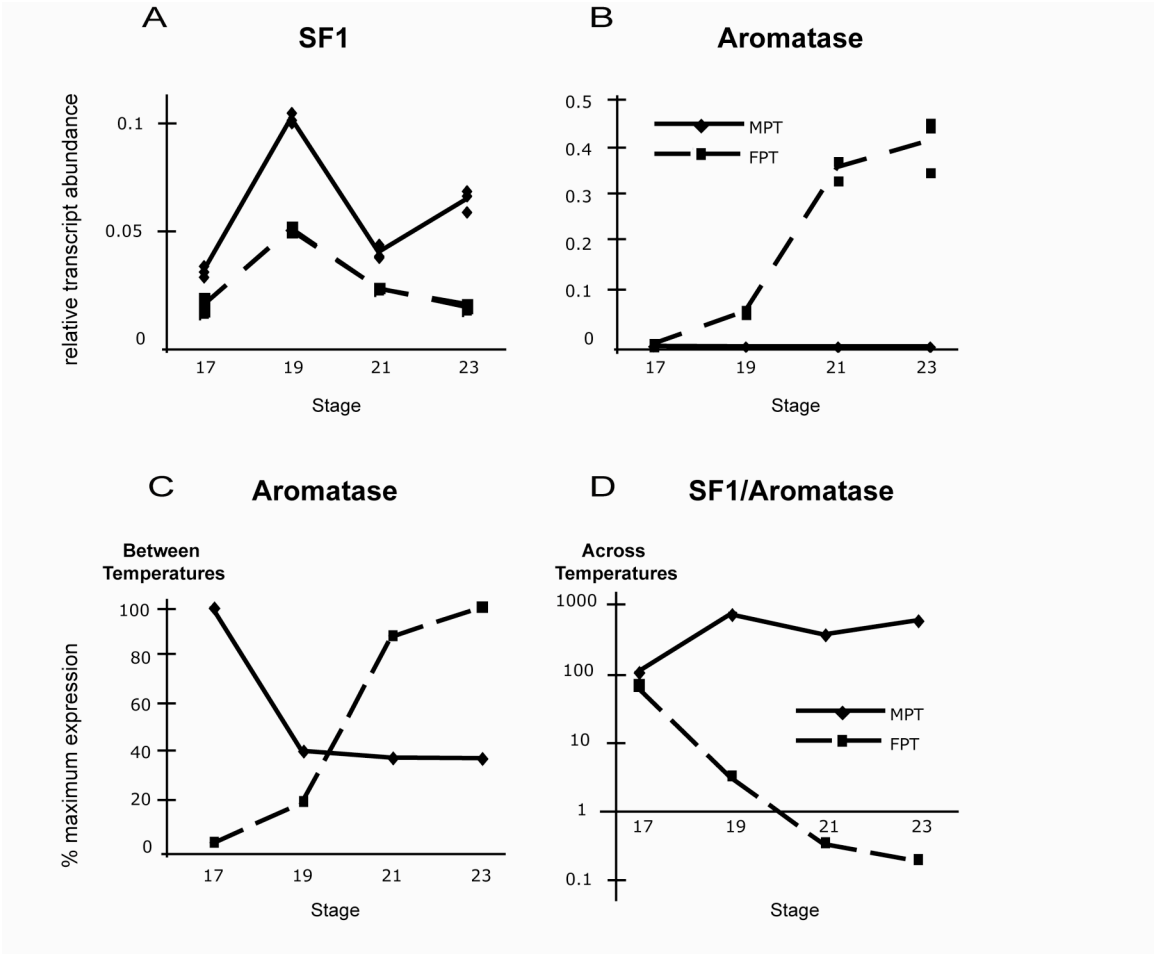
A
SF1
relative transcript abundance
0.1
0.05
0
17
19
21
23
Stage
B
Aromatase
0.5
0.4
0.3
0.2
0.1
0
MPT
FPT
17
19
21
23
Stage
C
Aromatase
Between Temperatures
% maximum expression
100
80
60
40
20
0
17
19
21
23
Stage
D
SF1/Aromatase
Across Temperatures
1000
100
10
1
0.1
MPT
FPT
17
19
21
23
Stage

Figure 2-6. Exogenous application of estradiol overcomes the male-producing temperature to produce ovaries and redirect patterns of *Sf1* and aromatase gonadal localization while treatment at the female-producing temperature creates a unique phenotype.

*Sf1* gonadal expression assumes a more diffuse, female-specific pattern of expression following application of estradiol to embryos incubating at male-producing temperatures (A-D). Aromatase expression is intensified following estradiol treatment, and spreads to the cortical compartment in the differentiating ovary at male-producing temperatures (G-J). At female-producing temperature temperatures, estradiol application results in enlarged cortical compartments as well as altered expression patterns for *Sf1* (E,F) and aromatase (K,L). MPT = male-producing temperature (26° C), FPT = female-producing temperature (31° C). Estradiol treatment occurred at the onset of the sex-determining phase of gonadal development (Stage 17), midway through the TSP. Control embryos were treated with EtOH vehicle (A, C, E for *Sf1*; G,I,K for aromatase). Whole mount gonads were sectioned at 40 μm thickness except I,J which were sectioned at 25 μm thickness. Bar = 10 μm.

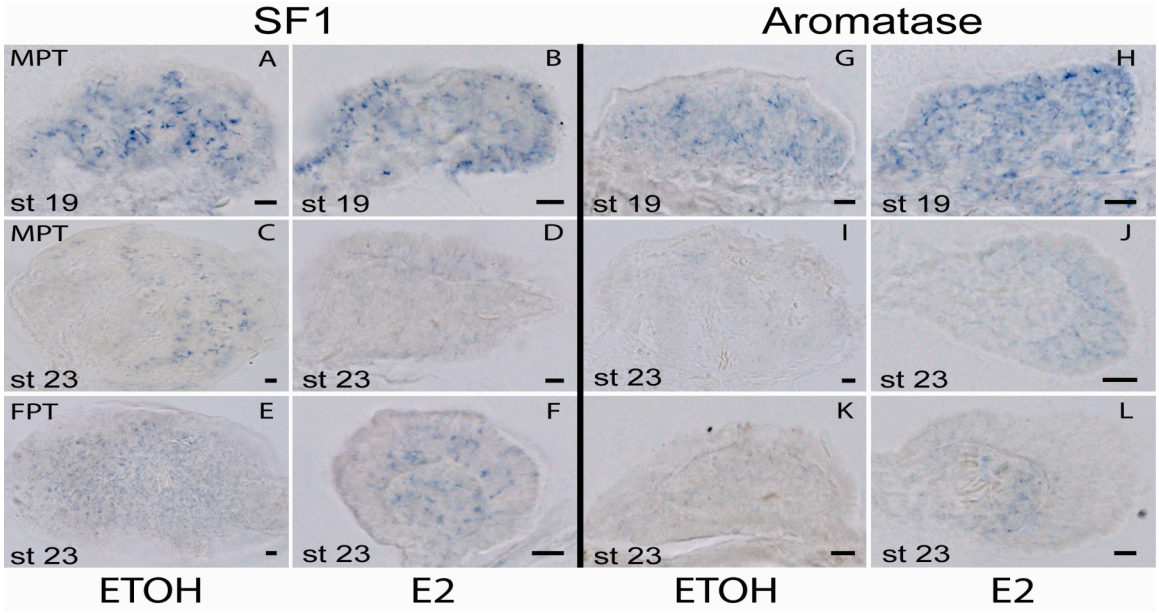

Figure 2-7. Inhibition of aromatase activity overcomes the female-biased temperature to produce testes and redirect patterns of *Sf1* and aromatase expression.

*Sf1* (A,B) and aromatase (E,F) exhibit delayed response to application of aromatase inhibitor (AI) to eggs incubating at a female-biased temperature. Each gene shows sex-specific changes to AI treatment (C,D for *Sf1*; G,H for aromatase) by the time of gonadal differentiation (Stage 23). FBT = female-biased temperature (29.4° C). AI treatment occurred at the onset of the sex-determining phase of gonadal development (Stage 17), midway through the TSP. Control embryos were treated with EtOH vehicle (A,C for *Sf1*; E,G for aromatase). Whole mount gonads were sectioned at 40 μm thickness. Bar = 10 μm.

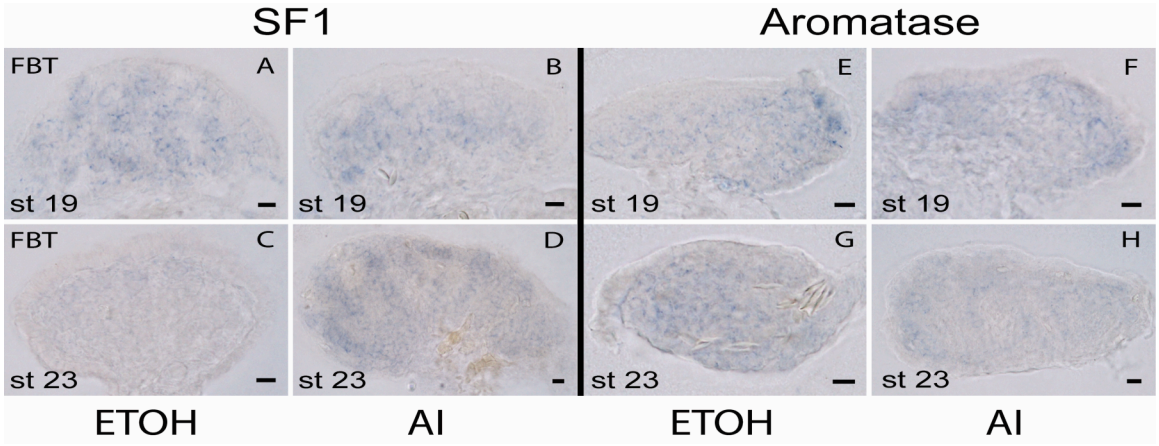

# Chapter 3: Steroid signaling system responds differently to temperature and hormone manipulation in the red-eared slider turtle (*Trachemys scripta elegans*), a reptile with temperature-dependent sex determination

## INTRODUCTION

Many egg-laying reptiles exhibit temperature-dependent sex determination (TSD) wherein sex is determined via a temperature cue (Bull, 1980). The red-eared slider turtle (*Trachemys scripta elegans*) is a TSD reptile where incubation temperature within a temperature-sensitive period (TSP) during the middle third of development determines gonadal sex (Wibbels et al., 1991b). In the slider turtle, warmer temperatures (31° C) produce female hatchlings, while cooler temperatures (26° C) produce male hatchlings. Intermediate temperatures produce mixed sex ratios, with a threshold temperature of 29.2° C producing 1:1 sex ratio (Crews et al., 1994).

Gonadal development in the slider turtle encompasses three major phases (Table 1). First is the formation of the bipotential genital ridge during which both sexes develop primitive medullary sex cords (Wibbels et al., 1991a; Yao et al., 2004). Next is the sex determination phase, during which the gonad becomes committed to either a testicular or ovarian fate. And finally, in the sex differentiation phase the sex cords develop into seminiferous tubules in the testis, while in the ovary the primitive sex cords degenerate into lacunae (Yao et al., 2004) and the cortical region (granulosa and germ cells) proliferates (Wibbels et al., 1991a). The TSP encompasses the bipotential and sex determination phases, and during this time gonadal sex outcome can be reversed by

shifting embryos from male- to female-, or female- to male-producing incubation temperatures (Wibbels et al., 1991a).

Gonadal sex determination in the slider turtle is also sensitive to steroid hormones, and the period of hormone sensitivity overlaps the TSP (Wibbels et al., 1991b). Estrogens exert a powerful effect on slider turtle sex determination, and application of exogenous estradiol ($E_2$) will feminize embryos incubating at male-inducing temperatures (Crews et al., 1991). In addition, modulating estrogen availability during this period by blocking aromatase, the enzyme that converts testosterone to $E_2$, results in male hatchlings at a female-biased temperature (Crews and Bergeron, 1994).

Androgens appear to play a more subtle but still important role in slider turtle sex determination. While exogenous androgen application will not override temperature if applied to eggs incubating at female-producing temperatures, treatment with the nonaromatizable androgen dihydrotestosterone (DHT) will masculinize embryos incubating at temperature regimens that would normally produce 1:1 sex ratios (Wibbels et al., 1992; Wibbels and Crews, 1995). Blocking reductase, the enzyme that converts testosterone to DHT, produces female hatchlings from a male-biased temperatures (Crews and Bergeron, 1994).

Steroid hormones act through binding to nuclear steroid hormone receptors, transcription factors that transduce steroid hormone effects on target gene transcription (Tsai and O'Malley, 1994), although nongenomic, rapid steroid hormone actions initiated at the cell membrane can also occur (Zhang and Trudeau, 2006). To the best of our knowledge, the possible role of these nongenomic mechanisms of action has not been

explored in TSD. We restrict our discussion here to estrogen receptor α (ERα) and estrogen receptor β (ERβ), and for androgens the androgen receptor (AR).

Considerable research has been conducted on differential estrogen synthesis in TSD reptiles (Smith et al., 1995; Jeyasuria and Place, 1998; Pieau et al., 1999; Willingham et al., 2000; Gabriel et al., 2001; Murdock and Wibbels, 2003; Ramsey et al., 2007), but comparatively little work has been done on the steroid hormone receptors themselves, although it is known that ERα is present in the gonads during development at both male- and female-producing temperatures (Bergeron et al., 1998).

Here we examine gonadal expression patterns for ERα, ERβ, and AR using real-time qPCR and *in situ* hybridization. We also report changes in steroid signaling in response to sex reversal via temperature and application of exogenous estrogen or aromatase inhibitor to eggs during the TSP.

## MATERIALS AND METHODS

### Tissue collection

Slider turtle eggs were purchased from Robert Clark (Clark Turtle Farms, Hammond LA) within one day of laying. Eggs were stored at room temperature until viability was established by candling. The eggs were then randomized and placed into incubators (Precision, Chicago, IL) at 26° C (male-producing temperature), 29.4° C (female-biased temperature), or 31° C (female-producing temperature). HOBO recording devices (Onset Computer Corporation, Bourne, MA) were used to monitor incubator temperature, and each incubator was also checked daily using calibrated shelf

thermometers. Egg trays were rotated daily within the incubator to avoid small temperature gradient effects.

Eggs were dissected at regular intervals to assess developmental stage (Yntema, 1968). Eggs were incubated at continual temperatures (26°, 31°, or 29.4° C) to assess sex/temperature-specific gene expression patterns. For the developmental analysis, adrenal-kidney-gonad (AKG) complex or gonad tissue was harvested at Stages 15, 17, 19, 21, and 23. In addition, subgroups of eggs received sex-reversing treatments at Stage 17, midway through the TSP (Ramsey et al., 2007). The treatment groups were as follows: (1) to assess the effect of temperature, eggs were shifted from male- to female-producing temperatures (26°→ 31° C) or from female- to male-producing temperatures (31°→ 26° C); (2) to assess the effect of exogenous estrogen application at a male-producing temperature, eggs were treated with 5 μg estradiol-17β (Sigma, St. Louis, MO) in 5 μl 95% EtOH or EtOH vehicle control; (3) to assess the effect of blocking estrogen production, eggs were treated with 100 μg of the aromatase inhibitor (AI) fadrozole (CGS16949A, Ciba-Geigy, Summit, NJ) in 5 μl 95% EtOH or EtOH vehicle control. Eggs assigned to the AI treatment (and EtOH controls) were incubated at the intermediate temperature of 29.4° C, a temperature that produces a female-biased sex ratio. AKG tissue from treated eggs was dissected at Stages 18, 19 and 23.

Gonad tissue destined for quantitative real-time PCR (qPCR) was rapidly dissected and stored in RNA Later (Ambion, Austin, TX) overnight at 4° C and then stored at -80° C or placed directly into Promega RNAgents Total RNA Isolation kit denaturing solution and stored at -80° C until total RNA was extracted (see below). AKG tissue destined for whole mount *in situ* hybridization was fixed overnight in 4%

PFA and then sequentially dehydrated with MeOH:PBTX solutions, ending in 100% MeOH for storage at -20° C. For each group, a subset of eggs was allowed to develop through hatching and was sexed by gross morphology of the gonad (see Ramsey et al., 2007 for hatchling sex ratios).

**Estrogen Receptor β gene cloning**

A nested degenerate cloning strategy was used to clone slider turtle ERβ gene. Human ERα and ERβ sequences were aligned using MacVector (Accelrys, Inc., San Diego, CA) software program to identify regions of sequence divergence between the two isoforms. Sequence spanning the variable hinge and ligand binding domains was chosen for primer design. Two sets of degenerate primers (Table 1) were designed in ERβ-specific gene regions using the CODEHOP (COnsensus-DEgenerate Hybrid Oligonucleotide Primer; http://blocks.fhcrc.org/codehop.html) website tool. Consensus sequences were derived from aligned human, rat, mouse, and chicken ERβ protein sequences. The first, outer cloning PCR reaction used single-stranded cDNA derived from adult slider turtle testis. The second, inner cloning PCR reaction used 1$^{st}$ round product as target. A 548 bp ERβ clone was isolated and ligated into pCR 4-TOPO vector (Invitrogen, Carlsbad, CA) according to the manufacturer's protocol. Sequence identity was confirmed by sequencing (see below for Accession number). PCR parameters were as follows: 1$^{st}$ (outer) round - 1 denaturing cycle (1 min at 94° C) followed by 35 amplification cycles (45 sec at 94° C, 2 min at 61° C, and 1:30 min at 72° C) and 1 final elongation cycle (10 min at 72° C. 2$^{nd}$ (inner) round - 1 denaturing cycle (1 min at 94° C) followed by 30 amplification cycles (45 sec at 94° C, 1:30 min at 61° C, and 2 min at 72° C and a final 10 min elongation cycle (72° C).

The cloning of slider turtle ERα has been described (Bergeron et al., 1998). AR was cloned previously (D. Crews and J.K. Skipper, unpublished data), however the cloning primers are reported in Table 1.

**Probe preparation**

DIG-labeled slider turtle ERα (596nt; Accession **DQ848987**), ERβ (601nt; Accession **DQ848988**), and AR (448nt; Accession **DQ848989**) antisense and sense (control) probes were transcribed using Megascript High Yield Transcription kit (Ambion, Austin, TX) with 33% labeled digoxigenin-11-UTP (Roche, Indianapolis, IN) and 67% unlabeled UTP, following the manufacturer's protocol. Probe integrity and abundance were assessed through gel electrophoresis. For each gene, the same probe was used in both Northern and whole mount *in situ* hybridization experiments.

**Northern hybridization**

For preparation of Northern blots, total RNA was extracted from an adult slider turtle testis as well as pooled (20-50 individuals/sample) AKG tissue incubating at male- and female-producing temperatures at Stages 15, 17, 19, 21, and 23. RNA was extracted using Promega RNAgents Total RNA Isolation kit (Promega, Madison, WI) according to the manufacturer's protocol. 25 μg of testis or AKG total RNA, or Ambion Millenium marker RNA (5 μg) was loaded/lane and transferred onto BrightStar-Plus membrane (Ambion, Austin, TX) using Ambion's NorthernMax kit following the manufacturer's protocol.

Blots were hybridized overnight at 65° C (AR) or 68° C (ERα, ERβ) with either DIG-labeled AR (100 ng/ml), ERα (5 ng/ml), or ERβ (5 ng/ml) using Ambion Ultrahyb solution. Hybridization and washing steps were performed following Ambion's NorthernMax protocol. CDP-Star chemiluminescence (Roche, Indianapolis, IN) was used to detect DIG-labeled probe binding following the manufacturer's protocol.

**Real-time quantitative PCR (qPCR)**

All qPCR assays were run on single-stranded cDNA synthesized from pooled gonad (20-50/sample) total RNA. The gonad is a relatively small part of the heterogenous AKG tissue, so to avoid adrenal- or kidney-specific gene expression confounding gonadal expression analysis, gonads were rapidly dissected away from the surrounding tissue for processing. Total RNA was then extracted using RNAgents Total RNA Isolation kit (Promega, Madison, WI) following the manufacturer's protocol. Total RNA abundance and purity was assessed through spectophotometry readings at 260 nm and 280 nm.

Prior to cDNA synthesis, total RNA was DNase-treated using Turbo DNA-Free kit (Ambion) following the manufacturer's protocol. Single-stranded cDNA was then reverse-transcribed at a concentration of 1 μg total RNA/20 μl synthesis reaction primed with oligo-dT and random hexamers using Superscript First Strand Synthesis for RT-PCR kit (Invitrogen) according to the manufacturer's protocol for real-time PCR template synthesis.

Real-time primer sequences and amplicon size are described in Table 1. Estrogen receptor α, ERβ, and AR PCR primers were designed using MacVector software program. All primers were engineered to cross exon boundaries (estimated from human gene structure) to eliminate possible signal contamination from genomic DNA. Specificity of target was verified by gel electrophoresis. Housekeeping gene PP1 (protein phosphatase 1 gamma) real-time PCR primers have been previously described (Ramsey, et al., 2007).

Real-time qPCR experiments were conducted on ABI Prism 7900 real-time PCR machine (Applied Biosystems). Each sample was run in triplicate. Each well comprised a 10 μl reaction containing 2 μl (ERα, AR, PP1) or 3 μl (ERβ, PP1) cDNA template, 5 μl 2x Platinum SYBR Green qPCR SuperMix UDG (Invitrogen), and 5 pmol (ERα, ERβ, AR) primers or 3 pmol (PP1) primers. Real-time qPCR parameters were 2 min at 50° C, 2 min at 95°C for denaturing, followed by 40 cycles at 15 sec 95° C, 15 sec 60° C, and 15 sec 72° C. For each gene, primers gave no specific signal in no-template and no-RT control wells, and dissociation curve analysis confirmed target specificity in experimental wells.

Gene expression levels were assessed using SYBR green detection chemistry with Applied Biosystems Sequence Detection System software (SDS 2.2.1). Relative quantification was performed by a modified comparative critical threshold (CT) method that corrects for different PCR amplification efficiencies among primer pairs (Simon, 2003). PP1 housekeeping gene was used to normalize qPCR results as described (Ramsey, et al., 2007). Normalized gene expression is given as MNE (mean normalized expression) = $(E_{pp1}\text{^meanCT}_{pp1})/(E_{ER\alpha,\ ER\beta,\ or\ AR}\text{^meanCT}_{ER\alpha,\ ER\beta,\ or\ AR})$, where E= PCR

efficiency (E=10^-(1/slope)) (Pfaffl, 2001) and meanCT is the average CT across the three replicates. For each gene, values were then calibrated to Stage 17 FPT.

**Whole mount in situ hybridization**

Whole mount *in situ* hybridization (ISH) experiments were conducted using AKG tissue from 4 embryos/stage/treatment (N= 88 embryos/gene). ISH experiments were conducted as described (Ramsey, et al 2007). Briefly, slider turtle AKG complexes were hybridized overnight at 65° C in hybridization solution containing 4-8 μl of DIG-labeled antisense (or sense control) probe. After washing, AKG complexes were then incubated overnight (4° C) with anti-digoxigenin-AP antibody (Roche) preabsorbed with embryo powder derived from whole body and AKG embryonic turtle tissue. BM purple AP substrate (Roche) was used for colorimetric detection. Detection time was optimized for each gene/stage and allowed to proceed until visible signal could be detected (4 to 7 hours). For each gene, all groups within an ISH were stopped simultaneously. Following detection, AKG complexes were fixed in 4% PFA and stored in glycerol (4° C) until processed.

Representative whole mount-hybridized AKG complexes from Stage 15 male- and female-producing embryos are shown in Figure 3. All three steroid hormone receptors are expressed at both temperatures, so we opted to section the whole mount AKGs in order to detect temperature-specific changes in expression within the gonad itself. In addition, ERβ is expressed in relatively few cells during key stages of slider turtle development (see higher magnification inset, Figure 3B and E), making gonadal expression difficult to assess from external views. Therefore, whole mount tissue was cryoprotected (30% sucrose/PBS), embedded in either TFM (Triangle Biomedical

Services, Inc., Durham, NC) or Neg50 (Richard-Allen Scientific, Kalamazoo, MI) and then sectioned at 40 μm on a Microm HM 500 OM cryostat (Microm International, Germany). All section photomicrographs were taken on a Nikon Eclipse 80i microscope using NIS-Elements BR 220 visualization software with LUT settings 125-black, 255-white, and gamma .76 except for AR Stage 15 (Figure 5G) taken at 90-black, 255-white, and gamma .76. Whole mount photomicrographs were taken on an Olympus SZX12 dissecting scope.

## RESULTS

### Northern blot hybridization

A Northern blot containing adult testis and embryonic AKG total RNA was probed sequentially with DIG-labeled AR and ERα. Band sizes for each probe were consistent across all developmental stages 15, 17, 19, 21, and 23 and at both male- and female-producing temperatures. Representative Stage 17 AKG results are shown in Figure 1A. In both adult testis and embryonic AKG, AR hybridized to a major band at approximately 9.5Kb and an alternate transcript at approximately 0.75Kb (Figure 1A). In embryonic AKG, ERα hybridized to a single ~7Kb band (Figure 1A), while adult testis tissue produced the 7Kb band and a testis-specific alternate transcript at ~1Kb (alternate transcript shown in Figure 1B).

Estrogen receptor β was cloned subsequent to the AR and ERα Northern blot shown in Figure 1A, and tissue was not available to repeat the developmental Northern for ERβ. However, to establish that our ERα and ERβ probes were isoform-specific and did not cross-hybridize, we probed a Northern blot loaded with adult slider turtle testis

total RNA (Figure 1B). Results were consistent with the earlier blot for ERα (bands at ~7kb and a testis-specific alternate transcript at ~1kb). Estrogen receptor β hybridized to a single band at approximately 4Kb, with faint second transcript at 2Kb.

**Developmental qPCR measurement of isolated gonad tissue**

Estrogen receptor α, ERβ, and AR transcript levels were measured in developing gonads at male- and female-producing temperatures using real-time qPCR (Figure 2). Estrogen receptor α and ERβ exhibit distinct patterns of expression throughout development, while ERα and AR patterns are similar.

Estrogen receptor α transcript levels are equivalent at male- and female-producing temperatures midway through the TSP (Stage 17; Figure 2A). Late in the TSP as gonadal sex is being determined at the female-producing temperature (Stage 19), ERα levels spike at both temperatures, but the peak at female-producing temperature is 5-fold greater than at the male-producing temperature. As development continues, ERα levels decline in both sexes and are maintained at similar levels throughout gonadal differentiation (Stages 21 and 23).

Estrogen receptor β transcript abundance is unchanging from the middle of the TSP (Stage 17) through sex determination and the onset of gonadal differentiation at both temperatures (Stages 19 and 21), although it is always slightly higher at the female-producing temperature (Figure 2B). Estrogen receptor β exhibits a female-specific increase (3-fold higher at the female-producing temperature than at the male-producing temperature) as ovarian differentiation is completed at Stage 23.

Androgen receptor expression is similar to ERα (Figure 2C). Levels are initially equivalent during the TSP (Stage 17), but increase late in the TSP (Stage 19). As with ERα, the increase in AR at the female-producing temperature is greater than at the male-producing temperature. Androgen receptor expression subsequently drops in both temperatures/sexes as gonadal differentiation commences (Stage 21) although both exhibit a slight increase as differentiation is completed (Stage 23).

**Developmental *in situ* hybridization**

All three steroid hormone receptors are present in the gonad at both temperatures throughout the bipotential, sex determination, and sex differentiation phases of gonadal development. Whole mount *in situ* hybridization results on AKG tissue early in the TSP (Stage 15) for each receptor are shown in Figure 3. For all three phases of gonadal development (represented by Stages 15, 17, 19, 23), internal localization patterns within the gonad are depicted in sectioned whole mounts for ERα (Figure 4), ERβ (Figure 5), and AR (Figure 6). For each gene, localization patterns are roughly equivalent between temperatures during early development (bipotential and sex determination phases), and exhibit sexually dimorphic patterns only after morphological differentiation was evident (sex differentiation phase).

***Estrogen Receptor α***

Estrogen receptor α is strongly expressed at both temperatures at the onset of the TSP (Stage 15; Figure 3A and D; Figure 4A and G), and expression persists through the middle of the TSP (Stage 17; Figure 4B and H). At both temperatures, ERα is localized into circular patterns that may represent expression in the supporting cell lineage around

putative germ cells, as well as scattered punctate expression throughout the medullary region of the gonad. Late in the TSP as the gonad begins to differentiate (Stage 19; Figure 4C and I) ERα expression coalesces along the developing medullary sex cords at the male-producing temperature, while maintaining a more diffuse, scattered medullary expression coupled with occasional circular patterns at the female-producing temperature. Later in development (Stage 23; Figure 4D and J), ERα is light but detectable along the developing seminiferous tubules at the male-producing temperature, while expression remains primarily medullary in ovaries produced at the female-producing temperature.

***Estrogen Receptor β***

Early in the TSP (Stage 15; Figure 3B and E and inset; Figure 5A and G), ERβ is generally confined to circular patterns, although nonspecific expression scattered throughout the gonad can also be seen. As the TSP progresses (Stage 17; Figure 5B and H), ERβ predominately maintains the more scattered-type expression pattern, although occasional circular structures remain at both temperatures (data not shown). As the gonads begin to differentiate late in the TSP (Stage 19; Figure 5C and I), ERβ is expressed along the developing seminiferous tubules at the male-producing temperature, and is primarily localized to the medullary compartment in the developing ovary at the female-producing temperature, although expression occasionally extends into the cortical compartment (data not shown). Later in development (Stage 23; Figure 5D and J), ERβ continues to be expressed along the testis cords and throughout the differentiating ovary, although one of four sectioned ovaries did not show detectable signal (data not shown).

### *Androgen Receptor*

AR is expressed in the bipotential gonad at both temperatures (Stage 15; Figure 3C and F; Figure 6A and G), and continues to be expressed throughout the gonad at both temperatures through the middle of the TSP (Stage 17; Figure 6B and H). Expression is mostly seen scattered throughout the gonad, but at both temperatures can also be observed in circular patterns (data not shown). Late in the TSP, AR expression is predominantly medullary (Stage 19; Figure 6C and I). At the male-producing temperature, AR is expressed along the developing sex cords, while at the female-producing temperature AR is expressed throughout the medullary region in both scattered and circular patterns. In the differentiated testis (Stage 23; Figure 6D), AR is expressed within the seminiferous tubules. Androgen receptor expression is detectable in differentiated ovaries (Figure 6J), but this expression is disorganized and scattered throughout the medullary compartment.

## Response to temperature

Temperature shifts during the TSP reverse gonadal sex outcome in slider turtle embryos. We assayed ERα (Figure 4), ERβ (Figure 5), and AR (Figure 6) expression following temperature shifts at Stage 17 from male- to female-producing temperature (MPT→FPT) as well as from female- to male-producing temperature (FPT→MPT). Gonads were sampled at Stages 19 (while reversal is underway) and 23 (when the shifted gonad has committed to final sex outcome). For all three receptors, temperature shifts altered localization patterns during sex reversal. Following MPT→FPT, ERα and AR are maintained in the medullary region while ERβ could only be detected in the cortical

compartment. Following FPT→MPT, ERα and ERβ became confined to the cortical compartment while AR medullary organization was altered.

***Estrogen Receptor α***

Two developmental stages after the MPT→FPT shift (Figure 4E), some cortical development is already evident, indicating the gonad has begun to switch to an ovary-producing trajectory. Most ERα expression is medullary and remains prominent along the sex cords. Later in development (Stage 23; Figure 4F) ERα expression is medullary and similar to an un-shifted ovary (Figure 4J and F), although expression tends to coalesce along the medullary/cortical boundary rather than throughout the entire medullary region.

Following the corresponding FPT→MPT shift, ERα medullary expression is reduced compared to unshifted control two stages after the shift (Figure 4I and K), and what expression does remain tends to be located in the cortical region. By Stage 23, ERα displays testis-typical patterns and is expressed along the developing seminiferous tubules (Figure 4L).

***Estrogen Receptor β***

Estrogen receptor β medullary expression is reduced two stages after the MPT→FPT shift compared to the un-shifted control (Stage 19, Figure 5C and E), although some ERβ expression remains in the cortical compartment. At Stage 23, ERβ is expressed along the medullary/cortical boundary of the shifted ovary (Figure 5F).

Estrogen receptor β medullary expression is also reduced compared to the un-shifted control two stages following the corresponding FPT→MPT shift (Stage 19; Figure 5I and K). As with the MPT→FPT treatment, any ERβ expression that remains is generally confined to the more cortical portion of the gonad. Later in development, ERβ exhibits male-typical expression along the developing seminiferous tubules of the shifted testis (Stage 23; Figure 5L).

***Androgen Receptor***

Two stages after the MPT→FPT shift, AR expression exhibits a striping localization pattern similar to that seen in the un-shifted controls (Stage 19; Figure 6C and E) although the sex cords seem less organized in the shifted gonads. By Stage 23, AR is expressed in a more diffuse pattern in the differentiating ovary, and expression tends to localize more toward the medullary/cortical boundary than ovaries produced under constant incubation at the female-producing temperature (Figure 6F and J).

Androgen receptor expression is mostly contained within the medullary compartment two stages after the opposing FPT→MPT shift (Stage 19; Figure 6I and K). Androgen receptor is coalesced into circular structures as well as exhibiting light, punctate signal scattered throughout the gonad. As development progresses to a differentiated testis (Stage 23; Figure 6L), AR is expressed within the developing seminiferous tubules.

**Response to exogenous estradiol at a male-producing temperature**

During the TSP, application of exogenous estrogen to slider turtle eggs incubating at male-producing temperatures results in 100% female hatchlings (Crews et al., 1991, 1996). Estrogen receptor α, ERβ, and AR expression patterns were assayed following $E_2$ treatment at Stage 17. Gonads were sampled during sex reversal (Stages 18, 19) and after estrogen-induced ovarian differentiation (Stage 23). Localization patterns for all three receptors were altered following $E_2$ (Figure 7). Both ERα and ERβ became primarily localized in the cortical region, but the response in ERα expression preceeded that of ERβ. Androgen receptor medullary expression was also reduced following $E_2$ treatment, but this response was transient.

***Estrogen Receptor α***

Expression of ERα responds rapidly to $E_2$ treatment. By the first timepoint assayed (Stage 18, Figure 7A and D), ERα expression is reduced throughout the medullary region compared to EtOH-treated control gonads, and most remaining signal localizes to the developing medullary/cortical boundary. This altered localization pattern continues as sex reversal progresses (Stage 19, Figure 7B,E). In the differentiated ovary (Stage 23, Figure 7F), ERα expression is maintained in the medullary region, but also extends into the cortex. In the EtOH-treated controls, ERα displayed testis-typical expression along the developing seminiferous tubules (Figure 7A,B,C).

***Estrogen Receptor β***

Unlike ERα, ERβ expression intensity is not rapidly reduced following $E_2$ treatment compared to EtOH-treated controls after exogenous estradiol application (Stage

18; Figure 7G and J). However, expression in $E_2$-treated gonads has become much less organized along medullary cord structures. By two stages after $E_2$ application, (Stage 19; Figure 7H and K) light medullary signal can be detected along the degenerating sex cords, and expression now extends into the developing cortical compartment. By Stage 23 (Figure 7L), ERβ is expressed in the cortex and along the medullary/cortical boundary of $E_2$-treated ovaries (although some individuals continue to show medullary expression as well; data not shown).

***Androgen Receptor***

Androgen receptor expression is not altered one stage after treatment with $E_2$ (Stage 18; Figure 7M and Q). However, by two stages after application, AR expression differentially localizes to the medulla/cortex boundary in estradiol-treated gonads (Stage 19; Figure 7N and R). In differentiated gonads, (Stage 23; Figure 7O and S), AR is expressed throughout the medullary compartment as well as along the medullary/cortical boundary in $E_2$-treated ovaries. In EtOH controls, AR is expressed in male-typical pattern within the developing seminiferous tubules.

**Response to aromatase inhibitor treatment**

Application of aromatase inhibitor (AI) midway through the TSP results in male hatchlings from a female-biased temperature (Crews and Bergeron, 1994). After AI treatment at Stage 17, we assayed ERα, ERβ, and AR expression patterns at Stages 19 and 23. While ERα and ERβ did not exhibit localization changes following AI treatment until after gonadal morphological differentiation was evident, AR localization was altered during sex reversal and before obvious testis differentiation.

***Estrogen Receptor α***

Both AI- and EtOH-treated gonads show some cortical development two stages after AI application (Stage 19; Figure 8A and C), and ERα expression, while primarily light and medullary, can extend up into the cortical compartment regardless of treatment. Later in development, AI-treated testes express ERα along the seminiferous tubules, while EtOH-treated ovaries show light and diffuse ERα expression throughout the medullary compartment (Stage 23; Figure 8D and B).

***Estrogen Receptor β***

Two stages after AI-treatment (Stage 19, Figure 8E and G), ERβ expression is barely detectable in both AI- and EtOH-treated gonads, but when it is present, ERβ is scattered throughout the medullary region. At Stage 23, AI-created testes show ERβ expression along the seminiferous tubules, while EtOH-treated ovaries uniformly showed very light medullary/undetectable signal (Figure 8F and H).

***Androgen Receptor***

Two stages after treatment, AR expression intensity is not markedly different between AI- and EtOH-treated gonads, but there is a change in localization pattern (Stage 19, Figure 8I and K). Aromatase inhibitor-treated gonads exhibit very light, scattered medullary expression, while EtOH-control gonads exhibit circular patterns of AR localization towards the cortical region of the gonad. At Stage 23, AI-treated testes

express AR within the developing seminiferous tubules, while expression is diffuse throughout EtOH-treated ovaries (Figure 8J and L).

## DISCUSSION

Sex steroid hormone action requires the presence of a protein receptor in target tissues. In the slider turtle, ERα, ERβ, and AR are expressed in the gonad throughout development at all incubation temperatures, indicating a role for steroid signaling pathways in both testis and ovarian development. However, disruption of normal gonadal development with sex-reversing treatments produces strikingly different patterns of steroid receptor expression, particularly for ERα.

To establish the expression patterns of the sex steroid signaling pathway during steady male- and female-development, we assayed ERα, ERβ, and AR transcript levels via qPCR and *in situ* hybridization throughout gonadal development. By qPCR, ERα and AR exhibit similar expression patterns. Both show a spike in expression during a key phase of gonadal development late in the TSP. As this spike occurs, the TSP is closing for the female-producing temperature, but sex is still somewhat labile at the male-producing temperature (Wibbels et al., 1991a). For both, the peak in expression is higher at the female-producing temperature (Figure 2). Interestingly, female-specific increases in aromatase expression are also evident at this stage (Ramsey et al., 2007). Higher gonadal estrogen levels coupled with increased ERα and AR expression may indicate greater steroid sensitivity at the female-producing temperature just as ovarian fate is determined and differentiation commences. However, while aromatase levels continue to increase as the ovary develops (Ramsey et al., 2007), both ERα and AR levels drop back

to earlier levels and do not exhibit any sex-specific differences in transcript levels during gonadal differentiation.

In contrast, ERβ expression levels are unchanged as ovarian fate is determined. Levels are steady throughout the TSP and sex determination phase of gonadal development at both temperatures. However, late in ovarian differentiation, ERβ exhibits a female-specific increase in expression. Ovarian differentiation in the slider turtle is marked by a proliferation of granulosa cells and germ cells (Wibbels et al., 1991a), and ERβ is expressed in granulosa cells in the developing mouse ovary (Jefferson et al., 2000). It is possible our qPCR measures reflect granulosa cell proliferation in the developing ovary. This increase occurs well after ovarian commitment and female-specific increases in aromatase transcript (Ramsey et al., 2007), indicating that ERβ is probably only indirectly responsive to increased estrogen production and is downstream in the ovarian differentiation cascade.

Several genes known to be important in sex determination/differentiation across vertebrate groups such as *Sox9*, *Dmrt1*, *Sf1*, *FoxL2*, and aromatase are differentially expressed in the slider turtle before the onset of obvious morphological sexual differentiation (Fleming et al., 1999; Kettlewell et al., 2000; Loffler et al., 2003; Ramsey et al., 2007; Shoemaker et al., 2007). In contrast, under constant temperature regimens, ERα, ERβ, and AR do not exhibit early differences in gonadal localization across temperatures, and may be key in gonadal formation for both sexes, although as mentioned above, there is a quantitative female-specific increase in ERα and AR expression as ovarian fate is committed. This increase in ERα during ovarian determination was not evident in the whole mount *in situ* hybridization. Our qualitative

whole mount can illustrate localization patterns and detect changes in these patterns (ie – the shift in ERα expression out of the medulla and into the cortex following exogenous $E_2$ treatment), but is not an effective method for detecting quantitative changes in gene expression levels particularly across developmental stages. Because of developmental differences in tissue differentiation/permeability, each stage in a whole mount assay must be optimized for probe penetration into the gonad (see methods), therefore overall abundance cannot be compared across stages.

ERβ expression patterns were also not always consistent between qPCR and across whole mount *in situ* assays. The female-specific expression evident in the qPCR measurements was not consistently observed in differentiated ovaries via the *in situ* method. One of four sectioned 31° C (female-producing temperature) ovaries did not exhibit detectable ERβ expression, and all 29.4° C (female-biased temperature) EtOH-treated ovaries lacked signal (n=3, the fourth individual was a testis with male-typical ERβ signal along the sex cords; data not shown). This variability may result from individual variation in the timing of granulosa cell differentiation/proliferation in the developing ovary. However, ERβ expression was also noticeably light/absent in 29.4° C gonads earlier in development (Figure 8E and G). Estrogen receptor β may be below the limits of detection by *in situ* method in some ovaries and in undifferentiated gonads incubating at the female-biased temperature.

Androgen receptor is expressed in the medullary compartment of both sexes during the differentiation phase of gonadal development, and coalesces around the dominant medullary structure in each gonad (seminiferous tubules in testis, degenerating primitive sex cords/lacunae in ovary). Although we cannot definitively assign cell type,

AR is consistently found in the interior of the developing seminiferous tubules (Figure 6,7,8). This interior localization may indicate Sertoli cell expression and a role for androgens in organizing sex cords in the slider turtle. This pattern is in contrast to mammalian ontogeny, where AR protein is barely detectable in Sertoli cells in the rat (Majdic et al., 1995) and undetectable in sheep (Sweeney et al., 1997). Work with marsupials (Butler et al., 1998) demonstrate AR transcript in early gonads but did not reliably detect AR protein, indicating either differential assay sensitivity or post-transcriptional regulation of AR. Our assays examined mRNA expression, and gonadal AR protein could also be regulated post-transcription in the slider turtle. However, while mammalian testis formation is androgen-independent (Yeh et al., 2002), steroid hormones may be important for testis formation in the slider turtle. As mentioned earlier, exogenous DHT treatment creates male hatchlings from a threshold temperature (expected 1:1 sex ratio), and blocking the enzyme that converts testosterone into DHT sex-reverses embryos incubating at a male-biased temperature (Wibbels and Crews, 1995; Crews, 1998). Androgen receptor expression in the developing seminiferous tubules may provide the mechanism for androgen action in slider turtle testis development.

Because sex steroid receptor expression patterns were not markedly different between temperatures during the time of sex determination at constant temperature, we would predict no response (or late response) to sex-reversing temperature shifts until after morphological differentiation of the shifted gonad was obvious. However, all three receptors responded to temperature shifts and displayed altered localization patterns before differentiation to the destination sex had occurred.

Following the shift from male- to female-producing temperatures, both ERα and AR were expressed along the sex cords in the medullary compartment of the gonad, while ERβ medullary expression was reduced compared to unshifted controls. The strong ERα and AR signal may mean that both receptors retain male-typical cord localization two developmental stages after the shift, and that any alteration in steroid signaling towards ovarian development is well downstream from a temperature cue. However, ovarian formation in the slider turtle involves two developmental processes – degeneration of the medullary sex cords and proliferation of the cortical compartment (Wibbels et al., 1993), and both of these processes may be mediated by increased estrogen production at the female-producing temperature (Ramsey et al., 2007). Medullary ERα expression after the feminizing shift may indicate a role for ERα in mediating degeneration of medullary cords. While the genomic regulatory sequences of male-specific genes involved in sex cord development are not known in the slider turtle, it is worth noting that genomic screens have identified ER binding sites (estrogen response elements (ERE) sequences) in the promoter region of Sertoli cell markers Sox9 and MIS (Frasor et al., 2003; Jin et al., 2005). The reduction in ERβ medullary expression may support the idea of differential roles for ERα and ERβ isoforms during temperature-mediated feminization. Indeed, ERβ localized solely to the nascent cortical compartment following the shift, and may participate in female-specific cortical development, although expression did not appear to be widespread.

Following the opposing female- to male-producing temperature shift, ERα, ERβ, and AR medullary expression was reduced compared to unshifted controls. If estrogen mediates ovarian medullary degeneration, this reduction in ERα and ERβ may indicate the first signs of temperature-induced alteration of sex steroid signaling towards a testis-

determining pathway. Since both isoforms are also expressed in the differentiated testis, this down-regulation following the temperature shift may be transient, and indeed both receptors are expressed along the developing seminiferous tubules in shifted testes (Figures 4L and 5L). Androgen receptor expression also appeared less organized in the medullary compartment than unshifted gonads (Figure 6) prior to ultimate testis differentiation (when AR displayed testis-typical expression along the seminiferous tubules). If androgens do have a role in testis cord formation in the slider turtle, this transient disorganization may reflect the time needed to redirect gonadal architecture towards testis formation. However, it does appear that androgen signaling is downstream from initial temperature-based testis-determining gene expression.

Estrogen and androgen signaling networks are responsive to estrogen treatment (Lauber et al., 1991; Menuet et al., 2004; Pelletier et al., 2004). In the slider turtle, sex reversal via application of exogenous $E_2$ at the male-producing temperature causes differential changes in sex steroid receptor expression. Estrogen receptor $\alpha$ expression was reduced compared to EtOH-treated controls throughout the medullary region within one stage of E2 treatment (Figure 7). This medullary reduction was maintained throughout ovarian development in the E2 treatment group, and was coupled with increased cortical expression – a pattern not typical of temperature-created ovaries (Figure 4,8). ER$\beta$ also responded to $E_2$ treatment, but the shift towards cortical localization was not as rapid as with ER$\alpha$ (Figure 7). Aromatase expression is also expanded into the cortical region in E2-created ovaries (Ramsey et al., 2007), indicating long-lasting changes in the estrogen signaling network in E2-created versus temperature-created ovaries. Cortical estrogen synthesis and transduction may be needed to maintain ovarian development at a male-producing temperature.

Unlike $E_2$ application, modulating estrogen availability through treatment with aromatase inhibitor (AI) did not markedly change ERα or ERβ expression until after gonadal commitment to testis outcome was evident (Figure 8). Aromatase inhibitor treatment inhibits new embryonic estrogen synthesis, but does not interfere with estrogen already present in the system. This delayed response to AI treatment has also been seen in studies on slider turtle Sf1 and aromatase expression (Fleming and Crews, 2001; Ramsey et al., 2007). During testis differentiation at the male-producing temperature, ERα and ERβ are expressed in the absence of embryonic estrogen production (Ramsey et al., 2007), and AI-created testes at the female-biased temperature exhibit robust ERα and ERβ expression as well (Figure 8). Receptor presence in the absence of estrogen probably explains the sensitivity to estrogen in male embryos when treated with exogenous $E_2$, but may also indicate a role for ligand-independent ER action in testis formation.

In contrast, AR localization was altered two stages after AI treatment (Figure 8). The cessation of estrogen production perturbed androgen signaling before any changes in ERα or ERβ localization were evident. This may result from increased androgen availability, but testosterone levels have not been measured following AI treatment.

Estrogen receptor α, ERβ, and AR are present in the gonad throughout development, and do not exhibit sexually dimorphic patterns of expression before gonadal differentiation when incubated at constant male- and female-producing temperatures. However, all three receptors respond differentially to sex-reversing treatments, and feminization via $E_2$ treatment at a male-producing temperature

profoundly changed the expression patterns for all three receptors, particularly ERα. Although sex reversal via temperature shift to warmer, female-producing temperature and estrogen treatment both result in the same endpoint (ovarian development), our data indicate potential different steroid signaling patterns between temperature- and estrogen-induced feminization.

Table 3-1 *Trachemys scripta* developmental timeline

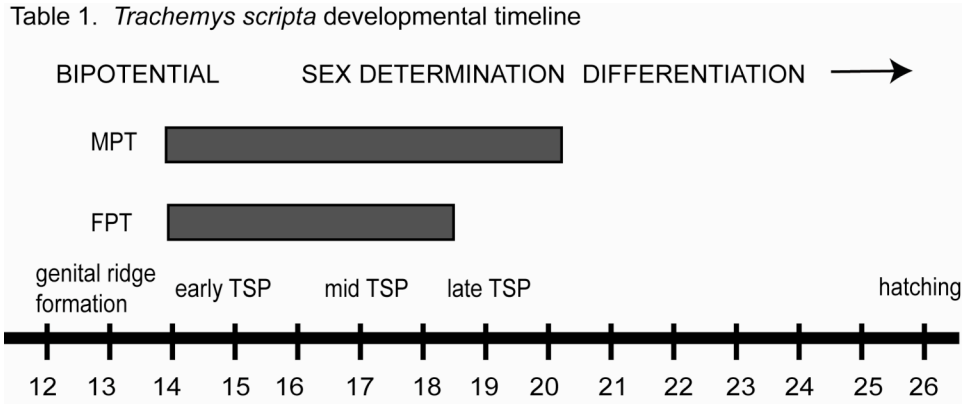

Table 3-2. Primer sequences

Table 2. Primer sequences

| Gene | Length (bp) | Primer sequence |
|---|---|---|
| ERβ cloning outer | 1028 | For 5' - GAGCCGCAGAAGTCCCCNTGGTGYGARG - 3'<br>Rev 5' - TTGGCGATCACCCACACNARNGCRTC - 3' |
| ERβ cloning inner | 548 | For 5' - CGGCGGGAGCGGTGYGGNTAYNG - 3'<br>Rev 5' - GCCTTCACGCACAGGTACTCYTTRTGYTG - 3' |
| AR cloning | 448 | For 5' - TGYTAYGARGCIGGIATGAC - 3'<br>Rev 5' - CCA(I/C)CCCATNGCRAANACCAT - 3' |
| ERα real time PCR | 92 | For 5' - TGATGATTGGCTTAGTCTGGCG - 3'<br>Rev 5' - GCACTTCCCTTGATTCCTGTCC - 3' |
| ERβ real time PCR | 112 | For 5' - TCCTAATGTGTTGCTGGTGAGTCG - 3'<br>Rev 5' - GGCCCAACCAATCATGTGAACCAA - 3' |
| AR real time PCR | 93 | For 5' - CCAGCCTGAATGAGCTTGGG - 3'<br>Rev 5' - GGTCATCCACATGCAAGTTACGG - 3' |

Figure 3-1. Northern blot analysis of estrogen receptor α, estrogen receptor β, and androgen receptor expression.

Northern blot analysis of ERα, ERβ, and AR expression in adult testis and AKG tissue in the slider turtle. A: AR and ERα were sequentially probed onto a blot containing developmental AKG and adult testis total RNA. Lane 1: Stage 17 AKG MPT, Lane 2: Stage 17 AKG FPT, Lane 3: adult testis. In AKG and adult testis, AR hybridized to a major band at ~9kb (alternate transcript at ~0.75kb not shown). ERα hybridized to a band at ~7kb in all tissue types with a testis-specific alternate transcript of ~1kb (not shown in A; see B). B: ERα and ERβ were probed onto a blot containing adult testis total RNA. Lane 1: ERα, Lane 2:, ERβ. ERα results in B were identical to blot shown in A. ERβ hybridized to a major band at ~4kb with a faint alternate transcript at ~2kb. AKG = adrenal-kidney-gonad complex. MPT = male-producing temperature (26° C). FPT = female-producing temperature (31° C). Stage 17 AKG MPT and FPT results were identical to those for MPT and FPT Stages 15,19,21,23 (data not shown).

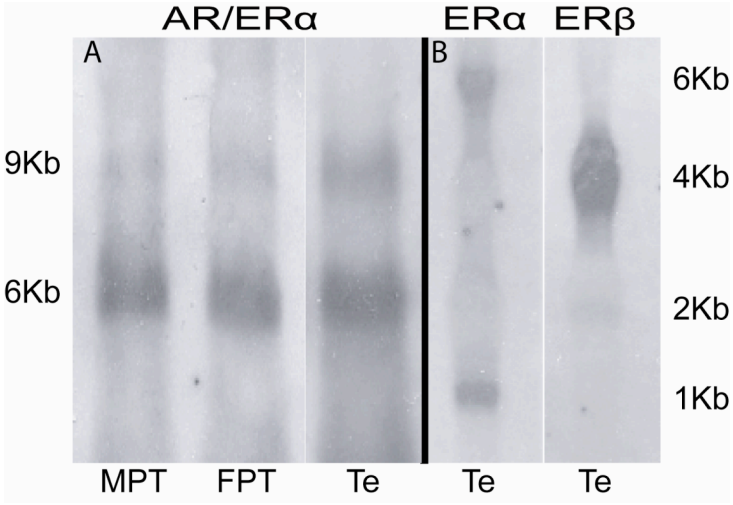

Figure 3-2. Quantitative real time PCR (qPCR) analysis of estrogen receptor α, estrogen receptor β, and androgen receptor expression at female- and male-producing incubation temperatures.

ERα, ERβ, and AR transcript abundance was measured by qPCR. ERα was expressed at both temperatures (A), and for both temperatures, expression spiked at Stage 19, although the peak at FPT was higher than for MPT. ERβ was also expressed at both temperatures (B), but levels remained stable throughout the sex-determining period of development (Stages 17-21). ERβ produced a moderate sex-specific peak at Stage 23 at the FPT. AR abundance showed a similar pattern to ERα, and as with ERα, the peak at Stage 19 was greater at FPT than MPT. Target tissue for qPCR analyses consisted of pooled gonad tissue from 30-50 individuals/stage/temperature. Individual data points of the triplicate wells are graphed onto panels A, B, and C but are not always distinct due to similarity of measurements across replicates. Levels were normalized relative to PP1 housekeeping gene (see Materials and Methods) and then calibrated across temperatures to the normalized Stage 17 FPT value for each gene. For each gene, Stage 17 FPT=1, and other values reflect the ratio of gene expression level/temp and stage to Stage 17 FPT. FPT = female-producing temperature (31° C). MPT = male-producing temperature (26° C).

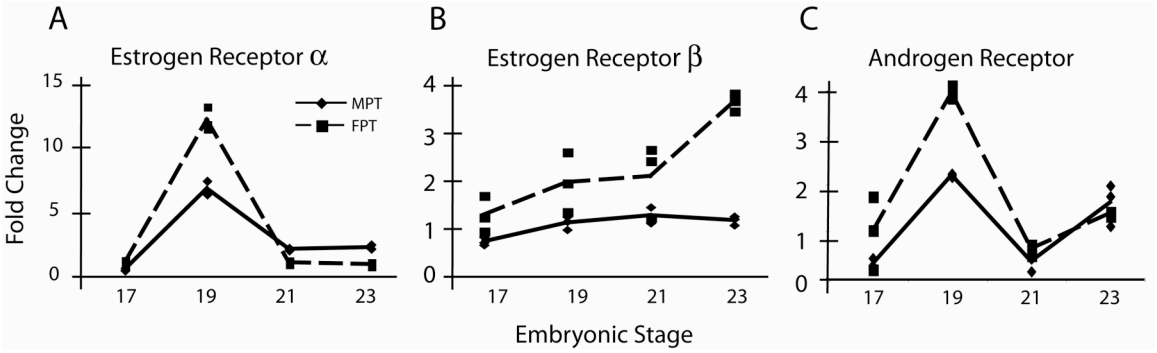

Figure 3-3. Representative whole mount *in situ* hybridization adrenal-kidney-gonad (AKG) complexes.

Whole mount *in situ* hybridization of slider turtle AKG tissue reveal gonad-specific expression at the beginning of the TSP (Stage 15). ERα was strongly expressed at the onset of the TSP at both MPT and FPT (A,D). ERβ expression was much less abundant but was specifically localized into circular structures possibly reflecting expression around putative germ cells. ERβ-probed gonad tissue is difficult to distinguish from the underlying mesonephros, but a high magnification inset shows specific localization (B,E). AR is moderately expressed at both temperatures at the onset of the TSP (C,F). Although not shown for ERα and AR, specific circular structures can be observed at high magnification in all gonads. AKG = adrenal/kidney/gonad complex; TSP = temperature-specific period. Bar = 250μm. Representative whole mount pictures taken at 20x magnification; high magnification insets (B,E) were taken at 90x. Box outlines representative circular structures seen in high magnification inset.

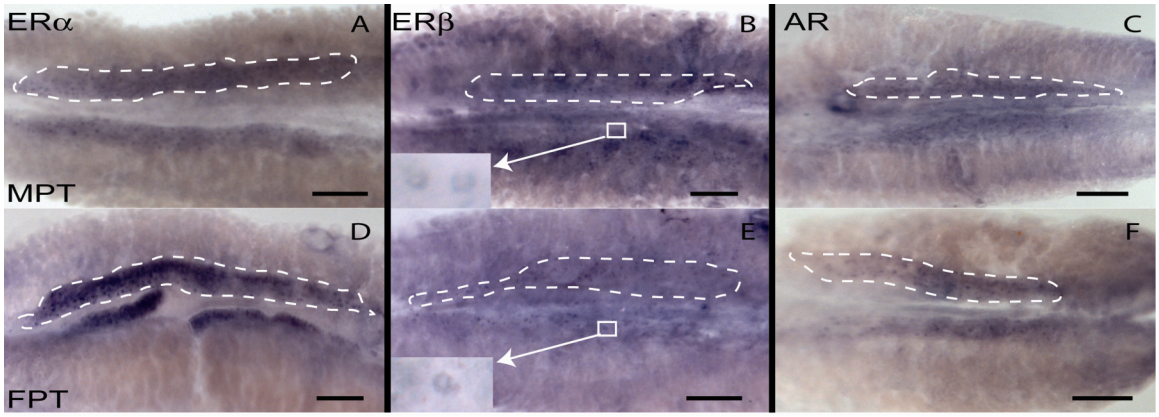

Figure 3-4. Developmental expression of estrogen receptor α during gonadal sex determination and differentiation and following temperature shift.

ERα is expressed in the gonad throughout sexual development at male-producing (A-D) and female-producing (G-J) temperatures. Embryos were shifted midway through the TSP (Stage 17). ERα responded to temperature shifts from male- to female-producing temperatures (E,F) and female- to male-producing temperatures (K,L). MPT = male-producing temperature (26° C); FPT = female-producing temperature (31° C). MPT→FPT shift = 26°→31°; FPT→MPT shift = 31°→26°. Whole mount gonads were sectioned at 40 μm thickness. Bar = 10 μm.

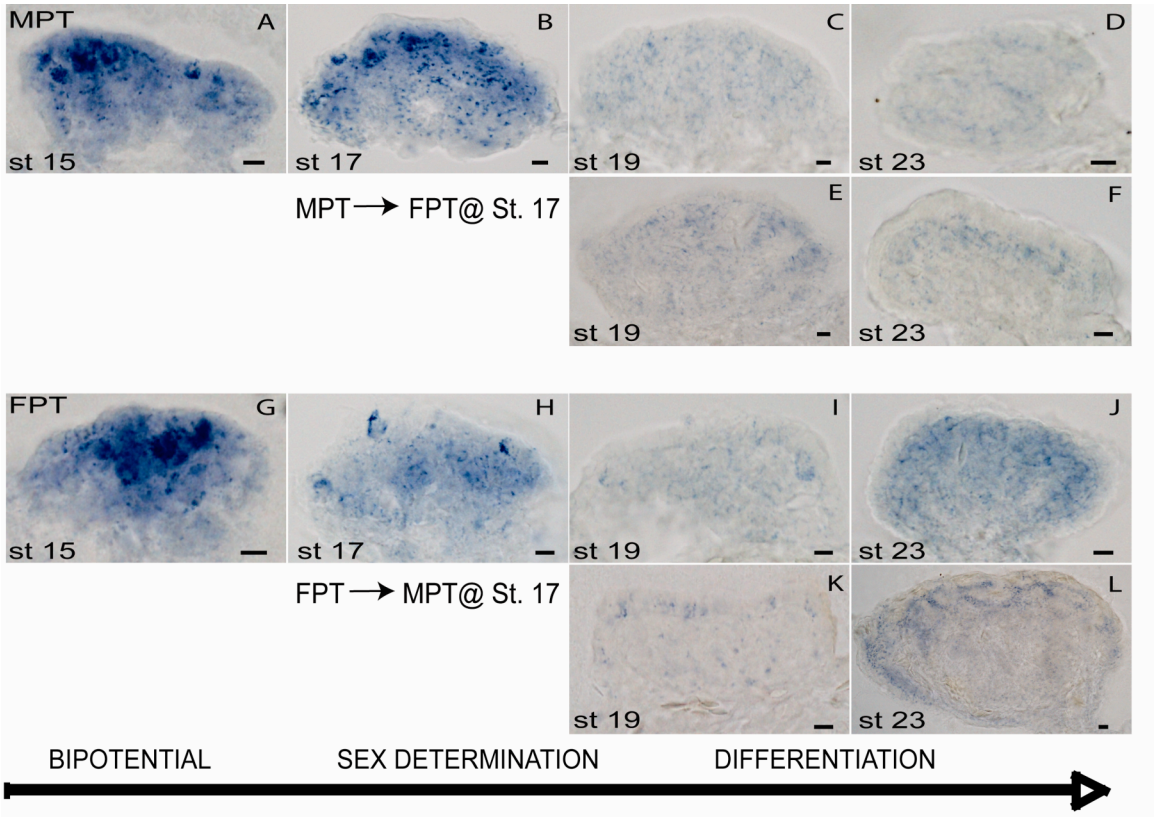

Figure 3-5. Developmental expression of estrogen receptor β during gonadal sex determination and differentiation and following temperature shift.

ERβ is expressed in the gonad throughout sexual development at male-producing (A-D) and female-producing (G-J) temperatures. Embryos were shifted midway through the TSP (Stage 17). ERβ responded to temperature shifts from male- to female-producing temperatures (E,F) and female- to male-producing temperatures (K,L). MPT = male-producing temperature (26° C); FPT = female-producing temperature (31° C). MPT→FPT shift = 26°→31°; FPT→MPT shift = 31°→26°. Whole mount gonads were sectioned at 40 μm thickness. Bar = 10 μm.

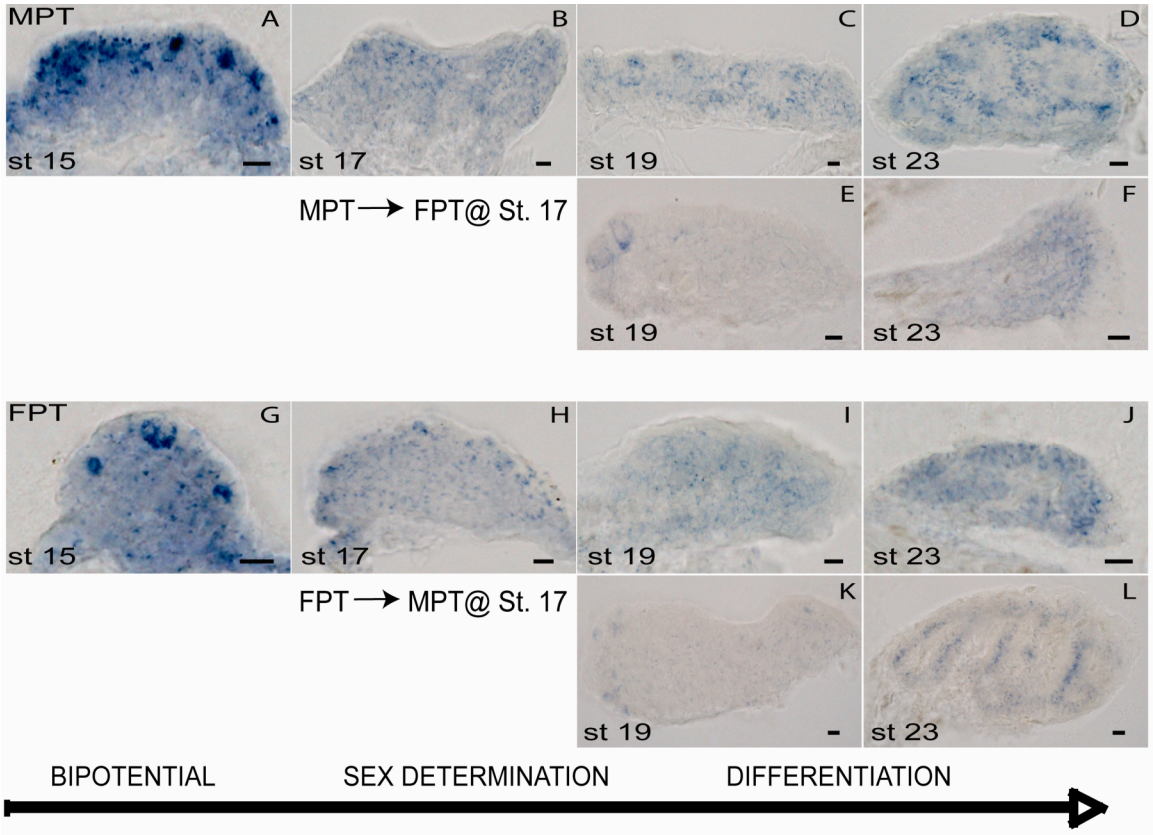

Figure 3-6. Developmental expression of androgen receptor during gonadal sex determination and differentiation and following temperature shift.

AR is expressed in the gonad throughout sexual development at male-producing (A-D) and female-producing (G-J) temperatures. Embryos were shifted midway through the TSP (Stage 17). AR responded to temperature shifts from male- to female-producing temperatures (E,F) and female- to male-producing temperatures (K,L). MPT = male-producing temperature (26° C); FPT = female-producing temperature (31° C). MPT→FPT shift = 26°→31°; FPT→MPT shift = 31°→26°. Whole mount gonads were sectioned at 40 μm thickness. Bar = 10 μm.

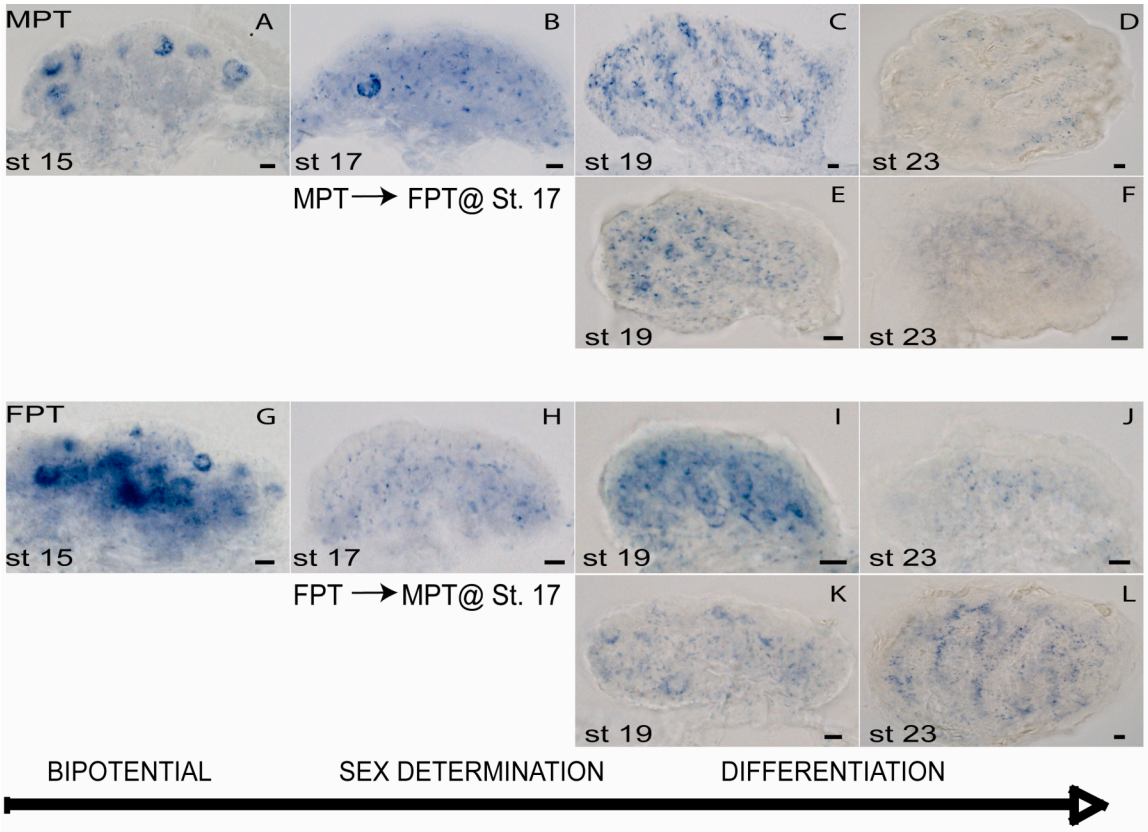

Figure 3-7. Effect of exogenous estradiol application at a male-producing temperature on estrogen receptor α, estrogen receptor β, and androgen receptor expression patterns.

ERα medullary expression is reduced following exogenous $E_2$ treatment (D,E,F) compared to EtOH-treated controls (A,B,C) incubated at the male-producing temperature. ERβ medullary expression is altered following $E_2$ treatment (J,K,L) compared to EtOH-treated controls (G,H,I). ERα and ERβ expression is extensive in the cortical compartments of ovaries created at the male-producing temperature (F,L). AR exhibits a delayed response to $E_2$ treatment, but does show a transient reduction in medullary expression after $E_2$ application (Q,R,S) compared to EtOH-treated controls (M,N,O). Male-producing temperature = 26° C. $E_2$ = estradiol-17β. Whole mount gonads were sectioned at 40 μm thickness. Bar = 10 μm.

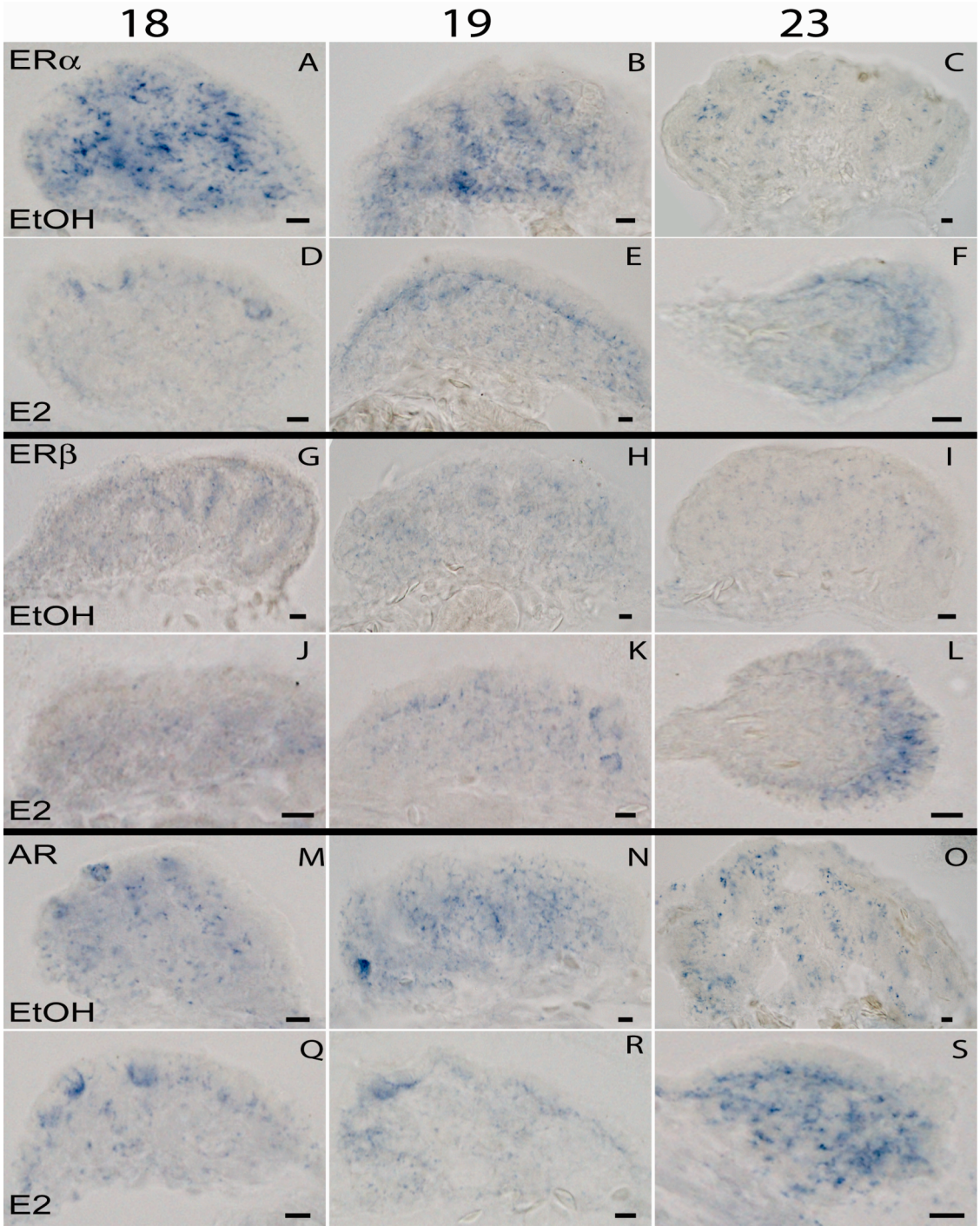
18
19
23
ERα
A
B
C
EtOH
D
E
F
E2
ERβ
G
H
I
EtOH
J
K
L
E2
AR
M
N
O
EtOH
Q
R
S
E2

Figure 3-8. Effect of aromatase inhibitor (AI) treatment at a female-biased temperature on estrogen receptor α, estrogen receptor β, and androgen receptor expression patterns.

ERα exhibits a delayed response to application of AI at the female-biased temperature (A,C), but does show sex-specific changes in localization later in development (B,D). ERβ expression is light/undetectable in both AI- and EtOH-treated embryos two stages after application (E,G), but shows strong signal along developing seminiferous tubules in AI-treated individuals (H). AR medullary expression is less organized following AI treatment when compared with EtOH-treated controls (I,K), and exhibits sex-specific localization patterns as the gonad differentiates (J,L). Arrow indicates circular patterns of expression within the seminiferous tubules of AI-created testes (L). Female-biased temperature = 29.4° C. AI = aromatase inhibitor. Whole mount gonads were sectioned at 40 μm thickness. Bar = 10 μm.

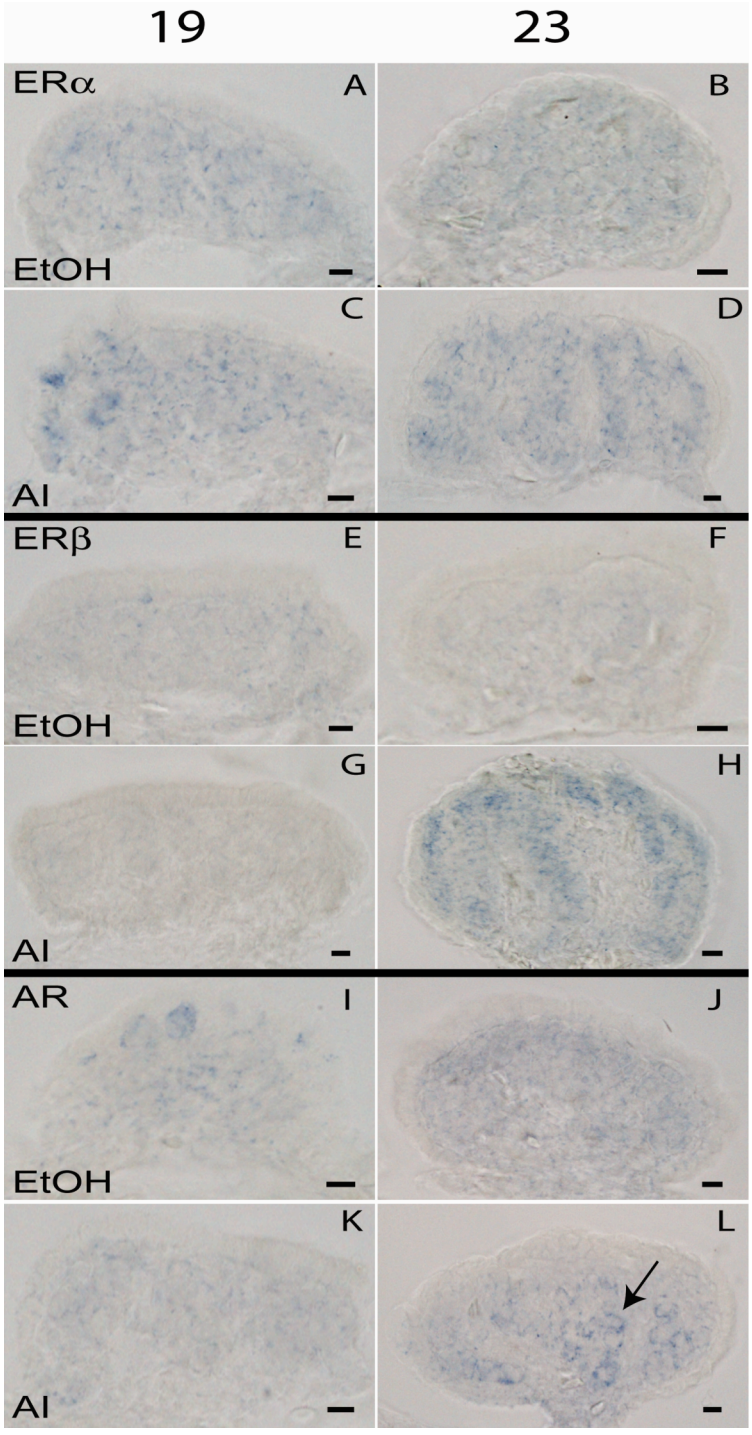
19
23
ERα
A
B
EtOH
C
D
AI
ERβ
E
F
EtOH
G
H
AI
AR
I
J
EtOH
K
L
AI

# Chapter 4: Adrenal-kidney-gonad complex measurements do not predict gonad-specific changes in gene expression patterns during temperature-dependent sex determination in the red-eared slider turtle (*Trachemys scripta elegans*)

## INTRODUCTION

Reptiles with temperature-dependent sex determination (TSD) are useful model organisms for studying genes involved in sex determination and sex differentiation because the gonad is truly bipotential until a temperature cue acts to determine sex. Many reptiles, including the red-eared slider turtle (*Trachemys scripta elegans*), exhibit temperature-dependent sex determination (TSD), where the sex of the developing embryo is determined by egg incubation temperature during a critical temperature-sensitive period (TSD) of development (Bull, 1980; Wibbels et al., 1991). The mechanism by which temperature is transduced into a sex-determining cue is not known, although much current research in TSD reptiles examines differential gene expression in the gonad prior to or at the onset of the TSP (Fleming et al., 1999; Kettlewell et al., 2000; Western et al., 2000; Maldonado et al., 2002; Murdock and Wibbels, 2003b; Murdock and Wibbels, 2003a; Ramsey et al., 2007; Shoemaker et al., 2007).

The reptilian gonad arises as a bipotential genital ridge along the medial ventral mesonephros, and is part of a heterogenous tissue complex that also includes the developing adrenal gland in addition to the mesonephros (from which the Wolffian and Mullerian ducts develop) and later, metanephros which will become the kidney (Raynaud and Pieau, 1985). For the sake of convention, this organ complex will be referred to as

the adrenal-kidney-gonad (AKG) complex. Gene expression from the adrenal and kidney compartments may mask gonad-specific changes in gene expression during development, including during the TSP while sex is being determined. However, because of the difficulty in separating the gonad from the surrounding mesonephros tissue, the AKG complex is frequently used as the tissue source in gene expression studies looking at sex determination and differentiation in reptiles (Spotila et al., 1998; Kettlewell et al., 2000; Murdock and Wibbels, 2003a; Murdock and Wibbels, 2003b; Takada et al., 2004). Many of the genes involved in amniote gonadal sex determination and differentiation are also expressed in adjacent adrenal and kidney tissue (Vainio and Lin, 2002; Parviainen et al., 2007; Shoemaker et al., 2007), and early, subtle gonad-specific changes in gene expression may be diluted by expression in other compartments. In addition, there may be unexpected sex differences in developmental adrenal or kidney gene expression, as has been measured in mouse fetal adrenal (Mukai et al., 2002) and newborn and adult mouse kidney (Janmohamed et al., 2004; Rinn et al., 2004).

Here we report gene expression levels in intact AKG tissue for five genes important in gonadal sex determination and differentiation in the slider turtle, and compare these expression patterns with those for isolated adrenal-kidney (AK) and G (gonad) tissue sources. The genes measured include the steroid hormone receptors androgen receptor (AR), estrogen receptor α (ERα), estrogen receptor β (ERβ), as well as aromatase, the enzyme that converts testosterone to estradiol, and steroidogenic factor-1 (*Sf1*), a master regulator for steroidogenic enzymes. Our results indicate that all 5 genes exhibit different patterns of expression depending on the tissue source of measurement.

## MATERIALS AND METHODS

### Tissue collection

Red-eared slider turtle *(Trachemys scripta)* eggs were purchased from Robert Clark (Clark Turtle Farms, Hammond LA) within 24 hours of laying and randomized on site to control for clutch effects. Eggs were held at room temperature in Texas until candled to establish viability. Eggs were then further randomized, placed into trays containing 1:1 vermiculite and water mix and placed in incubators (Precision, Chicago, IL) at 26° C (male-producing temperature) or 31° C (female-producing temperature). Incubator temperatures were monitored continuously with HOBO recording devices (Onset Computer Corporation, Bourne, MA) and verified daily with calibrated shelf thermometers. To avoid small temperature gradient effects, the egg trays were also rotated daily within the incubator. Eggs were dissected at regular intervals to assess developmental stage (Yntema, 1968). Embryos were harvested at Stages 17, 19, 21, and 23. Adrenal-kidney-gonad (AKG), adrenal-kidney (AK) or isolated gonad (gonad or G) tissue was rapidly dissected and processed for experimental use.

### Total RNA preparation and cDNA synthesis

For the AK and gonad measurements, we dissected gonad tissue off the AK component of the AKG for processing. Therefore, the AK and gonad samples represent tissue from the same individuals. The gonad is a very small component of the AKG, therefore to ensure adequate material for qPCR assays, tissue from multiple individuals (30-50/sample) were pooled for AK and gonad measurements. AKG tissue was pooled from 10-30 individuals. After dissection, AKG, AK, or gonad tissue was placed in RNAlater (Ambion) for overnight incubation at 4° C followed by storage at -80° C, or

placed directly into Promega RNAgents Total RNA Isolation kit denaturing solution and stored at -80° C. Total RNA was extracted using RNAgents Total RNA Isolation kit (Promega, Madison, WI) following the manufacturer's protocol. Abundance and purity was assessed through spectophotometry readings at 260 nm and 280 nm.

Total RNA was treated with DNase to eliminate any genomic DNA contamination in the RNA samples using Turbo DNA-Free kit (Ambion) following the manufacturer's protocol. Single-stranded cDNA was reverse-transcribed (1 μg total RNA/20 μl reaction concentration) using Superscript First Strand Synthesis for RT-PCR kit (Invitrogen). cDNA synthesis was primed with both oligo-dT and random hexamers using a modified manufacturer's protocol (Invitrogen).

**Real-time qPCR**

Gene sequences, real-time PCR primer sequences and amplicon sizes have been described (Ramsey and Crews,in review; Ramsey et al., 2007). For all genes, specificity of target was verified by gel electrophoresis. Expression levels were normalized to PP1 (protein phosphatase 1 gamma) housekeeping gene. PP1 was chosen based on stability of expression under experimental conditions and relative level of abundance compared to AR, ERα, ERβ, aromatase, and *Sf1* (Ramsey et al., 2007).

Real-time qPCR experiments were conducted on ABI Prism 7900 real-time PCR machine (Applied Biosystems). Reaction conditions have been described (Ramsey and Crews, in review; Ramsey et al., 2007). Relative gene expression levels were assessed using SYBR green detection chemistry. Dissociation curve analysis was performed after each assay to determine target specificity. Each sample was run in triplicate. For each

gene, AKG, AK, and gonad samples were run on the same plate to eliminate inter-run variability.

### Real-time qPCR data analysis

Assay results were first analyzed using the Applied Biosystems Sequence Detection System software (SDS 2.2.1). Relative quantification was performed by a modified comparative critical threshold (CT) method that corrects for different PCR amplification efficiencies among primer pairs (Simon, 2003). Gene expression normalized to PP1 housekeeping is given as MNE (mean normalized expression) = ($E_{pp1}$^meanCT $_{pp1}$)/( $E_{exp\ gene}$^meanCT $_{exp\ gene}$), where E= PCR efficiency (E=10^-(1/slope)) (Pfaffl, 2001), meanCT is the average CT across the three replicates, and exp gene = AR, ERα, ERβ, aromatase, or *Sf1*. Normalized gene expression levels were then calibrated to a baseline measurement (Stage 17 measurement at the female-producing temperature).

## RESULTS

Androgen receptor, ERα, ERβ, aromatase, and *Sf1* transcript abundance was measured using quantitative real-time PCR (qPCR). Intact AKG, isolated AK, and isolated gonad tissue was used as template for qPCR measurements, and the resulting patterns were compared between temperatures and across stages.

### Adrenal-kidney-gonad complex

Androgen receptor, ERα, ERβ, aromatase, and *Sf1* are all expressed in the AKG (Figure 1A,D,H,K,N). Androgen receptor and ERα expression patterns are similar in the

AKG. Androgen receptor is slightly higher at the male-producing temperature during the TSP (Stage 17), but expression at the male-producing temperature steadily declines throughout the phases of gonadal commitment and differentiation (Figure 1A), while at the female-producing temperature there is a moderate increase during gonadal commitment before declining. Similarly, ERα is slightly higher in the middle of the TSP (Stage 17) at the male-producing temperature, declining slightly throughout gonadal differentiation (Figure 1D); at the female-producing temperature ERα expression remains unchanging throughout the TSP (Stages 17-19), and then declines slightly as ovarian differentiation commences (Stage 21) but remains level through Stage 23.

Estrogen receptor β and aromatase are both expressed slightly higher at the female-producing temperature, but with differing patterns of expression. At both incubation temperatures ERβ expression is equivalent at Stage 17, but expression drops steadily at the male-producing temperature until leveling out at the onset of testis differentiation (Stage 21; Figure 1H); at the female-producing temperature ERβ increases slightly as ovarian commitment begins (Stage 19), but then declines as differentiation continues. Aromatase is also equivalent between the two temperatures during the TSP (Stage 17), and then exhibits a drop in expression at the male-producing temperature as sex is being determined and then remains stably expressed as testis differentiation continues (Figure 1K). At the female-producing temperature, aromatase expression is unchanged through the TSP (Stages 17-19), and after a brief decline as the ovary is being determined and ovarian differentiation commences (Stage 21), expression begins a female-specific increase as ovarian differentiation is completed (Stage 23).

Steroidogenic factor 1 expression is slightly higher at the male-producing temperature throughout the TSP and into gonadal commitment and differentiation, but levels at both temperatures decline slightly throughout development (Figure 1N).

**Adrenal-kidney**

Androgen receptor, ERα, ERβ, aromatase, and *Sf1* are all expressed in the AK compartment of the AKG (Figure 1B,E,I,L,O). Androgen receptor gene expression is not differential by temperature in the AK (Figure 1B). Estrogen receptor α is expressed at a constant level throughout AK development at the male-producing temperature (Figure 1E). At the female-producing temperature, levels are steady during the TSP, but drop slightly at the female-producing temperature between Stages 19 and 21.

Estrogen receptor β expression is also relatively constant through development in the AK compartment (Figure 1I). As with the AKG measurement, levels are slightly higher at the female-producing temperature. At both temperatures, ERβ increases slightly after the TSP has closed, although the increase at the female-producing temperature can be seen at Stage 21, while male-producing temperature levels do not increase until Stage 23. Like AR, aromatase levels are not differential by temperature in the AK (Figure 1L).

The SF1 AK expression pattern in unique and does not match either the AKG or gonad patterns (Figure1N,O,P). Expression is steady at the male-producing temperature, but there is a slight peak at the female-producing temperature at Stage 19. For all five genes, expression levels for AK Stage 23 at the female-producing temperature were

eliminated due to inter-well variability caused by low target abundance in the preparation.

**Gonad**

Androgen receptor, ERα, ERβ, aromatase, and *Sf1* are all expressed in the gonad compartment of the AKG (Figure 1C,F,J,M,P). Gonad-specific gene expression patterns have been described for all five genes (Ramsey and Crews, ; Ramsey et al., 2007). For AR, expression is equivalent during the middle of the TSP (Stage 17) rather than higher at the male-producing temperature (Figure 1C,A) as measured with AKG tissue. The female-specific peak in expression as ovarian commitment occurs (Stage 19) is much higher in the G-only assay (the peak is twice as high in females as compared to males in isolated G, vs. a normalized difference of only .5 for the same comparison in AKG).

Like AR, ERα exhibits a female-specific peak at Stage 19 in the isolated gonad tissue (Figure 1F,D) that is barely perceptible in the AKG measurement (5-fold higher peak at the female-producing temperature according to G measure versus .3 normalized difference in the AKG measure).

Estrogen receptor β patterns exhibit two primary differences between gonad and AKG measurements. In the isolated gonad tissue, ERβ is higher at the female temperature during the middle of the TSP (Stage 17), whereas in the AKG measurement levels are equivalent between (Figure 1H,J). Also, the female-specific increase in ERβ as the ovary is differentiating (Stage 23) is specific to the gonad measurement and is not detectable in AKG.

Aromatase exhibits a much different pattern in gonad vs AKG tissue. In both, aromatase levels are equivalent midway through the TSP (Stage 17), but whereas aromatase increases throughout ovarian development when measured in isolated gonad tissue, the AKG measurements at the female-producing temperature decline at Stage 21 and only show a modest increase at Stage 23 (Figure 1M,K).

Like ERβ, *Sf1* follows a qualitatively similar pattern in gonad and AKG tissue. However, the magnitude of difference is attenuated in the AKG measurement, and the male-temperature specific peaks observed at Stages 19 and 23 are not detected in AKG (Figure 1P,N).

## DISCUSSION

Heterogenous AKG tissue is frequently used as source tissue for experiments looking at temperature-specific changes in gonadal gene expression (Spotila et al., 1998; Kettlewell et al., 2000; Murdock and Wibbels, 2003a; Murdock and Wibbels, 2003b; Takada et al., 2004). During the TSP, the AKG contains not just the developing gonad, adrenal, and embryonic kidneys, but also the Wolffian and Mullerian ducts (Raynaud and Pieau, 1985; Wibbels et al., 1999) – all potential sources of differential gene expression that cannot be distinguished in an AKG tissue preparation. Here, we show that expression patterns for AR, ERα, ERβ, aromatase, and *Sf1* do not correspond in isolated gonad versus AKG measurements. Temperature-specific differences in gonadal gene expression are at best attenuated, and at times are completely undetectable in AKG tissue measurements.

Isolated gonad tissue exhibits different patterns of expression than AKG tissue in all five genes examined here. In all cases, measuring gene expression in isolated gonad tissue versus AKG tissue results in more interpretable results. For example, in the gonad AR and ERα demonstrate quantitative differences (higher at the female-producing temperature) late in the TSP and as sex is being determined (Figure 1C,F). In both cases, the increase at the female temperature can be seen in the AKG measurement, but cannot be distinguished from expression at the male-producing temperature (Figure 1A,D).

Aromatase was the only gene with an increase at the female-producing temperature that was consistent across AKG and isolated gonad measurements, but the AKG increase was later in development than the gonad measurement (Figure 1K,M). Temperature-based differential aromatase activity has been hypothesized as an upstream marker of ovarian commitment in TSD reptiles (Crews et al., 1994; Pieau et al., 1999), and aromatase assays using isolated gonad tissue in the pond turtle (*Emys orbicularis*) measured increased aromatase activity at female-producing temperatures late in the TSP (Desvages and Pieau, 1992). However, other researchers measuring aromatase expression using AKG target tissue did not detect differences in aromatase expression or activity during the TSP in the slider turtle (Willingham et al., 2000; Murdock and Wibbels, 2003a) or in the alligator (Smith et al., 1995; Gabriel et al., 2001). Using isolated gonad tissue as target, we were able to detect higher levels of aromatase expression during the TSP while sex is not yet determined (Ramsey et al., 2007), adding evidence to support aromatase as an early responder to female-producing temperature in TSD reptiles.

This loss of temporal resolution in temperature-specific gonadal gene expression can also be seen with *Sox9*, a gene involved in male sexual development across vertebrate groups. Early reports using AKG tissue did not detect a difference in *Sox9* expression until late in male development (Spotila et al., 1998). In isolated gonads, higher *Sox9* expression can be detected at the male-producing temperature during the TSP itself (Shoemaker et al., 2007). Differences in gene expression are attenuated until later in development even in cases where AKG and gonad expression patterns are qualitatively similar. For example *Dmrt1*, a highly conserved gene involved in male sexual development, can be detected at higher levels in the male-producing temperature early in the TSP using AKG tissue (Kettlewell et al., 2000; Murdock and Wibbels, 2003b), but differences are more profound in isolated gonad tissue (Shoemaker et al., 2007).

In AK tissue, only *Sf1* demonstrated temperature-based changes in expression during the sex-determining phase of the TSP. In the AK, *Sf1* was higher at the female-producing temperature at a stage when it was higher at the male-producing temperature in the gonad. For *Sf1*, AKG patterns may be attenuated from isolated gonad patterns due to a masking effect of differential expression in the developing AK. For AR, ERα, ERβ, and aromatase, the discordance between patterns of expression the AKG and isolated gonad during the TSP do not appear to result from temperature-specific differences in AK component gene expression. In the absence of temperature-specific expression differences in the AK compartment, any temperature-specific differences in gene expression in the AKG measurements should be due to gonad compartment contribution. However, the AKG patterns do not reflect the patterns in gonad tissue, presumably due to dilution of the gonadal contribution to the AKG transcript pool.

These results suggest that AKG assays can detect genes such as *Dmrt1* that display large differences between male- and female-producing temperatures, but may miss more subtle temperature-specific changes taking place in the gonad. Taken together these results indicate that measurements based on AKG tissue can obscure important temporal relationships between temperature and gene expression within the gonad.

Figure 4-1. Quantitative real time PCR (qPCR) analysis of AR, ERα, ERβ, aromatase, and Sf1 expression and female- and male-producing temperatures using different compartments of the developing adrenal-kidney-gonad complex patterns during temperature-dependent sex determination in the red-eared slider turtle (*Trachemys scripta elegans*).

Gene expression patterns were compared between adrenal-kidney-gonad complex (AKG), adrenal-kidney (AK), and isolated gonad (G) tissues. AKG (A,D,H,K,N) patterns do not predict isolated gonad (C,F,J,M,P) patterns although AK (B,E,I,L,O) did not differ by temperature across development. Target tissue for qPCR analyses consisted of pooled AKG, AK or gonad tissue from 30-50 individuals/stage/temperature. Levels were normalized relative to PP1 housekeeping gene (see Materials and Methods) and then calibrated across temperatures to the normalized Stage 17 FPT value for each gene. For each gene, Stage 17 FPT=1, and other values reflect the ratio of gene expression level/temp and stage to Stage 17 FPT. AKG = adrenal-kidney-gonad complex. AK = adrenal-kidney complex. G = gonad. FPT = female-producing temperature (31° C) and is represented by the dashed line in all graphs. MPT = male-producing temperature (26° C). Data points for all five genes for AK tissue at Stage 23 at the female-producing temperature are absent due to inter-well variability, presumably due to degradation in the original total RNA preparation.

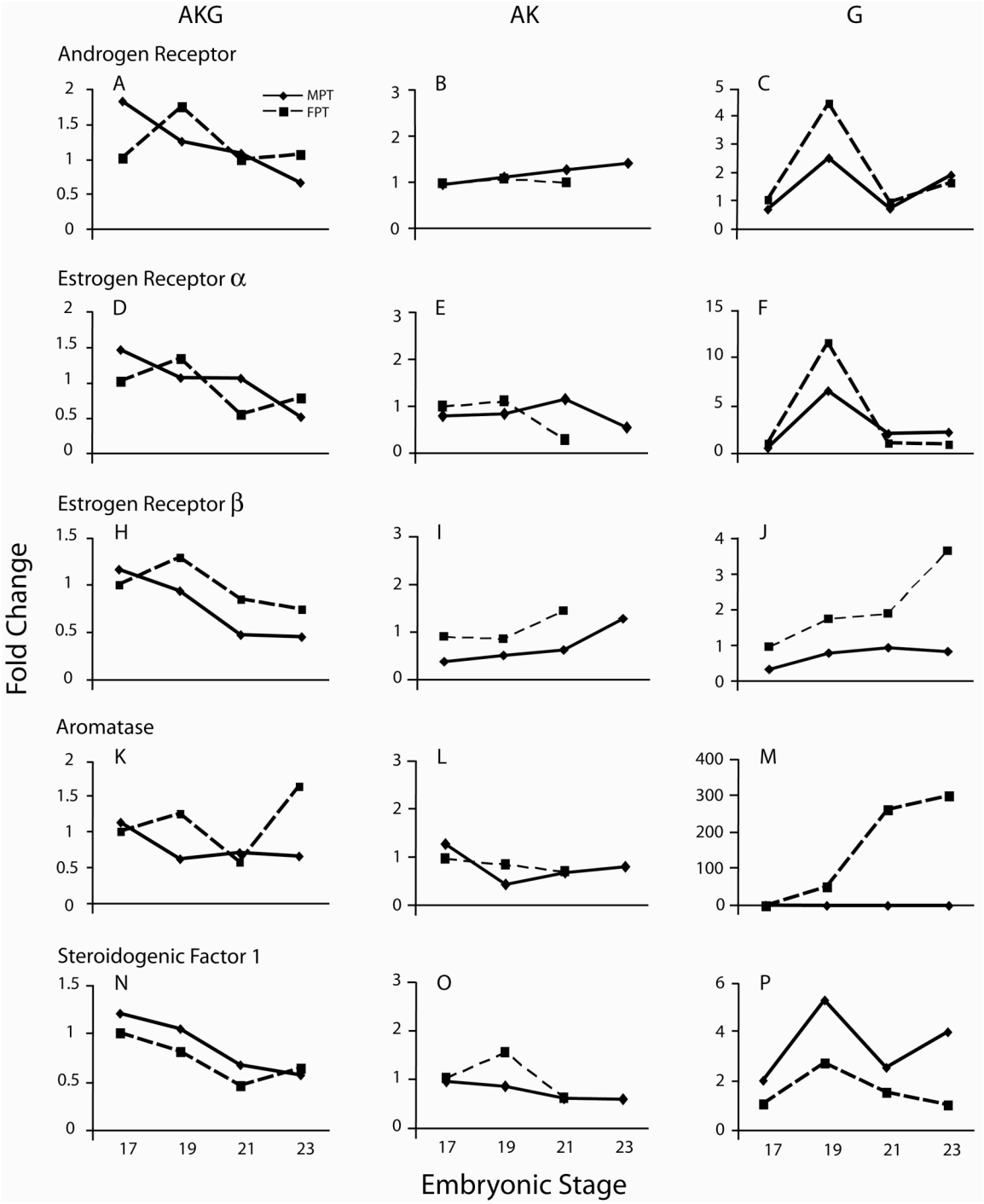
AKG
AK
G
Androgen Receptor
Estrogen Receptor α
Estrogen Receptor β
Aromatase
Steroidogenic Factor 1
A
B
C
D
E
F
H
I
J
K
L
M
N
O
P
MPT
FPT
Fold Change
Embryonic Stage
17
19
21
23

# Chapter 5: Conclusion

The aim of the present research was to elucidate the molecular mechanisms underlying steroid hormone action in temperature-dependent sex determination. In the red-eared slider turtle, gonadal sex is determined by egg incubation temperature during the temperature-sensitive period (TSP) of development (Wibbels et al., 1991). The gonad is also sensitive to steroid hormones during this phase of development, and sex can be reversed with both $E_2$ and AI application (Wibbels et al., 1993; Crews and Bergeron, 1994). Because steroid hormones can override a temperature cue, they may be the proximate mechanism through which temperature exerts its actions (Crews et al., 1994). The current work provides the first localization expression analysis for aromatase in a TSD reptile during sex determination and differentiation, as well as the first comparison between aromatase and *Sf1* expression patterns during gonadal development. In addition, expression patterns for three critical steroid hormone receptors in steroid signaling are described. While preliminary expression analysis for ERα has been described (Bergeron et al., 1998), the current work presents the first expression analysis for ERα following sex reversal, as well as the first developmental (and sex reversal) analysis for ERβ and AR in a TSD reptile. This has led to a series of hypotheses that represent conclusions as well as suggestions for future research (Table 1).

In Chapter 2, aromatase and *Sf1* expression patterns were assayed during development at male- and female-producing temperatures. Quantitative real-time PCR (qPCR) analysis reveals that aromatase is expressed in a female-specific manner, while *Sf-1* is expressed at higher levels at the male-producing temperature. Importantly,

increases in aromatase expression at the female-producing temperature occur during the TSP itself, while temperature is exerting its action and before ovarian differentiation is committed. **This finding adds to the hypothesis that aromatase may be an early target of temperature in ovarian sex determination/differentiation (Hypothesis 1)**.

In addition to differences in overall gonadal abundance, aromatase and *Sf1* exhibited different localization patterns starting in the middle of the TSP - before differential aromatase expression can be detected via qPCR, and before sex is determined. In the early bipotential gonad, germ cells are located throughout the outer germinal epithelium regardless of temperature, and will either proliferate in the cortical region in ovarian development, or migrate into the medullary region where they are enveloped by sex cords in the developing testis (Wibbels et al., 1991). Although my experimental protocol does not allow assignment of cell type, sectioned whole mount *in situ* analysis reveals that aromatase and *Sf1* are both localized around circular structures in the outer gonad. Given their location and size, these structures are probably germ cells. If so, aromatase is more tightly organized in the somatic cell lineage surrounding putative germ cells at the female-producing temperature while *Sf1* is more organized at the male-producing temperature. After sex determination and the closure of the TSP, aromatase expression is maintained at the female temperature and falls to negligible levels at the male temperature. *Sf1* is maintained at the male temperature while falling to lower levels (albeit still present) at the female-producing temperature. These data support Hypothesis 1**.** Higher aromatase expression as well as differential localization around putative germ cells may be creating a female-specific microenvironment critical for ovarian determination and differentiation. Secondly, my data, while correlative, suggest that ***Sf1*** **does not regulate female-specific aromatase expression during the**

**TSP and** the sex determination phase of gonadal development **in the slider turtle (Hypothesis 2)**.

Chapter 2 also assays aromatase and *Sf1* expression following sex reversal via temperature shift and steroid hormone treatment. Within two stages of treatment, aromatase begins to assume a more female-like expression pattern following M→F shift, and loses female-typical organization following the corresponding F→M. By contrast, *Sf1* organization becomes more diffuse following M→F shift while increasing in organization around developing medullary sex cords following F→M shift. Exogenous estrogen treatment at the male-producing temperature resulted in a maintenance of aromatase expression throughout the gonad while *Sf1* medullary expression becomes diffuse. Interestingly, aromatase expression is increased in the cortical region of $E_2$-created ovaries at the male-producing temperature, a pattern that was also seen with both estrogen receptors (see Chapter 3 and below). Inhibition of aromatase activity does not alter aromatase or *Sf1* expression patterns two stages after treatment. However, as development progressed both genes assume sex-specific expression patterns: aromatase is reduced to near negligible levels in the AI-created testis while *Sf1* continues to be expressed along the developing seminiferous tubules.

The biological actions of steroid hormones are mediated by their protein receptors. Therefore, to understand how steroid signals are transduced in the developing gonad, I explored the expression patterns of ERα, ERβ), and AR in Chapter 3. As with Chapter 2, I used qPCR and sectioned whole mount *in situ* hybridization to assess gonadal patterns in abundance and localization while incubating at constant male- and female-producing temperatures, then I used whole mount *in situ* method to explore

changes in gonadal localization following sex reversal via temperature or manipulation of estrogen availability.

Estrogen receptor α, ERβ, and AR are expressed in the slider turtle gonad at both male- and female-producing temperatures, and may be important in both testis and ovarian development. According to qPCR analysis on isolated gonad tissue, ERα, ERβ, and AR exhibit distinct patterns of expression. ERα and AR are equivalent between male-and female-producing temperatures midway through the TSP, but both exhibit a spike in expression at the close of the TSP that is higher at the female-producing temperature. Both then drop and are equivalent between sexes throughout the phase of gonadal differentiation. Importantly, the female-specific spike in expression correlates with the time of ovarian sex determination as well as increased aromatase expression at the female-producing temperature. **This leads to a third Hypothesis – that ovarian sex determination is accompanied by an increase in steroid sensitivity.** This sensitivity is transient and not required for ovarian differentiation, however, as levels for both ERα and AR drop later in development while aromatase continues to increase.

Estrogen receptor β exhibits a unique pattern of expression according to qPCR. Levels are constant at both temperatures throughout the TSP and the sex determination phase of gonadal development. Later in development, a female-specific increase in ERβ is observed in the differentiated ovary while levels in the testis remained constant. In mammals, ERβ is predominantly expressed in granulosa cells of the ovary (Fitzpatrick et al., 1999; Jefferson et al., 2000), and the late, female-specific expression pattern observed in the slider turtle ovary coincides with the timing of cortical cell proliferation in the slider turtle ovary (Wibbels et al., 1991). If ERβ cell type expression is conserved

between mammals and the slider turtle, then this increase may reflect granulosa cell proliferation. **The distinct levels of expression for ERα and ERβ during slider turtle gonadal development lead to a fourth Hypothesis – that ERα and ERβ may have distinct roles in slider turtle ovarian development**. Estrogen receptor β increases well after estrogen levels increase at the female-producing temperature, and this suggests that unlike ERα, ERβ is not an early target of estrogen in ovarian determination

While ERα and AR did exhibit quantitative differences in expression prior to gonadal differentiation, none of the steroid receptors are differentially localized within the gonad under constant temperature regimens until after morphological differentiation is evident in both testes and ovaries. Reversing gonadal sex via temperature shifts or steroid hormone treatment during the TSP allows us to examine changes in gene expression while temperature- or hormone-based sex determining cues are being reset. Unlike patterns during constant incubation conditions, ERα, ERβ, and AR did respond differentially to sex reversal via both temperature and steroid hormone manipulation. Following the M→F shift, ERα and AR were maintained in the medullary region of the shifted gonad, while ERβ medullary expression was reduced. After the corresponding F→M shift, ERα and ERβ medullary expression was reduced and AR medullary localization became transiently less organized.

Ovarian differentiation is marked by two key events – the degeneration of the primitive sex cords in the medullary compartment, and proliferation of cells comprising the cortical compartment (Wibbels et al., 1991). Increased estrogen availability may mediate one or both of these events, and earlier work implicates estrogen action in medullary degeneration (Wibbels et al., 1993). Although ERα may be maintaining

medullary patterns of expression following the M→F simply because it is not an early target of female-inducing temperature, it may be mediating medullary cord degeneration. In the pond turtle (*Emys orbicularis*), aromatase increases after M→F shift (Desvages and Pieau, 1992), and Chapter 2 indicates that in the slider turtle aromatase expression begins to exhibit a more organized female-typical expression pattern only two stages after the shift. If aromatase expression does increase following the feminizing shift, then ERα may be acting along the sex cords to downregulate male-specific gene expression. Although the regulatory relationships among slider turtle testis-determining genes are not currently known, it is known that many of the genes involved in the core pathway of amniote testis determination/differentiation are expressed during slider turtle testis development (Fleming et al., 1999; Kettlewell et al., 2000; Murdock and Wibbels, 2003b; Shoemaker et al., 2007). Two of these conserved genes, *Sf1* and *Dmrt1*, are downregulated in response to exogenous estrogen (Fleming and Crews, 2001; Murdock and Wibbels, 2006). In addition, the Sertoli cell markers *Sox9* and *Mis* have ER binding sites (estrogen response elements sequences) in their regulatory promoter regions according to genomic screens on mammalian sequences (Frasor et al., 2003; Jin et al., 2005).

If estrogen signaling mediates female-specific degeneration of the medullary sex cords, then the drop in aromatase, ERα, and ERβ medullary expression following the F→M shift may indicate that temperature acts to reset towards testis development in part by relieving repression on testis-determining genes along the primitive sex cords. This reduction is transient, however, and both ERs – but not aromatase - are expressed in the testis.

AR expression is also disrupted by the F→M shift. In the slider turtle, AR expression is generally specific to the medullary compartment and coalesces around the developing sex cords during testis differentiation and the degenerating primitive sex cords/lacunae in the ovary. Disrupted AR organization following the F→M shift may reflect the time the shifted gonad needs to reset towards a testis-determining trajectory. Although AR does not appear to be an early target of a male-inducing temperature cue (and as discussed above is actually higher at female-producing temperatures), it is clear that **both the androgen and estrogen signaling networks interact with temperature in slider turtle gonadal development (Hypothesis 5)**.

Medullary expression of ERα, ERβ, and AR is reduced following exogenous $E_2$ treatment. Estrogen receptor α reduction precedes that of ERβ, again suggesting that ERα is upstream while ERβ is downstream in steroid signaling response to estrogen in slider turtle ovarian development. Localization for both ERs shifts to the cortical region, a pattern mirrored by aromatase (Chapter 2). **These data lead to Hypothesis 6 – the estrogen signaling network responds differently to ovarian sex determination via warm temperature versus exogenous estrogen.** Expression of aromatase, ERα, and ERβ in the cortical region of $E_2$-created ovaries at the male-producing temperature suggest that increased estrogen production and signal transduction may be necessary to form and maintain the cortical region at the male-producing temperature.

Androgen receptor localization is altered following both $E_2$ and AI treatment, indicating that **the androgen signaling network responds to changes in estrogen availability (Hypothesis 7)**. Following $E_2$ treatment, AR medullary organization is transiently disrupted, but unlike the ERs, AR is later expressed throughout the medullary

compartment of $E_2$-created ovaries. Androgen receptor organization is altered within two stages following AI application. Aromatase inhibitor treatment blocks the synthesis of estrogen, but does not affect estrogen already present. Therefore, changes in gene expression following masculinizing AI treatment can be delayed, as seen with *Sf1* and aromatase (Chapter 2) or the ERs (Chapter 3). During sex reversal following AI treatment, AR maintained diffuse medullary expression, but localization around cortically located circular structures (presumptive germ cells?) seen in EtOH-treated gonads at the female-biased temperature was absent in AI treated gonads. While somewhat subtle, this response indicates that androgen signaling is affected by reduced estrogen availability prior to an obvious response in estrogen signaling. Although testosterone levels following AI treatment have not been measured in our lab, AI treatment presumably increases local testosterone concentration since it can no longer be aromatized to $E_2$. If testosterone levels are increased, this would explain why AR might exhibit an earlier sensitivity to AI treatment than components of the estrogen signaling network.

Uncovering differential gene expression during the TSP and prior to sex determination is key to elucidating the mechanisms underlying TSD. The gonad is a small component of the AKG, and is difficult to separate from the AK, particularly during earlier phases of gonadal development. Therefore, studies looking at temperature-based differences in gene expression have often used the AKG rather than isolated gonad as tissue source (Spotila et al., 1998; Kettlewell et al., 2000; Murdock and Wibbels, 2003a; Murdock and Wibbels, 2003b; Takada et al., 2004). In Chapter 4, I used qPCR to examine expression levels for *Sf1*, aromatase, ERα, ERβ, and AR in three tissue types – adrenal-kidney-gonad (AKG), isolated adrenal-kidney (AK), and isolated gonad. All five genes are expressed in AKG, AK, and isolated gonad. In all cases, gonad-specific

patterns of gene expression are attenuated in AKG tissue. Inclusion of AKG tissue results in reduced sensitivity and obscures important temporal patterns in gene expression.

Taken together, my data indicate a pivotal role for steroid hormones in slider turtle testis and ovarian development. In particular, expression patterns for aromatase, ERα, and ERβ suggest a central role for estrogen in ovarian determination as well as differentiation.

Table 5-1. Molecular mechanisms underlying steroid hormone action during sex determinatin in the red-eared slider turtle

Table 1. Molecular mechanisms underlying steroid hormone action during sex determination in the red-eared slider turtle

| | |
|---|---|
| **Hypothesis 1** | **Aromatase is an early target of temperature in ovarian sex determination/differentiation.** |
| **Hypothesis 2** | **Sf1 does not regulate female-specific aromatase expression during the TSP and through sex determination in the slider turtle.** |
| **Hypothesis 3** | **Ovarian sex determination is accompanied by an increase in steroid sensitivity.** |
| **Hypothesis 4** | **ER$\alpha$ and ER$\beta$ have distinct roles in slider turtle ovarian development.** |
| **Hypothesis 5** | **Both the estrogen and androgen signaling networks interact with temperature in slider turtle gonadal development.** |
| **Hypothesis 6** | **The estrogen signaling network responds differently to ovarian sex determination via warm temperature versus exogenous estrogen.** |
| **Hypothesis 7** | **The androgen signaling network responds to changes in estrogen availability.** |

## References


Andrews JE, Smith CA, Sinclair AH. 1997. Sites of estrogen receptor and aromatase expression in the chicken embryo. General and Comparative Endocrinology 108:182-190.

Baroiller J-F, Guiguen Y, Fostier A. 1999. Endocrine and environmental aspects of sex differentiation in fish. CMLS 55:910-931.

Bergeron JM, Gahr M, Horan K, Wibbels T, Crews D. 1998. Cloning and *in situ* hybridization of estrogen receptor in the developing gonad of the red-eared slider turtle, a species with temperature-dependent sex determination. Develop. Growth Differ. 40:243-254.

Bowden RM, Ewert MA, Nelson CE. 2002. Hormone levels in yolk decline throughout development in the red-eared slider turtle (*Trachemys scripta elegans*). General and Comparative Endocrinology 129:171-177.

Brinkmann A, Jenster G, Ris-Stalpers C, van der Korput H, Bruggenwirth H, Boehmer A, Trapman J. 1996. Molecular basis of androgen insensitivity. Steroids 61:172-175.

Britt KL, Drummond AE, Dyson M, Wreford NG, Jones MEE, Simpson ER, Findlay JK. 2001. The ovarian phenotype of the aromatase knockout (ArKO) mouse. Journal of Steroid Biochemistry and Molecular Biology 79:181-185.

Britt KL, Kerr J, O'Donnell L, Jones MEE, Drummond AE, Davis SR, Simpson ER, Findlay JK. 2002. Estrogen regulates development of the somatic cell phenotype in the eutherian ovary. FASEB Journal 16:1389-1397.

Bull JJ. 1980. Sex determination in reptiles. The Quarterly Review of Biology 55:3-21.

Bull JJ, Gutzke WHN, Crews D. 1988. Sex reversal by estradiol in three reptilian orders. General and Comparative Endocrinology 70:425-428.

Bull JJ, Wibbels T, Crews D. 1990. Sex determining potencies vary among female incubation temperatures in a turtle. Journal of Experimental Zoology 256:339-341.

Butler CM, Harry JL, Deakin JE, Cooper DW, Renfree MB. 1998. Developmental expression of the androgen receptor during virilization of the urogenital system of a marsupial. Biology of Reproduction 59:725-732.

Carreau S, Bourguiba S, Lambard S, Galeraud-Denis I, Genissel C, Bilinska B, Benahmed M, Levallet J. 2001. Aromatase expression in male germ cells. Journal of Steroid Biochemistry and Molecular Biology 79:203-208.

Chang WY, Wilson MJ, Birch L, Prins G. 1999. Neonatal estrogen stimulates proliferation of periductal fibroblasts and alters the extracellular matrix composition in the rat prostate. Endocrinology 140:405-415.

Clinton M. 1998. Sex determination and gonadal development: A bird's eye view. Journal of Experimental Zoology 281:457-465.

Couse JF, Hewitt SC, Bunch DO, Sar M, Walker VR, Davis BJ, Korach KS. 1999. Postnatal sex reversal of the ovaries in mice lacking estrogen receptors A and B. Science 286:2328-2331.

Coveney D, Shaw G, Renfree MB. 2001. Estrogen-induced gonadal sex reversal in the tammar wallaby. Biology of Reproduction 65:613-621.

Crews D. 1996. Temperature-dependent sex determination: The interplay of steroid hormones and temperature. Zoological Science 274:1-13.

Crews D. 1998. On the organization of individual differences in sexual behavior. American Zoologist 38:118-132.

Crews D, Bergeron JM. 1994. Role of reductase and aromatase in sex determination in the red-eared slider (*Trachemys scripta*), a turtle with temperature-dependent sex determination. Journal of Endocrinology 143:279-289.

Crews D, Bergeron JM, Bull JJ, Flores D, Tousignant A, Skipper JK, Wibbels T. 1994. Temperature-dependent sex determination in reptiles: Proximate mechanisms, ultimate outcomes, and practical applications. Developmental Genetics 15:297-312.

Crews D, Bull JJ, Wibbels T. 1991. Estrogen and sex reversal in turtles: a dose-dependent phenomenon. General and Comparative Endocrinology 81:357-364.

Crews D, Fleming A, Willingham E, Baldwin R, Skipper JK. 2001. Role of steroidogenic factor 1 and aromatase in temperature-dependent sex determination in the red-eared slider turtle. Journal of Experimental Zoology 290:597-606.

Crews D, Lou W, Fleming AS, Ogawa S. 2006. From gene networks underlying sex determination and gonadal differentiation to the development of neural networks regulating sociosexual behavior. Brain Research (in press).

Desvages G, Pieau C. 1992. Aromatase activity in gonads of turtle embryos as a function of the incubation temperature of eggs. J. Steroid Biochem. Molec. Biol. 41:851-853.

Dupont S, Dennefeld C, Krust A, Chambon P, Mark M. 2003. Expression of *Sox9* in granulosa cells lacking the estrogen receptors, ER A and ER B. Developmental Dynamics 226:103-106.

Dupont S, Krust A, Gansmuller A, Dierich A, Chambon P, Mark M. 2000. Effect of single and compound knockouts of estrogen receptors alpha (ER A) and beta (ER B) on mouse reproductive phenotypes. Development 127:4277-4291.

Elbrecht A, Smith RG. 1992. Aromatase enzyme activity and sex determination in chickens. Science 255:467-470.

Elkin M, Cohen I, Zcharia E, Orgel A, Guatta-Rangini Z, Peretz T, Vlodavsky I, Kleinman HK. 2003. Regulation of heparanase gene expression by estrogen in breast cancer. Cancer Research 63:8821-8826.

Fisher CR, Graves KH, Parlow AF, Simpson ER. 1998. Characterization of mice deficient in aromatase (ArKO) because of targeted disruption of the *cyp19* gene. PNAS 95:6965-6970.

Fitzpatrick SL, Funkhouser JM, Sindoni DM, Stevis PE, Deecher DC, Bapat AR, Merchenthaler I, Frail DE. 1999. Expression of estrogen receptor b protein in rodent ovary. Endocrinology 140:2581-2591.

Fleming A, Crews D. 2001. Estradiol and incubation temperature modulate regulation of steroidogenic factor 1 in the developing gonad of the red-eared slider turtle. Endocrinology 142:1403-1411.

Fleming A, Wibbels T, Skipper JK, Crews D. 1999. Developmental expression of steroidogenic factor 1 in a turtle with temperature-dependent sex determination. General and Comparative Endocrinology 116:336-346.

Foidart A, Lakaye B, Grisar T, Ball GF, Balthazart J. 1999. The estrogen receptor beta in quail: cloning, tissue expression and neuroanatomical distribution. Journal of Neurobiology 40:327-342.

Frasor J, Danes JM, Komm BS, Chang KCN, Lyttle CR, Katzenellenbogen BS. 2003. Profiling of estrogen up- and down-regulated gene expression in human breast cancer cells: insights into gene networks and pathways underlying estrogenic control of proliferation and cell phenotype. Endocrinology 144:4562-4574.

Gabriel WN, Blumberg B, Sutton S, Place AR, Lance VA. 2001. Alligator aromatase cDNA sequence and its expression in embryos at male and female incubation temperatures. Journal of Experimental Zoology 290:439-448.

Gahr M, Wibbels T, Crews D. 1992. Sites of estrogen uptake in embryonic *Trachemys scripta*, a turtle with temperature-dependent sex determination. Biology of Reproduction 46:458-463.

Govoroun M, Pannetier M, Pailhoux E, Cocquet J, Brillard J-P, Couty I, Batellier F, Cotinot C. 2004. Isolation of chicken homolog of the *FOXL2* gene and comparison of its expression patterns with those of aromatase during ovarian development. Developmental Dynamics 231:859-870.

Graves JAM. 2002. Sex chromosomes and sex determination in weird mammals. Cytogenetic and Genome Research 96:161-168.

Greco TL, Payne AH. 1994. Ontogeny of expression of the genes for steroidogenic enzymes P450 side-chain cleavage, 3b-hydroxysteroid dehydrogenase, P450 17a-hydroxylase/$C_{17-20}$ lyase, and P450 aromatase in fetal mouse gonads. Endocrinology 135:262-268.

Guan G, Kobayashi T, Nagahama Y. 2000. Sexually dimorphic expression of two types of DM (*Doublesex/Mab-3*)-domain genes in a teleost fish, the tilapia (*Oreochromis niloticus*). Biochemical and Biophysical Research Communications 272:662-666.

Gubbay J, Collignon J, Koopman P, Capel B, Economou A. 1990. A gene mapping to the sex-determining region of the mouse Y chromosome is a member of a novel family of embryonically expressed genes. Nature 346:245-250.

Haqq CM, Donahoe PK. 1998. Regulation of sexual dimorphism in mammals. Physiological Reviews 78:1-33.

Hinshelwood MM, Repa JJ, Shelton JM, Richardson JA, Mangelsdorf DJ, Mendelson CR. 2003. Expression of LRH-1 and SF-1 in the mouse ovary: localization in different cell types correlates with differing function. Molecular and Cellular Endocrinology 207:39-45.

Hu Y-C, Wang P-H, Yeh S, Wang R-S, Xie C, Xu Q, Zhou X, Chao H-T, Tsai M-Y, Chang C. 2004. Subfertility and defective folliculogenesis in female mice lacking androgen receptor. PNAS 101:11209-11214.

Hudson Q, Smith CA, Sinclair AH. 2005. Aromatase inhibition reduces expression of *FOXL2* in the embryonic chicken ovary. Developmental Dynamics 233:1052-1055.

Ikeda Y, Shen WH, Ingraham HA, Parker KL. 1994. Developmental expression of mouse steroidogenic factor-1, and essential regulator of steroid hydroxylases. Molecular Endocrinology 8:654-662.

Janmohamed A, Hernandez D, Phillips IR, Shephard EA. 2004. Cell-, tissue-, sex- and developmental stage-specific expression of mouse flavin-containing monoosygenases. Biochemican Pharmacology 68:73-83.

Janzen FJ, Paukstis GL. 1991. Environmental sex determinatin in reptiles: Ecology, evolution, and experimental design. Quarterly Review of Biology 66:149-179.

Jefferson WN, Couse JF, Banks EP, Korach KS, Newbold RR. 2000. Expression of estrogen receptor B is developmentally regulated in reproductive tissues of male and female mice. Biology of Reproduction 62:310-317.

Jeyasuria P, Place AR. 1997. Temperature-dependent aromatase expression in developing diamondback terrapin (*Malaclemys terrapin*) embryos. J. Steroid Biochem. Molec. Biol. 61:415-425.

Jeyasuria P, Place AR. 1998. Embryonic brain-gonadal axis in temperature-dependent sex determination of reptiles: A role for P450 aromatase (CYP19). Journal of Experimental Zoology 281:428-449.

Jin VX, Sun H, Pohar TT, Liyanarachchi S, Palaniswamy SK, Huang TH-M, Davuluri RV. 2005. ERTargetDB: an integral information resource of transcription regulation of estrogen receptor target genes. Journal of Molecular Endocrinology 35:225-230.

Katoh H, Ogino Y, Yamada G. 2006. Cloning and expression analysis of androgen receptor gene in chicken embryogenesis. FEBS Letters 580:1607-1615.

Kettlewell JR, Raymond CS, Zarkower D. 2000. Temperature-dependent expression of turtle *Dmrt1* prior to sexual differentiation. Genesis 26:174-178.

Krege JH, Hodgin JB, Couse JF, Enmark E, Warner M, Mahler JF, Sar M, Korach KS, Gustafsson J-A, Smithies O. 1998. Generation and reproductive phenotypes of mice lacking estrogen receptor B. PNAS 95:15677-15682.

Kuntz S, Chesnel A, Duterque-Coquilland M, Grillier-Vuissoz I, Callier M, Dournon C, Flament S, Chardard D. 2003. Differential expression of P450 aromatase during

gonadal sex differentiation and sex reversal of the newt *Pleurodeles waltl*. Journal of Steroid Biochemistry and Molecular Biology 84:89-100.

Lambard S, Carreau S. 2005. Aromatase and oestrogens in human male germ cells. International Journal of Andrology 28:254-259.

Lambard S, Galeraud-Denis I, Saunders PTK, Carreau S. 2004. Human immature germ cells and ejaculated spermatozoa contain aromatase and oestrogen receptors. Journal of Molecular Endocrinology 32:279-289.

Lauber AH, Mobbs CV, Muramatsu M, Pfaff DW. 1991. Estrogen receptor messenger RNA expression in rat hypothalamus as a function of genetic sex and estrogen dose. Endocrinology 129:3180-3186.

Loffler KA, Zarkower D, Koopman P. 2003. Etiology of ovarian failure in blepharophimosis ptosis epicanthus inversus syndrome: *FOXL2* is a conserved, early-acting gene in vertebrate ovarian development. Endocrinology 144:3237-3243.

Lubahn DB, Moyer JS, Golding TS, Couse JF, Korach KS, Smithies O. 1993. Alteration of reproductive function but not prenatal sexual development after insertional disruption of the mouse estrogen receptor gene. PNAS 90:11162-11166.

Majdic G, Millar MR, Saunders PTK. 1995. Immunolocalization of androgen receptor to interstitial cells in fetal rat testes and to mesenchymal and epithelial cells of associated ducts. Journal of Endocrinology 147:285-293.

Maldonado LCT, Piedra AL, Mendoza NM, Valencia AM, Martinez AM, Larios HM. 2002a. Expression profiles of Dax1, Dmrt1, and Sox9 during temperature sex determination in gonads of the sea turtle Lepidochelys olivacea. General and Comparative Endocrinology 129:20-26.

Maldonado LCT, Piedra AL, Moreno-Mendoza N, Valencia AM, Martinez AM, Merchant-Larios H. 2002b. Expression profiles of *Dax1, Dmrt1,* and *Sox9* during temperature sex determination in gonads of the sea turtle *Lepidochelys olivacea*. General and Comparative Endocrinology 129:20-26.

Manolakou P, Lavranos G, Angelopoulou R. 2006. Molecular patterns of sex determination in the animal kingdom: a comparative study of the biology of reproduction. Reproductive Biology and Endocrinology 4:59-81.

Marchal JA, Acosta MJ, Bullejos M, de la Guardia RD, Sanchez A. 2003. Sex chromosomes, sex determination, and sex-linked sequences in Microtidae. Cytogenetic and Genome Research 101:266-273.

Menuet A, Le Page Y, Torres O, Kern L, Kah O, Pakdel F. 2004. Analysis of estrogen regulation of zebrafish estrogen receptor reveals the distinct effect of ERa, ERb1 and ERb2. Journal of Molecular Endocrinology 32:975-986.

Moreno-Mendoza NA, Harley VR, Merchant-Larios H. 2001. Temperature regulates SOX9 expression in cultured gonads of *Lepidochelys olivacea*, a species with temperature sex determination. Developmental Biology 229:319-326.

Morohashi K-I, Omura T. 1996. Ad4BP/SF-1, a transcription factor essential for the transcription of steroidogenic cytochrome P450 genes and for the establishment of the reproductive function. FASEB Journal 10:1569-1577.

Mukai T, Kusaka M, Kawabe K, Goto K, Nawata H, Fujieda K, Morohashi K-I. 2002. Sexually dimorphic expression of Dax-1 in the adrenal cortex. Genes to Cells 7:717-729.

Murdock C, Wibbels T. 2003a. Cloning and expression of aromatase in a turtle with temperature-dependent sex determination. General and Comparative Endocrinology 130:109-119.

Murdock C, Wibbels T. 2003b. Expression of Dmrt1 in a turtle with temperature-dependent sex determination. Cytogenetic and Genome Research 101:302-308.

Murdock C, Wibbels T. 2006. Dmrt1 expression in response to estrogen treatment in a reptile with temperature-dependent sex determination. Journal of Experimental Zoology 306B:134-139.

Nakabayashi O, Kikuchi H, Kikuchi T, Mizuno S. 1998. Differential expression of genes for aromatase and estrogen receptor during the gonadal development in chicken embryos. Journal of Molecular Endocrinology 20:193-202.

Nilsson S, Makela S, Treuter E, Tujague M, Thomsen J, Andersson G, Enmark E, Pettersson K, Warner M, Gustafsson J-A. 2001. Mechanisms of estrogen action. Physiological Reviews 81:1535-1565.

Nishikimi H, Kansaku N, Saito N, Usami M, Ohno Y, Shimada K. 2000. Sex differentiation and mRNA expression of P450c17, P450arom and AMH in gonads of the chicken. Molecular Reproduction and Development 55:20-30.

Pannetier M, Fabre S, Batista F, Kocer A, Renault L, Jolivet G, Mandon-Pepin B, Cotinot C, Veitia RA, Pailhoux E. 2006. FOXL2 activates P450 aromatase gene transcription: towards a better characterization of the early steps of mammalian ovarian development. Journal of Molecular Endocrinology 36:399-413.

Parker KL, Rice DA, Lala DS, Ikeda Y, Luo X, Wong M, Bakke M, Zhao L, Frigeri C, Hanley NA, Stallings N, Schimmer BP. 2002. Steroidogenic factor 1: an essential mediator of endocrine development. Recent progress in hormone research 57:19-36.

Parviainen H, Kiiveri S, Bielinska M, Rahman NA, Huhtaniemi IT, Wilson DB, Heikinheimo M. 2007. GATA transcription factors in adrenal development and tumors. Molecular and Cellular Endocrinology 265-266:17-22.

Pelletier G, Labrie C, Labrie F. 2000. Localization of oestrogen receptor alpha, oestrogen receptor beta and androgen receptors in the rat reproductive organs. Journal of Endocrinology 165:359-370.

Pelletier G, Luu-The V, Labrie F. 2004. Localization and estrogenic regulation of androgen receptor mRNA expression in the mouse uterus and vagina. Journal of Endocrinology 180:77-85.

Pieau C, Dorizzi M. 2004. Oestrogens and temperature-dependent sex determination in reptiles: all is in the gonads. Journal of Endocrinology 181:367-377.

Pieau C, Dorizzi M, Richard-Mercier N. 1999. Temperature-dependent sex determination and gonadal differentiation in reptiles. CMLS 55:887-900.

Quirke LD, Juengel JL, Tisdall DJ, Lun S, Heath DA, McNatty KP. 2001. Ontogeny of steroidogenesis in the fetal sheep gonad. Biology of Reproduction 65:216-228.

Ramsey M, Shoemaker C, Crews D. 2007. Gonadal expression of Sf1 and aromatase during sex determination in the red-eared slider turtle (*Trachemys scripta*), a reptile with temperature-dependent sex determination. Differentiation in press.

Ramsey, M, Crews, D. Steroid signaling system responds differently to temperature and hormone manipulation in the red-eared slider turtle (*Trachemys scripta elegans*), a reptile with temperature-dependent sex determination. Sexual Development in press.

Raynaud A, Pieau C. 1985. Embryonic development of the genital system. In: Gans C, editor. Biology of the Reptilia. New York: Wiley. pp 151-300.

Rinn JL, Rozowsky JS, Laurenzi IJ, Petersen PH, Zou K, Zhong W, Gerstein M, Snyder M. 2004. Major molecular differences between mammalian sexes are involved in drug metabolism and renal function. Developmental Cell 6:791-800.

Robertson KM, O'Donnell L, Jones MEE, Meachem SJ, Boon WC, Fisher CR, Graves KH, McLachlan RI, Simpson ER. 1999. Impairment of spermatogenesis in mice lacking a functional aromatase (*cyp19*) gene. PNAS 96:7986-7991.

Sarre SD, Georges A, Quinn A. 2004. The ends of a continuum: genetic and temperature-dependent sex determination in reptiles. BioEssays 26:639-645.

Scheib D. 1983. Effects and role of estrogens in avian gonadal differentiation. Differentiation 23:S87-S92.

Schmidt D, Ovitt CE, Anlag K, Fehsenfeld S, Gredsted L, Treier A-C, Treier M. 2004. The murine winged-helix transcription factor Foxl2 is required for granulosa cell differentiation and ovary maintenance. Development 131:933-942.

Shibata K, Takase M, Nakamura M. 2002. The *Dmrt1* expression in sex-reversed gonads of amphibians. General and Comparative Endocrinology 127:232-241.

Shoemaker C, Ramsey M, Queen J, Crews D. 2007. Expression of *Sox9*, *Mis* and *Dmrt1* in the gonad of a species with temperature-dependent sex determination. Developmental Dynamics 236:1055-1063.

Simpson ER, Mahendroo MS, Means GD, Kilgore MW, Hinshelwood MM, Graham-Lorence S, Amarneh B, Ito Y, Fisher CR, Michael MD. 1994. Aromatase cytochrom P450, the enzyme responsible for estrogen biosynthesis. Endocrinol. Rev. 15:342-355.

Sinclair AH, Berta P, Palmer MS, Hawkins JR, Griffiths BL. 1990. A gene from the human sex-determining region encodes a protein with homology to a conserved DNA-binding motif. Nature 346:240-244.

Smith CA, Andrews JE, Sinclair AH. 1997. Gonadal sex differentiation in chicken embryos: Expression of estrogen receptor and aromatase genes. J. Steroid Biochem. Molec. Biol. 60:295-302.

Smith CA, Elf PK, Lang JW, Joss JMP. 1995. Aromatase enzyme activity during gonadal sex differentiation in alligator embryos. Differentiation 58:281-290.

Smith CA, Joss JMP. 1994. Uptake of $^{3}$H-estradiol by embryonic crocodile gonads during the period of sexual differentiation. Journal of Experimental Zoology 270:219-224.

Smith CA, Katz M, Sinclair AH. 2003. *DMRT1* is upregulated in the gonads during female-to-male sex reversal in ZW chicken embryos. Biology of Reproduction 68:560-570.

Smith CA, Sinclair AH. 2001. Sex determination in the chicken embryo. Journal of Experimental Zoology 290:691-699.

Smith CA, Smith MJ, Sinclair AH. 1999a. Expression of chicken steroidogenic factor-1 during gonadal sex differentiation. General and Comparative Endocrinology 113:187-196.

Smith CA, Smith MJ, Sinclair AH. 1999b. Gene expression during gonadogenesis in the chicken embryo. Gene 234:395-402.

Spotila LD, Spotila JR, Hall SE. 1998. Sequence and expression analysis of WT1 and Sox9 in the red-eared slider turtle, *Trachemys scripta*. Journal of Experimental Zoology 281:417-427.

Sweeney T, Saunders PTK, Millar MR, Brooks AN. 1997. Ontogeny of anti-Mullerian hormone, 2b-hydroxysteroid dehydrogenase and androgen receptor expression during ovine fetal gonadal development. Journal of Endocrinology 153:27-32.

Takada S, DiNapoli L, Capel B, Koopman P. 2004. Sox8 is expressed at similar levels in gonads of both sexes during the sex determining period in turtles. Developmental Dynamics 231:387-395.

Trant JM, Gavasso S, Ackers J, Chung B-C, Place AR. 2001. Developmental expression of cytochrome P450 aromatase genes (CYP19a and CYP19b) in zebrafish fry (*Danio rerio*). Journal of Experimental Zoology 290:475-483.

Tsai M-J, O'Malley BW. 1994. Molecular mechanisms of action of steroid/thyroid receptor superfamily members. Annual Review of Biochemistry 63:451-486.

Vainio S, Lin Y. 2002. Coordinating early kidney development: lessons from gene targeting. Nature Reviews Genetics 3:533-543.

Wallace H, Badawy GMI, Wallace BMN. 1999. Amphibian sex determination and sex reversal. CMLS 55:901-909.

Wennstrom K, Crews D. 1995. Making males from females: The effects of aromatase inhibitors on a parthenogenetic species of whiptail lizard. General and Comparative Endocrinology 99:316-322.

Western PS, Harry JL, Graves JAM, Sinclair AH. 1999. Temperature-dependent sex determination: Upregulation of SOX9 expression after commitment to male development. Developmental Dynamics 214:171-177.

Western PS, Harry JL, Graves JAM, Sinclair AH. 2000. Temperature-dependent sex determination in the American alligator: expression of *SF1*, *WT1*, and *DAX1* during gonadogenesis. Gene 241:223-232.

White RB, Thomas P. 1992a. Adrenal-kidney and gonadal steroidogenesis during sexual differentiation of a reptile with temperature-dependent sex determination. General and Comparative Endocrinology 88:10-19.

White RB, Thomas P. 1992b. Stimulation of the in vitro steroidogenesis by pituitary hormones in a turtle (*Trachemys scripta*) within the temperature-sensitive period for sex determination. Biology of Reproduction 47:952-959.

White RB, Thomas P. 1992c. Whole-body and plasma concentrations of steroids in the turtle, *Trachemys scripta*, before, during, and after the temperature-sensitive period for sex determination. Journal of Experimental Zoology 264:159-166.

Wibbels T, Bull JJ, Crews D. 1991a. Chronology and morphology of temperature-dependent sex determination. Journal of Experimental Zoology 260:371-381.

Wibbels T, Bull JJ, Crews D. 1991b. Synergism between temperature and estradiol: a common pathway in turtle sex determination? Journal of Experimental Zoology 260:130-134.

Wibbels T, Bull JJ, Crews D. 1992. Steroid hormone-induced male sex determination in an amniotic vertebrate. Journal of Experimental Zoology 262:454-457.

Wibbels T, Bull JJ, Crews D. 1994. Temperature-dependent sex determination: A mechanistic approach. Journal of Experimental Zoology 270:71-78.

Wibbels T, Crews D. 1992. Specificity of steroid hormone-induced sex determination in a turtle. Journal of Endocrinology 133:121-129.

Wibbels T, Crews D. 1994. Putative aromatase inhibitor induces male sex determination in a female unisexual lizard and in a turtle with temperature-dependent sex determination. Journal of Endocrinology 141:295-299.

Wibbels T, Crews D. 1995. Steroid-induced sex determination at incubation temperatures producing mixed sex ratios in a turtle with TSD. General and Comparative Endocrinology 100:53-60.

Wibbels T, Gideon P, Bull JJ, Crews D. 1993. Estrogen- and temperature-induced medullary cord regression during gonadal differentiation in a turtle. Differentiation 53:149-154.

Willingham E, Baldwin R, Skipper JK, Crews D. 2000. Aromatase activity during embryogenesis in the brain and adrenal-kidney-gonad of the red-eared slider turtle, a species with temperature-dependent sex determination. General and Comparative Endocrinology 119:202-207.

Yao HH-C, DiNapoli L, Capel B. 2004. Cellular mechanisms of sex determination in the red-eared slider turtle (*Trachemys scripta*). Mechanisms of Development 121:1393-1401.

Yeh S, Tsai M-Y, Xu Q, Mu X-M, Lardy H, Huang K-E, Lin H, Yeh S-D, Altuwaijri S, Zhou X, Xing L, Boyce BF, Hung M-C, Zhang S, Gan L, Chang C. 2002. Generation and characterization of androgen receptor knockout (ARKO) mice: An *in vivo* model for the study of androgen functions in selective tissues. PNAS 99:13498-13503.

Yoshida K, Shimada K, Saito N. 1996. Expression of $P450_{17a}$ hydroxylase and P450 aromatase genes in the chicken gonad before and after sexual differentiation. General and Comparative Endocrinology 102:233-240.

Zhang D, Trudeau VL. 2006. Integration of membrane and nuclear estrogen receptor signaling. Comparative Biochemistry and Physiology Part A 144:306-315.

# Vita

Mary Elizabeth Ramsey was born in Baytown, Texas on August 24, 1965, the daughter of Marjorie Greer Ramsey and Bruce Ramsey. After completing her work at Lee High School, Houston, Texas, in 1983, she entered Texas A&M University in College Station, Texas. She received the degree of Bachelor of Arts from Texas A&M University in May 1987. In September 1999 she entered the Zoology Program at the Graduate School of The University of Texas.

Permanent address: 8400 Appalachian Dr., Austin, Texas 78759

This dissertation was typed by the author.